Measurement of Electromagnetic Interference Rejection Ratio for Precision Instrumentation Amplifiers

Master Thesis

Submitted in Fulfillment of the
Requirements for the Academic Degree
M.Sc.

Dept. of Computer Science
Professorship of Computer Engineering

Submitted by: Preeti Udapudi
Matrikel Nr.: 619336
Master's Degree: Automotive Software Engineering
Submission date: 08.03.2022

Primary Supervisor: Prof. Dr. Dr. h. c. Wolfram Hardt
Secondary Supervisor: Mr. Reda Harradi
Technische Universitat Chemnitz
09111 Chemnitz, Germany

External Supervisor: Mr. Patrick Kammermayer
Texas Instruments Deutschland GmbH
85356 Freising, Germany

Abstract

Electro-Magnetic Interference(EMI) degrades the perfomance of electronic systems. So, Amplifiers which are the basic building blocks used in the front-end of analog and mixed-signal Integrated Circuits (ICs) must be evaluated for EMI. This work introduces the most intriguing figure of merit, Electro-Magnetic Interference Rejection Ratio (EMIRR) to measure the EMI immunity of precision Instrumentation Amplifiers (INAs) that helps to select the EMI robust INAs for EMI critical applications.

In this work, a new EMIRR measurement setup is implemented to measure the immunity of INAs for conducted EMI ranging from 10 MHz to 3 GHz. The shift in the DC offset voltage generated at the output of the INA due to RF rectification, is used to compute EMIRR. As part of the setup, the hardware evaluation board is designed and an automation test software is developed to run EMIRR measurements. Furthermore, EMIRR measurements are performed on several INAs with different specifications to compare and rank them on their EMI immunity levels. Additionally, with the help of EMIRR metric, suitable INAs for developing EMI-sensitive applications are proposed. Finally, the influence of amplifier bandwidth, the input capacitance, 50 Ω termination at the end of RF input trace, INA package parasitics and EMI filter bandwidth on EMIRR is analyzed with the measurement results.

Acknowledgement

I take this opportunity to thank all the people whose assistance was a milestone in the completion of my master thesis at Technical University of Chemnitz and Texas Instruments Deutschland GmbH.

My deepest gratitude goes to my industrial supervisor Mr. Patrick Kammermayer and my manager Mr. Tobias Oschmann for providing me the opportunity to work with them. Their insights and guidance throughout my tenure helped me in improving my technical and personal skills. A debt of gratitude is also owed to Mr. Mitchell Gallaher and Mr. Gerardo Rivera at Texas Instruments, Tucson for their kind help and co-operation throughout my thesis. I would like to express my further thanks to Mr. Raul Blecic and Mr. Karthikeyan Krishnamourthy for providing me the technical assistance during my research. My appreciation also extends to the colleagues of Precision Amplifiers team for being extremely helpful during my thesis work in Texas Instruments.

I would like to pay my special regards to my professor at the university Prof. Dr. Dr. h. c. Wolfram Hardt for providing me this opportunity to complete my master thesis under his professorship. I would also like to thank Mr. Reda Harradi for his guidance and valuable support throughout my thesis. Above ground, I am indebted to my family and friends, whose value to me only grows with age. I would not have been here without your love and support.

Table of Contents

Table of Contents . . . **iii**

List of Figures . . . **v**

List of Tables . . . **viii**

List of Abbreviations . . . **ix**

1 Introduction . . . **1**

1.1 Research Motivation . . . 1

1.2 Introduction to EMIRR . . . 2

1.3 Introduction to Precision Amplifiers . . . 3

1.3.1 The Precision Op-amps . . . 3

1.3.2 The Precision INAs . . . 4

1.4 Effect of EMI on Amplifiers . . . 5

1.5 Research Objectives . . . 6

1.6 Thesis Outline . . . 7

2 State of the Art . . . **9**

2.1 Theoretical Background . . . 9

2.1.1 Elements of EMI . . . 9

2.1.2 Sources of Electromagnetic Energy . . . 10

2.2 Related Work . . . 12

2.3 Research Methodology . . . 17

2.3.1 Built-in EMI Filtering in Amplifiers . . . 17

2.3.2 Calculating EMIRR . . . 18

2.3.3 Conducted EMI Measurement Technique in Op-amps . . . 19

2.4 Chapter Summary . . . 23

3 EMIRR Test Setup Correlation . . . **24**

3.1 Required Hardware Instruments . . . 24

3.2 Analyzing the Existing Op-amp Hardware Test Setup . . . 29

3.3 Hardware Test Board Design for INAs . . . 29

3.3.1 Applying RF Input to INAs . . . 29

3.3.2 Design of Evaluation Boards . . . 31
3.3.3 RF Design Guidelines that are Considered . . . 35
3.4 EMIRR Test Setup for INAs . . . 39
3.5 New(INA) Test Setup Correlation with the Old(Op-amp) Test Setup . 41
3.6 Chapter Summary . . . 41

4 Simulation and Test Software Implementation . . . 43
4.1 Signal Integrity Simulations . . . 43
4.1.1 Scattering parameters . . . 43
4.1.2 Signal Integrity Simulations in ADS . . . 44
4.1.3 Simulation Results . . . 47
4.2 Development of Test Software to Measure EMIRR . . . 50
4.2.1 About NI TestStand and NI LabVIEW . . . 50
4.2.2 Setting-Up the VNA to Measure S-Parameters . . . 51
4.2.3 Building the TestStand Sequence . . . 51
4.2.4 EMIRR Calculation . . . 54
4.3 Chapter Summary . . . 56

5 Results and Discussions . . . 58
5.1 EMIRR Measurements and Data Analysis . . . 58
5.1.1 Test Setup Verification by Measuring EMIRR for Op-amp Sample 58
5.1.2 EMIRR Measurement for INAs . . . 60
5.2 Some Investigations on EMIRR and Data Analysis . . . 63
5.2.1 Termination Resistor at the End of RF Input PCB Trace . . . 64
5.2.2 Device Package Test . . . 65
5.2.3 EMIRR Behavior for Different Amplitude Levels of RF . . . 67
5.2.4 EMIRR Response for Different Power Supply Voltages . . . 68
5.2.5 EMI Shielding Tent . . . 70
5.2.6 Coupling RF to Inverting and Non-Inverting Terminal of the Amplifier . . . 71
5.3 Comparison of the EMIRR Performance of INAs . . . 72
5.4 Influence of Amplifier Bandwidth, Input Capacitance on EMIRR . . . 76
5.5 Chapter Summary . . . 76

6 Conclusion . . . 78

Bibliography . . . 80

TUC References . . . 83

List of Figures

1.1 Acquisition Front-End Architecture in Sensor Applications [2] 2
1.2 EMIRR [4] 3
1.3 EMIRR IN+ [4] 3
1.4 Operational Amplifier [5] 4
1.5 The classic 3 op-amp INA [7] 4
1.6 Change in DC offset voltage for the detected RF signal[8] 5

2.1 Essential elements for EMI problems [11] 10
2.2 Common Impedance to Ground [4] 11
2.3 Capacitive Current Coupling [4] 12
2.4 Inductive Voltage Coupling [4] 12
2.5 EMI Measurement Techniques [11] 13
2.6 Examples of conducted and radiated emissions [12] 14
2.7 Test setup for immunity against magnetic fields using circular Helmholtz coils [14] 15
2.8 Measurement setup for EMI radiated immunity testing [11] 17
2.9 nMos differential input stage with input resistors [15] 18
2.10 Lumped circuit model [4] 19
2.11 Distributed circuit model [4] 20
2.12 Impedance Mismatch Causes Voltage and Current Reflections [4] 20
2.13 RF Input Signal Path for Measuring EMIRR [4] 21
2.14 Complex RF Input Environment [4] 21
2.15 Complete EMIRR Test Circuit Configuration [4] 22

3.1 Vector Network Analyzer 24
3.2 RF signal source 25
3.3 Bias Tee Circuit Model [4] 25
3.4 Bias Tee Circuit Model [4] 26

3.5 E3631A DC power supply . . . 26
3.6 TTE 8th order low pass filter . . . 27
3.7 Frequency response of 8th order passive low pass filter . . . 27
3.8 34410A Digital Multimeter . . . 28
3.9 Spectrum Analyzer . . . 28
3.10 Differential mode RF input to INA . . . 29
3.11 Common mode RF input to INA . . . 30
3.12 Input Capacitance Model [16] . . . 31
3.13 Schematic of INA for differential mode EMIRR measurement . . . 32
3.14 Schematic of INA for common mode EMIRR measurement . . . 33
3.15 INA SOIC8 EMIRR Test Board with Burr-Brown Pinout . . . 34
3.16 INA SOIC8 EMIRR Test Board with ADI Pinout . . . 35
3.17 Impedance Calculation for Microstrip trace [19] . . . 35
3.18 Coplanar waveguide analysis [20] . . . 36
3.19 Via shielding around the PCB trace . . . 37
3.20 Impedance characteristic of decoupling capacitor [22] . . . 39
3.21 Block Diagram of EMIRR Test Setup for In-amps . . . 40
3.22 EMIRR Measurement Setup in Lab . . . 41

4.1 S-parameters overview considering 2 ports [21] . . . 44
4.2 PCB layer stack-up for EM simulation . . . 45
4.3 The meshed layout of SOIC-8 BB pinout board in EM simulation . . . 46
4.4 S-parameter data of differential mode input trace . . . 47
4.5 S-parameters data of reference trace . . . 48
4.6 S-parameter data of common mode input trace . . . 49
4.7 EMIRR test software hierarchy . . . 52
4.8 EMIRR test software flowchart for the main sequence . . . 53
4.9 EMIRR test software flowchart for a submodule A . . . 55

5.1 OPA2227 EMIRR Curve compared with that of the datasheet curve . . . 59
5.2 DC Offset Voltage vs Frequency curve for OPA2227 . . . 59
5.3 EMIRR vs frequency for INA819 in Differential mode . . . 60
5.4 EMIRR vs frequency for INA819 in Common-mode . . . 61
5.5 DC offset voltage shift vs frequency for INA819 in differential mode . . . 61
5.6 DC offset voltage shift vs frequency for INA819 in common mode . . . 62
5.7 Coupon board . . . 62

5.8 INA819 EMIRR curve in differential mode with and without 50 Ω termination . . . 64
5.9 INA819 EMIRR curve in common mode with and without 50 Ω termination . . . 65
5.10 INA819 EMIRR curve in differential mode with D, DGK, and DRG packages . . . 66
5.11 INA819 EMIRR curve in common-mode with D, DGK, and DRG packages 66
5.12 INA818 EMIRR curves in differential mode for different RF power levels 67
5.13 INA818 EMIRR curves in the common mode for different RF power levels 68
5.14 INA819 EMIRR curves in differential mode for different supply voltages 69
5.15 INA819 EMIRR curves in the common mode for different supply voltages 69
5.16 EMIRR test board placed inside the EMI shielding tent . . . 70
5.17 INA819 EMIRR data with and without EMI shielding tent in differential mode . . . 70
5.18 INA819 EMIRR data with and without EMI shielding tent in common mode . . . 71
5.19 INA819 EMIRR measurement by coupling the RF to inverting and non-inverting input terminals . . . 72
5.20 EMIRR responses of INA819, INA821, INA828, and INA828 in differential mode . . . 73
5.21 EMIRR responses of INA819, INA821, INA828, and INA828 in common mode . . . 73

List of Tables

5.1 INAs with different specifications [26][27][28][29] 72
5.2 EMIRR values listed for the applications with the frequencies of interest [26][27] 75

List of Abbreviations

A/D Analog to Digital

AC Alternating Current

ADI Analog Device Incorporated

ADS Advanced Design Systems

ASP Analog Signal Processing

BB Burr-Brown

CMRR Common Mode Rejection Ratio

CW Continuous Wave

D/A Digital to Analog

DC Direct Current

DMM Digital Multi-Meter

DSP Digital Signal Processing

DUT Device Under Test

EMC Electro-Magnetic Compatibility

EMIRR Electro-Magnetic Interference Rejection Ratio

EMI Electro-Magnetic Interference

ESD Electro-Static Discharge

ESR Equivalent Series Resistance

GPIB General Purpose Interface Bus

GSM Global System for Mobile Communications

INA Instrumentation Amplifier0INVInverting

ISM Industrial, Scientific, and Medical

LPF Low Pass Filter

MOSFET Metal Oxide Semiconductor Field-Effect Transistor

MRI Magnetic Resonance Imaging

NI National Instruments

NINV Non-Inverting

Op-amp Operational Amplifier

PCB Printed Circuit Board

PDIP Plastic Dual Inline Package

PSRR Power Supply Rejection Ratio

RFI Radio Frequency Interference

RF Radio Frequency

RI Radiated Immunity

SMA Sub-Miniature Version A

SMPS Switch Mode Power Supply

SMT Surface-Mount Technology

SOIC-8 Small Outline Integrated Circuit-8

TDR Time Domain Reflectometer

UHF Ultra-High Frequency

VNA Vector Network Analyzer

VSWR Voltage Standing Wave Ratio

1 Introduction

1.1 Research Motivation

With the advancements in technologies of all the fields, electronic devices are gradually moving towards wireless communication, which is the primary cause of signal interference. Such signal interference includes EMI, which is also termed as Radio Frequency Interference (RFI) that has become a major challenge in recent years as the number of electronic devices across the world is increasing. Sensitive electronic applications such as the Magnetic Resonance Imaging (MRI) system and electrical nerve stimulation in the medical sector, infotainment systems in automobiles, radio communication, navigation systems, and many electronic devices that we use in day-to-day life such as television, radio are some of the examples that are susceptible to EMI. Internally, these applications are made up of electronic units for sensor signal conditioning, power management, load driving, etc., which are done with analog circuits based on amplifiers [1]. In such analog circuits, especially amplifiers are more prone to RF interferences.

Immunity to RF disturbances is a crucial requirement for electronic equipment to function safely and reliably. Therefore, the circuits of EMI-critical applications should be designed to be intrinsically immune to EMI by using components that are robust to such RF disturbances. Since, amplifiers are one of the most prominent analog building blocks used in such EMI-sensitive circuits [3], selecting an amplifier that is immune to EMI becomes a major challenge. As a result, we require a metric that can quantify the EMI robustness of amplifiers, enabling us to evaluate them and choose the one with the highest immunity for the EMI sensitive applications such as acquisition front-end architecture of sensor application that needs amplifiers with high immunity to EMI as illustrated in Figure 1.1. Since, amplifiers are used in the analog front end to condition the signals, it is crucial to avoid signal interferences affecting the amplifier

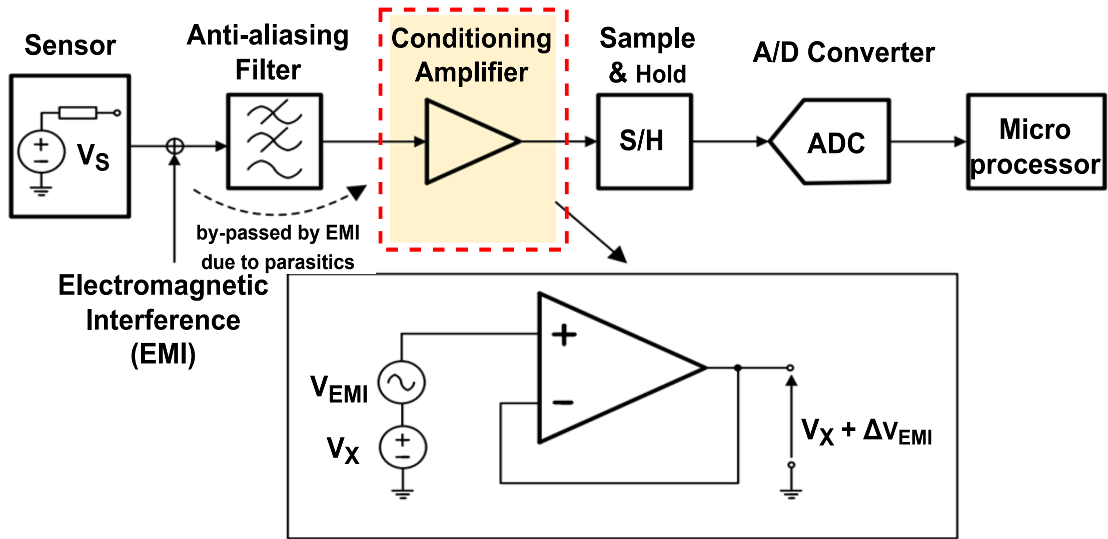

Figure 1.1: Acquisition Front-End Architecture in Sensor Applications [2]

circuit. Therefore, it is required to measure EMI immunity of amplifiers, so that the application designers can select the amplifiers based on their EMI requirements.

Newly designed amplifiers are incorporated with EMI filters to protect the device from RF noise by rejecting high-frequency interferences. And the rejection of RF interference can be estimated using a figure of merit, EMIRR. The EMIRR metric enables the user to directly compare the amplifiers in terms of EMI immunity. With this data, designers can now choose the best performing amplifier for EMI-critical applications. This method provides a considerable advantage to board and system-level designers while avoiding the high costs of additional design cycles [4]. In subsequent sections, the definition of EMIRR is described along with a method to measure it.

1.2 Introduction to EMIRR

Since the amplifiers are used to amplify and condition signals in a wide range of analog and mixed-signal integrated circuits, their EMI immunity is an important factor to be considered. EMIRR is a figure of merit used to quantify the EMI immunity of the amplifier and helps to compare and rank amplifiers based on their EMI robustness. By injecting an RF signal into any amplifier pin and measuring the subsequent DC offset shift (ΔV_{OS}) at the output of the amplifier, EMIRR can be calculated as featured in Figure 1.2. Sometimes, this parameter is referred to as EMIRR IN+ when the

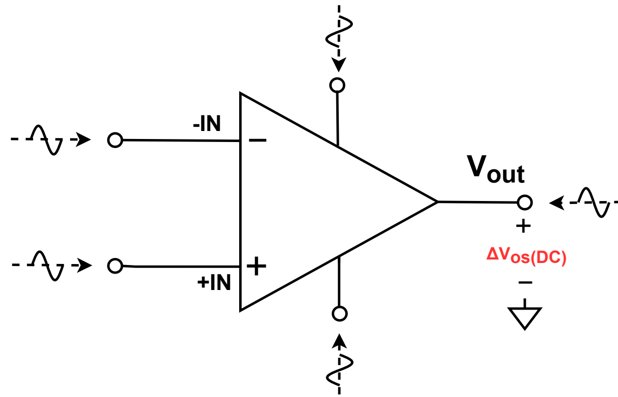

Figure 1.2: EMIRR [4]

non-inverting input pin of the amplifier is selected as a dedicated input pin for RF interference as shown in Figure 1.3 [4]. However, it is still designated as the EMIRR in this report irrespective of the dedicated input pin selected for RF injection.

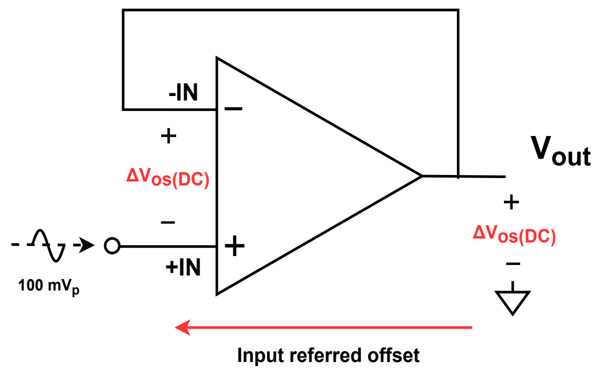

Figure 1.3: EMIRR IN+ [4]

1.3 Introduction to Precision Amplifiers

1.3.1 The Precision Op-amps

Amplifiers are integrated circuits that are used to amplify weak signals. Precision op-amps are amplifiers that have better specifications than normal amplifiers, such as lower bandwidth, precision offset, temperature drift, internal noise, input bias current, and so on. It is a 3-terminal electronic device with two high impedance inputs (inverting and non-inverting) and a low impedance output as shown in Figure 1.4. The main

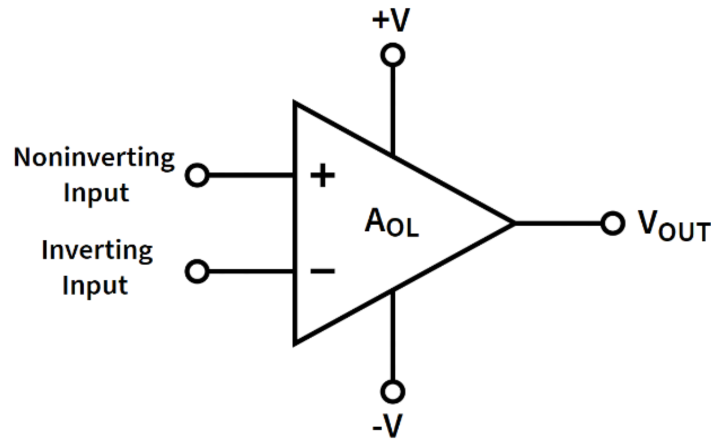

Figure 1.4: Operational Amplifier [5]

operation of an op-amp is to enhance or amplify the differential voltage signals between the inputs. An ideal op-amp has infinite input impedance, infinite open-loop gain (A_{OL}), zero output impedance, infinite bandwidth, and zero noise [6].

1.3.2 The Precision INAs

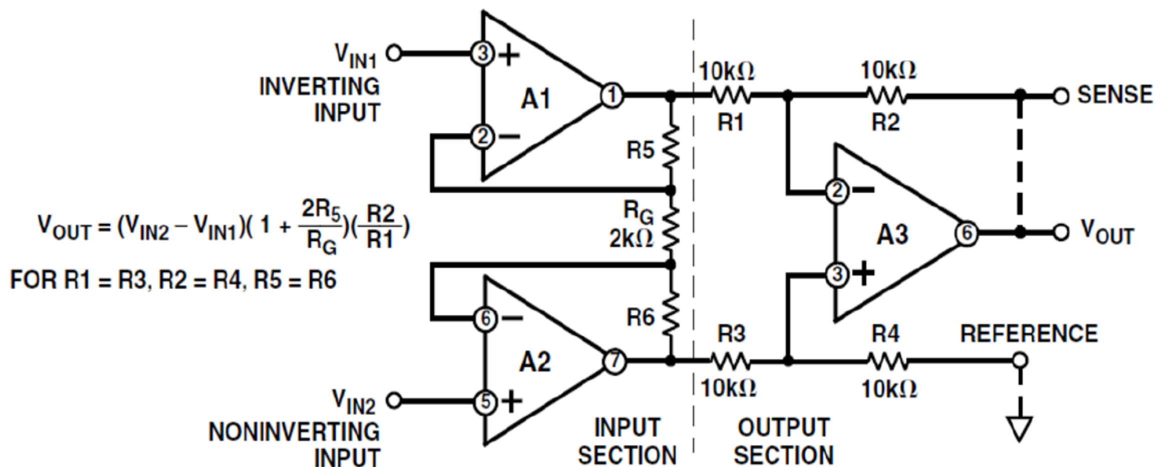

Figure 1.5: The classic 3 op-amp INA [7]

An INA is a precision differential amplifier with very high input impedance, low DC offset, low noise, low drift, and high Common Mode Rejection Ratio (CMRR) as compared to normal amplifiers, making it suitable for use in circuits requiring high accuracy and stability [7]. The amplifier's ability to reject a common signal given to both INV and NINV inputs is described as CMRR [TUC1]. INA's main function is

to amplify the differential signals between the inputs and reject the common-mode signals. Unlike other amplifiers, INA contains a reference input pin that is used to level-shift the output. Although the INA is schematically identical to a regular op-amp, it is almost always internally composed of three amplifiers. These are configured such that two input amplifiers (A1 and A2) will buffer the inverting and non-inverting inputs, and third amplifier(A3) produces the desired output with proper impedance matching for the function. Figure 1.5 depicts the basic 3 op-amps INA circuit. It is divided into two stages: the first is known as the input section, and the second is known as the output section.

1.4 Effect of EMI on Amplifiers

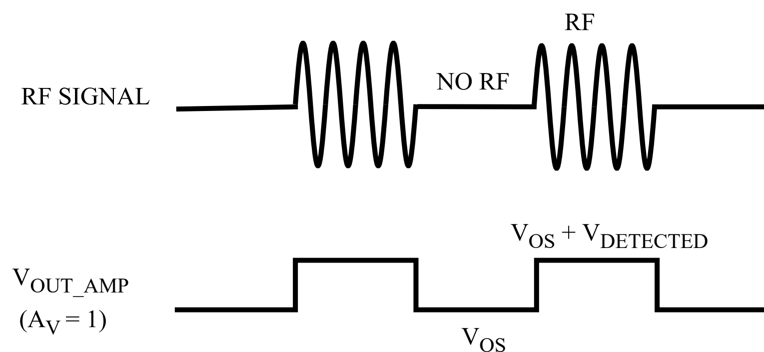

Figure 1.6: Change in DC offset voltage for the detected RF signal[8]

Op-amps are designed with non-linear elements such as diodes and transistors, which cause a small DC offset voltage to be generated when an op-amp is subjected to high-frequency EMI. This can be referred to the process of rectification because an AC signal is converted to a DC signal. Due to the rectification process in the op-amp signal path, there might be some offset error created in the system which can cause inaccuracies in the system. Figure 1.6 below clearly shows that when an RF signal is detected, the DC offset voltage on the amplifier's output is shifted to some extent. In this case, the op-amp is set to unity gain configuration, which implies the output voltage to be same as the input voltage since the gain is 1. The DC offset voltage varies when the RF signal is applied. This resulting DC offset voltage variation is used to calculate the EMIRR which is a useful metric to describe the RF immunity of

amplifiers [4].

1.5 Research Objectives

The main goal of this thesis is to analyze the existing EMIRR test setup for op-amps and optimize it for precision INAs to measure EMIRR of INAs and rank them according to their EMI robustness. This helps to select the suitable INAs for EMI-critical applications. In order to achieve this, as a first step, an EMIRR measurement setup should be implemented for INAs. This measurement setup shall consist of a hardware test board with an adapter board, RF signal generator with the frequency range up to 3 GHz or 5 GHz, bias tee, and low pass filter, power supply, spectral analyzer, high-resolution Digital Multi-Meter (DMM), and a lab computer to run the test software to measure EMIRR.

For the EMIRR test setup, it is expected to design a hardware test board to measure EMIRR for INAs. A test automation software must be developed using either National Instruments (NI) TestStand or LabVIEW (Laboratory Virtual Instrument Engineering Workbench) software to run EMIRR measurements by considering the different lab instruments used. The designed hardware PCB should be scalable to multiple packages of INAs. The small DC offset at the output terminal of the DUT - Device Under Test should be captured with the DMM and the EMIRR data should be computed. Data analysis can be done using the Spotfire tool.

This work is also aimed to analyze the following artifacts influencing EMIRR and to make possible conclusions:

1 **Influence of the test board on EMIRR**

To check the impact of the test board a 50 Ω termination resistor can be placed at the end of RF input trace to match setup impedance. By matching this impedance it is expected that the EMIRR results would improve as the input RF signal reaching the DUT is less reflected and the calibration values can be improved.

2 **The effect of INA package parasitics on EMIRR**

The same INA is available with various package types which implies that the different package parasitics. Thus, the influence of INA package parasitics on EMIRR should be checked because the bond-wire inductance or a capacitance to the lead-frame might have some impact on the seen impedance which further affects the signal reaching the inputs of the amplifier where the rectification happens.

3 **The impact of INA bandwidth, input capacitance on EMIRR**

The EMIRR should be measured to check the influence of INA characteristics such as bandwidth, input capacitance, and internal EMI filter cut-off frequency on EMIRR results.

4 **The influence of in-built EMI filter on INA on its EMIRR**

It is expected that EMI filter bandwidth can have significant impact on EMIRR as the EMI filter is placed at the input stage of INA where the rectification of RF signal takes place [9].

1.6 Thesis Outline

This thesis is composed of seven chapters.

Chapter 1 briefly introduces EMIRR and precision amplifiers (op-amps and INAs), discusses why EMIRR is important to be considered and then outlines the objectives of this thesis.

Chapter 2 describes the theoretical background of EMI, including the necessary elements required for EMI, sources of EMI, and two different EMI transmission types such as radiated immunity testing and conducted immunity testing. Some EMI measurement techniques are listed, including magnetic field immunity testing and radiated immunity testing, which are briefly explained. Finally, the study methodology outlines a more practical and precise way of measuring EMI immunity in amplifiers using the parameter EMIRR.

Chapter 3 finds a correlation between op-amp and INA test setups. All of the hardware instruments used in the EMIRR test setup is briefly described in terms of its purpose and functioning. The three-dimensional images of the proposed hardware evaluation boards are shown along with their schematics. Additionally, the RF guidelines that were followed while designing the boards are explained. Finally, a comprehensive block diagram of the EMIRR hardware measuring setup for INAs is demonstrated along with the EMIRR setup in the lab.

Chapter 4 deals with signal integrity simulations in Advanced Design Systems (ADS) software to assess the magnitude of the input RF signal reaching the device inputs. It also focuses on the proposed EMIRR test software implementation using NI TestStand software. Finally, flowcharts illustrating the flow of the test automation sequence are also provided.

Chapter 5 shows the EMIRR results for INAs and analyzes the data obtained to make possible inferences from the tests performed. Based on the EMIRR measurements on a couple of INAs with different bandwidths and input capacitances, a comparison was made on their EMI robustness. Finally, several RF applications with their operating frequencies were listed, and appropriate INAs for developing such applications were proposed based on the EMIRR values.

Chapter 6 summarizes the EMIRR research and measurements in this thesis and makes the conclusions.

2 State of the Art

2.1 Theoretical Background

Due to the increased level of environmental electromagnetic pollution, it has become mandatory to design electronic systems immune to RF interference signals. Indeed, the interconnections like wires and traces of printed circuit boards in electronic systems couple RF interference and translate it into current and voltages. These noise signals are then coupled with the system signals that reach the terminals of Integrated Circuit (IC) causing distortion in active non-linear devices and hence generating temporary or permanent errors in the functionality of the electronic system [10].

Analog circuits are more susceptible to EMI than digital circuits because they sense the weak noise as just another signal whereas digital circuits can only recognize the states like full on or full off. Hence, DSP - Digital Signal Processing is preferred over ASP- Analog Signal Processing in some applications. However, analog signal processing cannot be replaced in many electronic applications including the Analog-to-Digital (A/D) and Digital-to-Analog (D/A) conversions required in digital signal processing due to the intrinsic analog nature of information in the physical world [10]. Among analog circuits, op-amps can be extremely susceptible to RF interference. They demodulate RFI added to input signals, causing interference to corrupt the op-amp output signals. Due to the presence of a continuous-wave interference signal, unwanted DC output offset voltage will be generated in the system.

2.1.1 Elements of EMI

For an analog circuit to respond to EMI, three elements must be present in the system. First, there must be an EMI source that acts as a source of unintended interferences. Second, a channel or a medium is required to transfer the EMI signals to the circuit. Third, an energy-sensitive receptor, which reacts to these interferences

must be present as shown in Figure 2.1 [11]. A receptor can be an analog circuit or any other type of circuit that acts as an antenna. When these three components are present in an electronic system, the EMI effect may occur. The source must produce enough RF power at frequencies that the receptor can detect. To couple the RF signal to the receptor, a coupling source must be present and the receptor must be sensitive enough to that specific RF condition to produce an unwanted response. Although EMI arises as radiations initially, gradually it is converted to conducted EMI [TUC2], which can enter into other circuits.

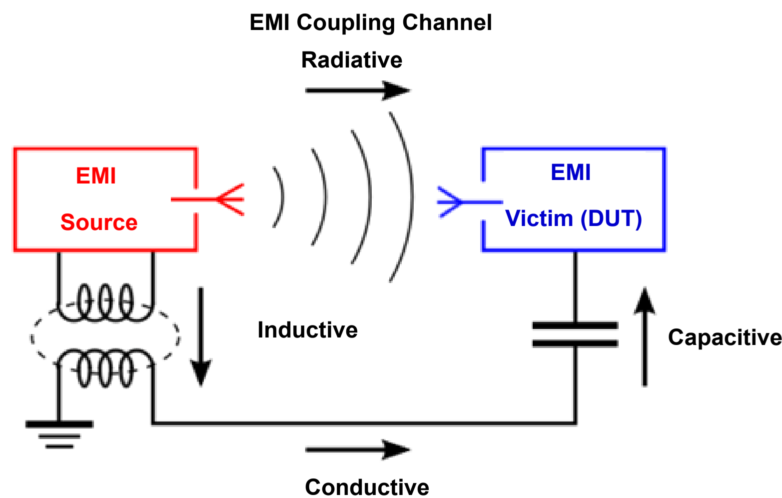

Figure 2.1: Essential elements for EMI problems [11]

2.1.2 Sources of Electromagnetic Energy

Many sources can generate RF interferences and are mainly segregated based on how the EMI enters the electronic system. Two such methods are given below:

1 **EMI by radiation:** RF Interference by radiation can occur when the DUT can detect the electromagnetic waves in the environment and receive them. It depends upon the frequency of the Interference wave and the sensitivity of the DUT to that frequency. Also, the susceptibility of the DUT is determined by the relative size of the DUT to the wavelength of the interfering EM wave. Examples of EMI radiating sources include cell phones, wireless routers, lightning, wireless Bluetooth devices, etc [8].

2 **EMI by conduction:** EMI by conduction occurs when the other devices nearby the DUT acts as receivers/antennas for EMI signals. Such devices can be, the cables or the traces on the PCB, which are connected to the DUT. Following that, the received signals such as voltages and currents are conductively transferred to the DUT which may interfere with the op-amp and degrade the functionality of the system. Examples of conductive EMI sources are RF transmitters, Switch Mode Power Supply (SMPS), clock circuitry in microcontrollers, electromechanical relays, etc [8]. It is sufficient to consider RF disturbances received conductively to determine the robustness of an analog circuit to EMI.

So, apart from these sources, EMI can also be generated within the circuits that are designed as illustrated below.

1 **Common impedance to ground:** If two circuits are sharing the common ground as depicted in Figure 2.2 then currents flowing from one circuit to ground can couple with another circuit, which causes ground bounce.

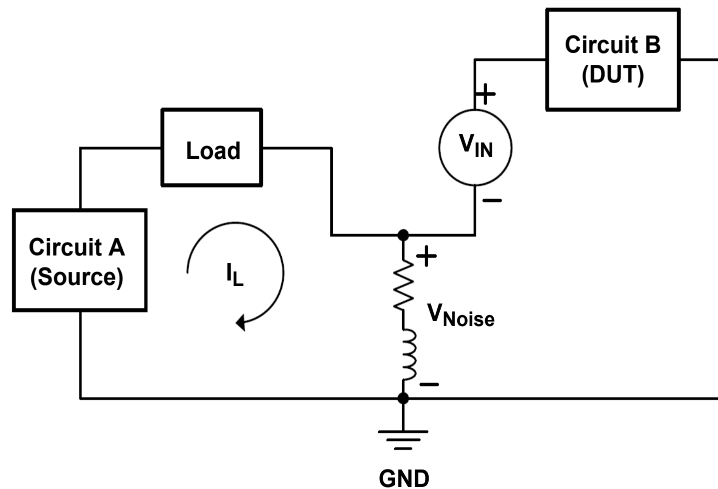

Figure 2.2: Common Impedance to Ground [4]

2 **Capacitive coupling:** Due to transient change in data and clock signals EMI can be generated inside a system that can couple capacitively with the neighboring circuits. As both circuits are capacitively coupled, some displacement currents are generated in circuit B as a result of the fast change in voltage in circuit A, which is shown in Figure 2.3.

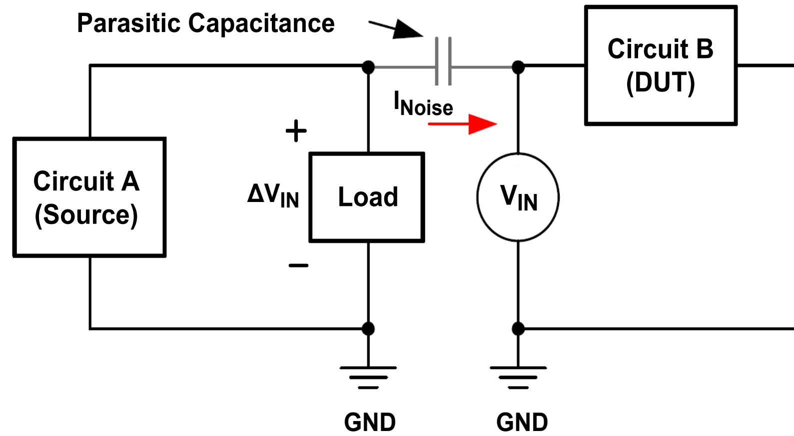

Figure 2.3: Capacitive Current Coupling [4]

3 **Inductive coupling:** Similar to capacitive coupling, two circuits that are inductively coupled can also create EMI, as voltage can be induced in circuit B because of the transient flow of current in circuit A, which is shown in Figure 2.4. This is called mutual inductance. Hence, it is important to design filtering and decoupling circuits at all interfaces and near to the sensitive devices because EMI interferences can be caused by both internal and external sources.

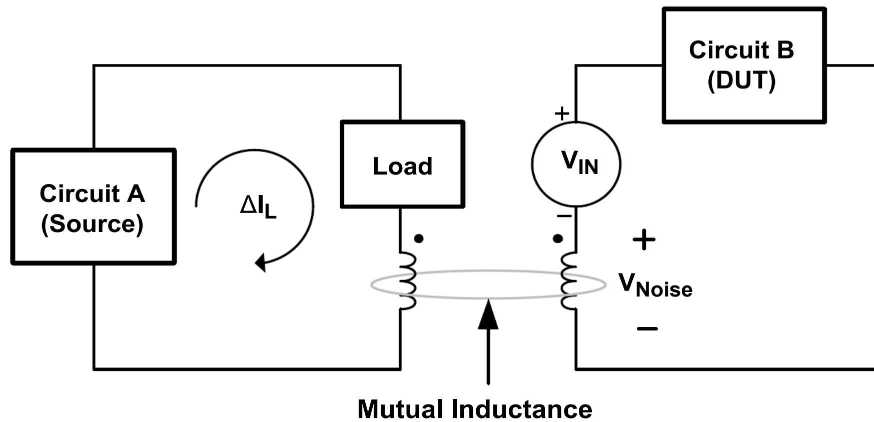

Figure 2.4: Inductive Voltage Coupling [4]

2.2 Related Work

Although a system is designed to be as immune to external noise effects as possible, sensitive analog circuits such as op-amps, converters, and regulators experience EMI

effects in the application. Since precision op-amps are mainly used on the analog front-end of the application, it makes more sense to evaluate how they react to EMI.

EMI Measurement Techniques

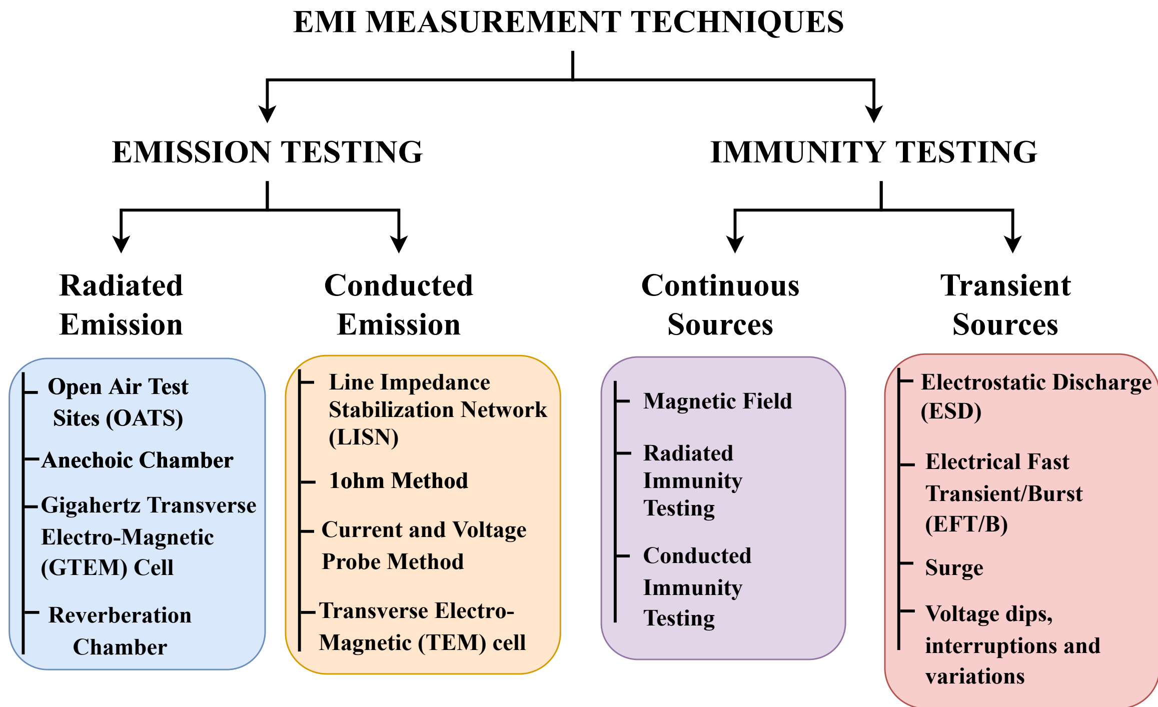

Figure 2.5: EMI Measurement Techniques [11]

There are many techniques to measure EMI that degrades electronic device performance. EMI testing is categorized into emission testing and immunity testing depending upon if the device is emitting EMI or suffering from EMI. So, these emitting EMI sources and subjected DUTs may be different systems, resulting in intersystem EMI, or they may be different sub-systems of a larger system, resulting in intra-system EMI.

Emission Testing

Emission testing is performed where the electronic instrument is acting as an EMI source intentionally or unintentionally and becoming the reason for electromagnetic pollution. In this type, the emitter is the DUT. The nature of the coupling medium is used to further characterize emission testing. Conducted emission testing is performed

when the coupling channel is conducting in nature and if the conducting medium is radiating in nature, then radiated emission testing is done. The EMI emissions may be conducted through the power cables or PCB traces in case of conducted emissions and antennas in case of radiated emissions. Hence, it is necessary to test such components to keep the electromagnetic environment clean and usable. The EMI effect of the coupling medium can be lowered by RF design guidelines while designing and routing the hardware test board, EMI shielding, and incorporating decoupling techniques [11].

(a) Power cables (b) Antenna

Figure 2.6: Examples of conducted and radiated emissions [12]

Some of the radiated emission testing methods such as Open-Air Test Sites (OATS), anechoic chamber, Gigahertz Transverse Electro-Magnetic (GTEM) cell, reverberation chamber illustrates the different kinds of testbeds for measurement setup to measure EMI emissions. Also, Line Impedance Stabilization Network (LISN), 1Ω method, current and voltage probe method, and Transverse Electro-Magnetic (TEM) cell methods are some of the popular conducted emission testing methods [13].

Immunity Testing

Immunity testing is exactly the opposite of emission testing, which is performed to quantify the EMI robustness of a DUT by subjecting it to an electromagnetically hostile environment and evaluating the performance of DUT for high-frequency EMI. If any change in the performance of the DUT is detected, then it is measured to quantify the immunity of the DUT for such EMI. Immunity testing is categorized into continuous source testing and transient source testing based on whether the EMI generating source is continuously affecting the electronic system or transiently. Some of the transient sources of EMI include lightning, EM pulses, Electrostatic Discharge (ESD), voltage fluctuations, and fast switching of relays. The tolerance of the electronic

systems for such transient effects can be measured by ESD test, electrical fast transient test, surge test, and by finding the voltage dips, interruptions, and variations as listed in Figure 2.5.

The objective of continuous immunity testing is to test whether the DUT will function in the desired manner when it is exposed to continuous noise sources such as signal generators, broadcast stations, magnetic fields, solar radiations, etc. These tests are carried out by continuously injecting the noise into the system to see how many high-frequency signals it can withstand and reject. This category of testing can be further classified into magnetic field immunity test, radiated immunity test, and conducted immunity test depending on the way coupling medium gets affected by EMI.

The magnetic field immunity testing and radiated immunity testing are briefly described below and the later part of this report is all about describing the conducted immunity testing method for amplifiers.

1 **Magnetic field immunity testing:**

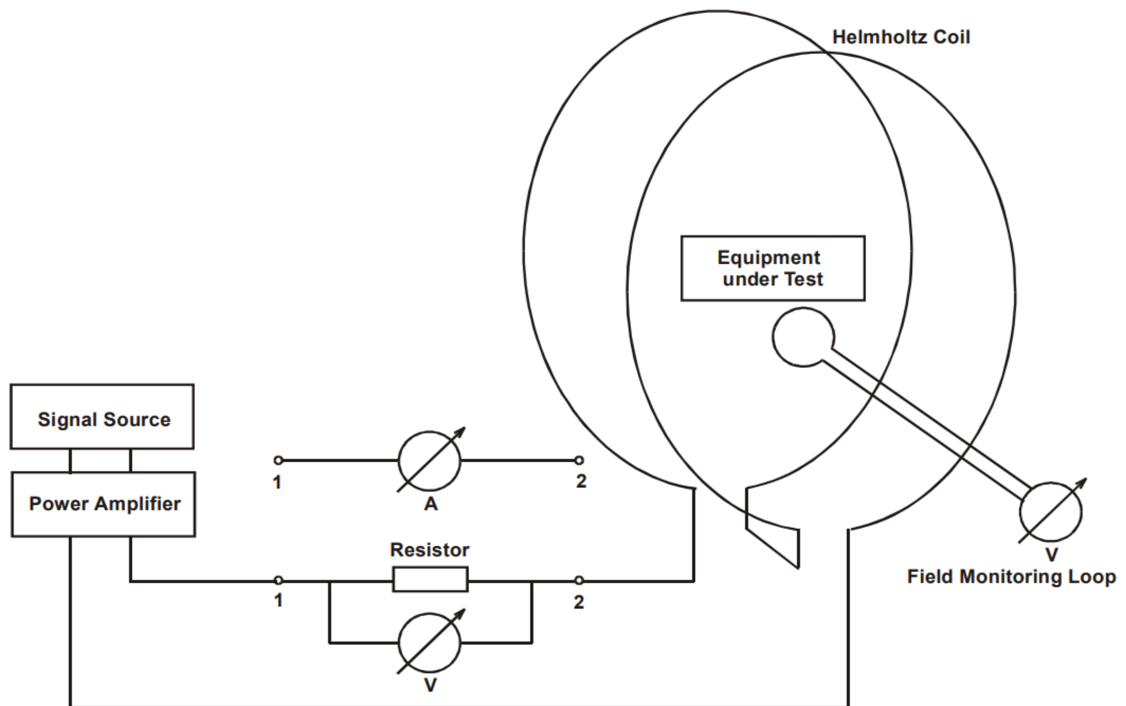

Figure 2.7: Test setup for immunity against magnetic fields using circular Helmholtz coils [14]

Magnetic fields are coupled by the cables and wires of an electrical instrument that can attack the components which are susceptible to magnetic fields such as amplifiers, relays, and monitors of the parent circuit and the instruments present nearby. Thus, it is necessary to ensure that the DUT can withstand such magnetic effects. The withstanding power of the device is measured using magnetic field immunity testing. The measurement setup consists of a signal source to generate RF signals and a power amplifier to amplify the generated signals. These are connected to circular Helmholtz coils which can establish uniform magnetic fields around DUT. The DUT is placed inside the coils and is subjected to a continuous magnetic field. A field monitoring loop along with the voltmeter is used to determine the magnetic field strength [13]. However, this method can be used only at lower frequencies of 10Hz to 100KHz.

2 **Radiated immunity testing:**

When a DUT is exposed to electromagnetic radiations, there are high chances that it is getting affected by the RF radiations if it is susceptible to EMI. Radiated Immunity (RI) tests are performed in anechoic chambers, OATS, GTEM cells, or reverberation chambers. Similar to the magnetic field immunity test setup, the RI test setup consists of an RF signal generator to continuously generate RF signals that are amplified by the power amplifier, an antenna that acts as a transmitter of the generated signals to the cell or chamber that creates a uniform electromagnetic environment [11]. The setup also has a field sensor, which monitors magnetic field strength inside the chamber, and a monitoring system to monitor DUT. The performance of the DUT is repeatedly evaluated by placing it to face towards the antenna by providing different frequencies with different signal strengths. A block diagram of radiated immunity testing is illustrated in Figure 2.8.

However, in 2009, Armstrong has pointed out some issues in RI testing regarding reliability test levels, angle of incidence, the polarization of the field within the cell/chamber and, the sensitivity of DUT towards certain frequencies [11]. Hence he claimed that RI testing might not be sufficient in the real-world scenario to quantify the immunity of the DUT.

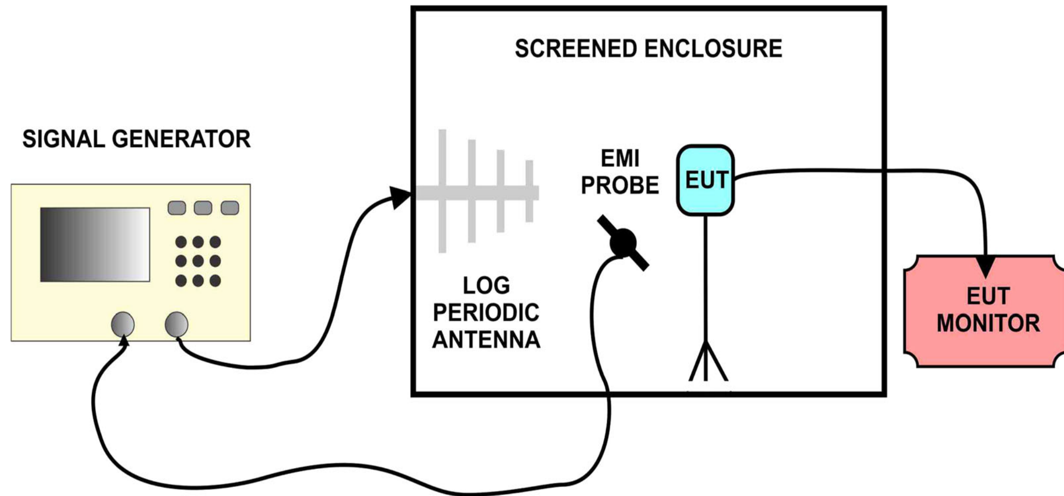

Figure 2.8: Measurement setup for EMI radiated immunity testing [11]

As discussed, the magnetic field immunity testing method is only applicable for lower frequency applications and radiated field immunity testing method has got some drawbacks and is not sufficient to measure the EMI performance of the DUT. Hence, we need an RF immunity testing method that can overcome these drawbacks. In the research methodology, conducted immunity testing method will be explained in detail, particularly with the application of precision amplifiers that are highly susceptible to RF interferences [1]. The immunity of these precision amplifiers is quantified into a figure of merit – EMIRR. This type of immunity test is practical, accurate, reliable, and will work for a broad range of frequencies from 10MHz to 10GHz. However, with the existing signal generator ranging from 10MHz to 3GHz, the immunity testing is performed for the range of 10MHz to 3GHz.

2.3 Research Methodology

2.3.1 Built-in EMI Filtering in Amplifiers

There is a continuous effort to improve the EMI robustness of op-amps. One of the solutions to reduce the EMI susceptibility of amplifiers was to design an integrated low pass filter in an amplifier that can attenuate the amplitude of RF signals at higher frequencies. There are multiple RF injection points in op-amp such as input, output, and supply pins. However, input pins are more susceptible to EMI compared to output and supply pins since they sense every signal that enters the amplifier. Therefore,

an EMI filter is designed at the input stage of an amplifier. Figure 2.9 depicts two input stages of an amplifier with two MOSFETs (M1 and M2) connected to the load resistors (ZL1 and ZL2 respectively). A low-pass filter is formed at inverting (VINV) and non-inverting (VNINV) inputs of the amplifier by two resistors (R – highlighted with red box) connected in series with input differential pair junction capacitances of an amplifier [10]. Since the common mode and differential capacitances are present in the input differential terminals of an amplifier, the inbuilt EMI filter is efficient in attenuating high frequency EMI.

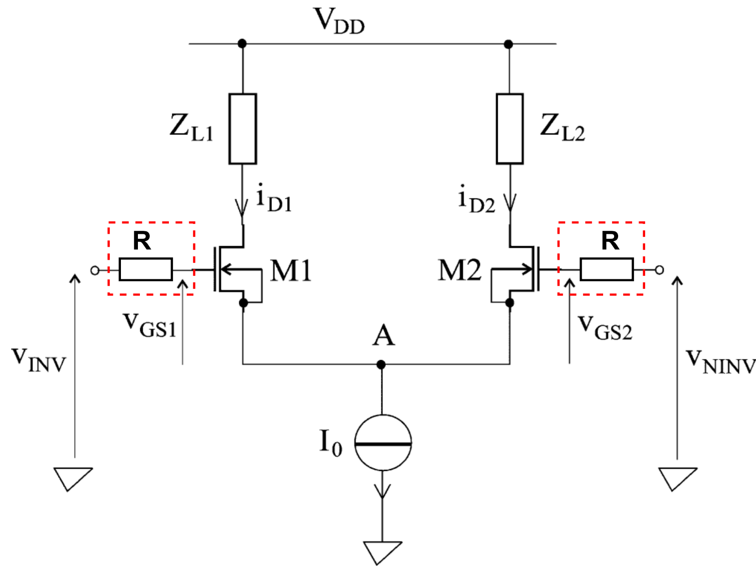

Figure 2.9: nMos differential input stage with input resistors [15]

The unity-gain bandwidth of the op-amp is commonly ranging from a few kHz to a few MHz, so the low pass filter cut-off frequency is well above it. That prevents the EMI filter from becoming a factor in the op-amp's normal AC response. However, the cut-off frequency of the low-pass filter is low enough to be effective in the filtering of 100MHz and higher frequencies. The series resistances (denoted with R) are chosen to determine the cut-off frequency of the EMI filter, but they should have lower value so that the low noise performance of the amplifier is not affected.

2.3.2 Calculating EMIRR

EMIRR is a logarithmic ratio of RF Peak Voltage (EMI signal injected to any of the op-amp terminals) input to the shift in DC offset voltage at the output of the amplifier.

Similar to CMRR and Power Supply Rejection Ratio (PSRR) parameters of the op-amp, EMIRR is also expressed in decibels (dB). The higher the value of EMIRR, the better is the rejection ratio which means the amplifier has higher immunity to EMI. EMIRR is calculated by equation (1).

For EMIRR calculation, a standard test condition of 100mVp is used.

$$EMIRR[dB] = 20 \cdot \log\left(\frac{V_{RF_PEAK}}{|\Delta Vos|}\right) + 20 \cdot \log\left(\frac{V_{RF_PEAK}}{100mV_p}\right) \tag{1}$$

Where,

V_{RF_PEAK} is the peak-amplitude of the applied RF voltage

ΔVos is the shift in DC offset voltage

$20 \cdot \log\left(\frac{V_{RF_PEAK}}{100mV_p}\right)$ term refers to the EMIRR to an input signal of $100mVp$

$$\Delta V_{OS} = \left(\frac{V_{RF_PEAK}}{100mV_p}\right) \cdot 10^{-\left(\frac{EMIRR[dB]}{20}\right)} \tag{2}$$

2.3.3 Conducted EMI Measurement Technique in Op-amps

Impedance matching

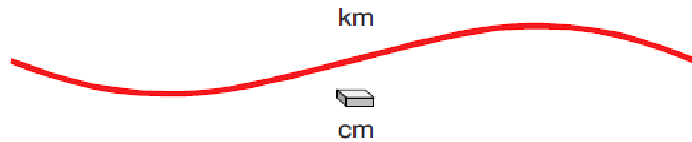

Figure 2.10: Lumped circuit model [4]

There are several circuit models to describe the circuit behavior, which include lumped and distributed circuit models. If the voltages and currents are uniform throughout the conductors, then that's a lumped circuit model, but the distributed circuit model may be depicted as a transmission line with variable voltage and current levels along the conductor as shown in Figure 2.11. The distributed circuit models are better for high-frequency applications as the impedance is distributed continuously throughout the material of the conductor.

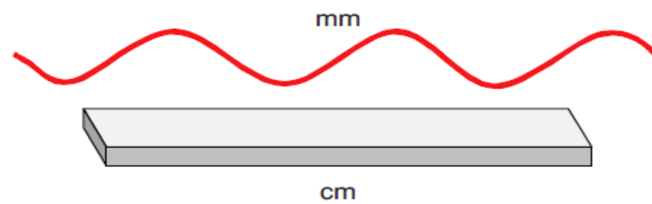

Figure 2.11: Distributed circuit model [4]

Impedance matching is the biggest challenge when working with RF systems. Change in the impedance at the interfaces will cause signal reflections which are proportional to the impedance mismatch. This concept is demonstrated in Figure 2.12. As a result of these signal losses, the intended magnitude of the voltage or current signal does not reach the amplifier input pins which might be the reason for incorrect measurements [4]. So, care must be taken to avoid such signal reflections.

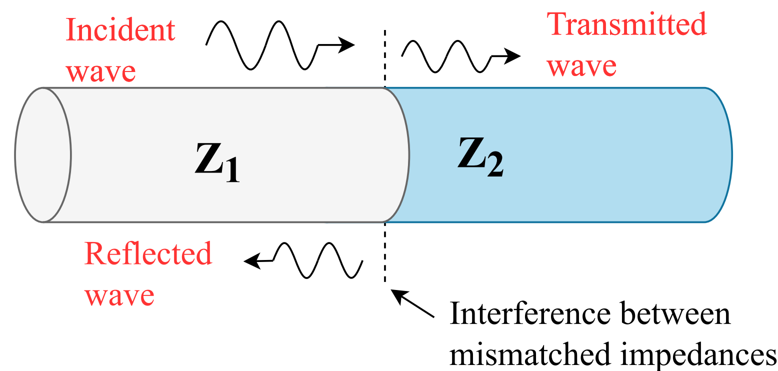

Figure 2.12: Impedance Mismatch Causes Voltage and Current Reflections [4]

Applying RF signal to EMIRR setup

To measure EMIRR, a high-frequency signal source that can generate and control the frequency and magnitude of RF signal is needed. This is a continuous conduction immunity testing, which means the RF interference/noise is injected into the op-amp through conduction and the measurement is carried out. The generated RF signal travels through the cable to a terminal of the bias tee, and then to the op-amp input via SMA connector and PCB trace. However, due to impedance mismatches, there will be signal reflections along this path. This RF path and the transmission line model are illustrated in Figure 2.13 and Figure 2.14 respectively.

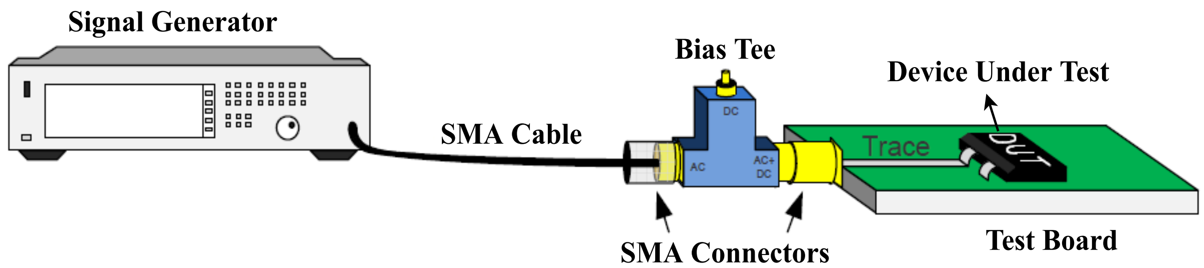

Figure 2.13: RF Input Signal Path for Measuring EMIRR [4]

The voltage reflections can be reduced by designing the entire RF signal path to 50 Ω to match the system impedance which is also 50 Ω. Nevertheless, op-amp has a high input impedance which will not be matched to 50 Ω impedance, and at higher frequencies, this will even change due to parasitic reactance in the op-amp input stage. Hence, it is difficult to match impedances consistently throughout the bandwidth of measurement. A VNA can be used to capture the reflection coefficients that can be compensated while calculating the EMIRR.

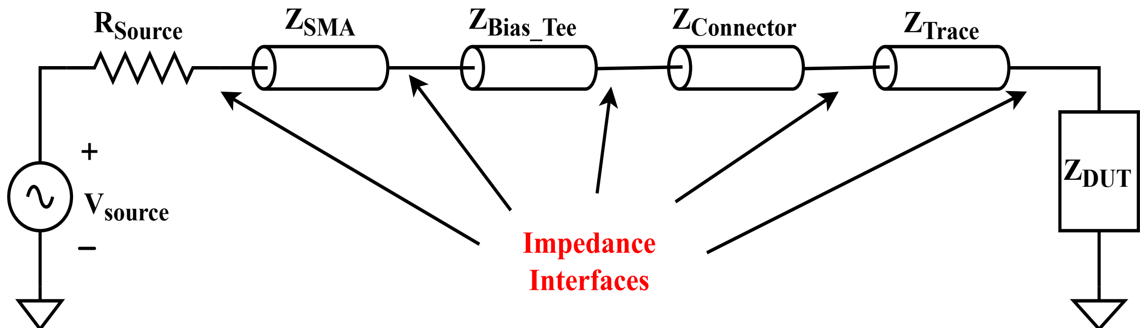

Figure 2.14: Complex RF Input Environment [4]

EMIRR test configuration and measurement procedure

The overall test circuit configuration of EMIRR is demonstrated in Figure 2.15 after the RF reflection coefficients have been measured from Vector Network Analyzer (VNA). The test setup consists of the signal generator connected to the non-inverting input of op-amp via a 50 Ω transmission path. The op-amp circuit is in buffer configuration (gain = 1). The output of the op-amp is connected to a low pass filter to attenuate the residual RF signal, which avoids aliasing effect by band limiting the

input RF signals. Then a DMM is connected to display DC offset voltages during the EMIRR measurement.

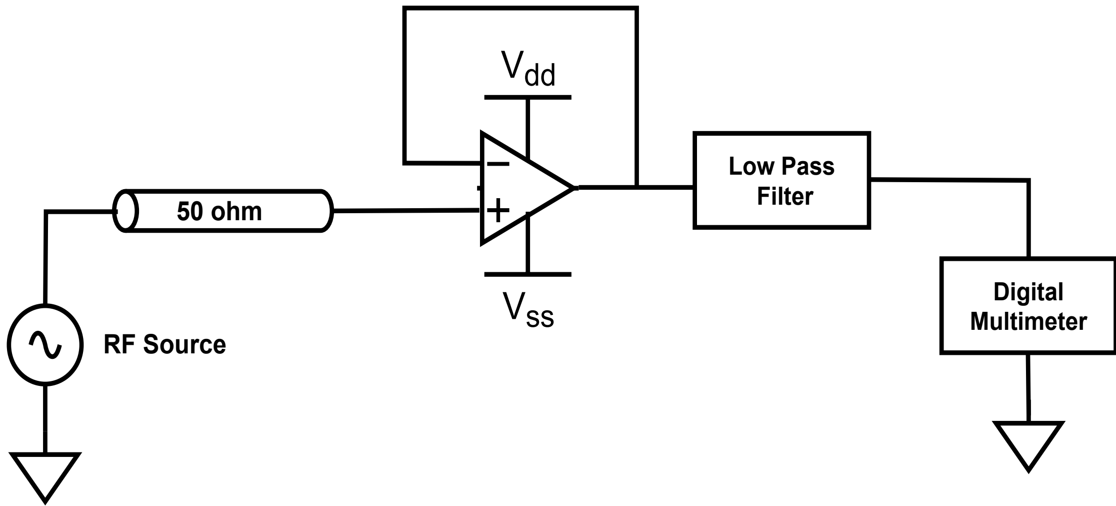

Figure 2.15: Complete EMIRR Test Circuit Configuration [4]

The following procedure can be used to measure the DC offset voltage shift and to calculate the EMIRR.

Step 1 Measure the output voltage (VOUT1) from DMM when the RF signal from the signal source is OFF.

Step 2 Then switch on the RF signal and measure the output voltage again (VOUT2).

Step 3 Convert the measured output voltages to input-referred voltages by dividing them with amplifier gain.

Step 4 Subtract the input-referred voltages and take the absolute value of the DC offset voltage shift.

Step 5 Calculate the EMIRR with equation (1).

If any offset voltage is present at the output of the op-amp before applying the RF signals, it should not be included in the EMIRR calculations. To remove this small DC offset voltage, two separate measurements are taken i.e., First measurement when the RF source is turned OFF and then second when the RF source is turned ON. The subtracted DC offset voltage shift value from these two measurements will give the

amount of DC offset generated after DC rectification of the injected RF signals. This measurement procedure is repeated for all the frequencies from 10 MHz to 3 GHz for which the EMIRR is assessed.

2.4 Chapter Summary

This chapter describes the theoretical background of EMI and the basic elements necessary for EMI to exist. As part of the related work, several techniques of EMI measurement are investigated, and two EMI immunity testing approaches such as magnetic field immunity testing and radiated immunity testing, are briefly explained. Some of the research questions that occurred while researching are posed in research questions, which will be addressed in the report's results and discussions section. Finally, the research methodology outlines a practical and more precise method of measuring EMI in amplifiers.

As part of the research methodology, how amplifiers are made EMI robust is examined. The metric EMIRR, which is a figure of merit that quantifies the immunity of op-amps to EMI signals, is defined. Additionally, the importance of RF considerations in matching system impedance is then demonstrated. Finally, how to apply an RF signal to the non-inverting input of op-amp and how to quantify EMIRR in op-amps are discussed, along with the test configuration. Overall, when compared to the other two EMI measurement approaches, the EMIRR method offers benefits such as precision, reliability, and it works well across a wide frequency range.

3 EMIRR Test Setup Correlation

3.1 Required Hardware Instruments

The following instruments are required to build the hardware test setup to measure EMIRR. Each instrument is accompanied by an example model that is used in the setup.

1 Vector Network Analyzer (VNA)

VNA is required to measure network parameters, specifically Scattering parameters (S-parameters) at higher frequencies. Generally, in signal integrity checks, 1-port or 2-port VNAs are used. 1 port VNA calibration needs three known standards such as open, short, and load whereas 2 port VNA requires four standards SOLT (Short, Open, Load, and Through). The goal of VNA is to extract the signal reflection data (S-parameters) of the transmission lines/PCB traces, before starting the EMIRR measurement. The collected data can be compensated while computing the EMIRR in the test software. So, HP 8753D two-port network analyzer with a frequency range from 30kHz to 6GHz is used in the EMIRR setup.

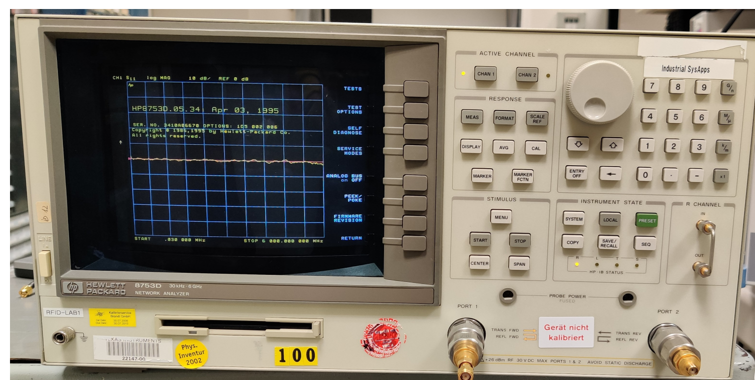

Figure 3.1: Vector Network Analyzer

2 RF signal source

Signal generator is connected to the amplifier's pin under test through bias tee used to generate the high-frequency RF interference which can be injected into the amplifier to see the rejection ability of an amplifier. In the current setup, RSSMA100 from Rhode and Schwarz is used that can generate signals from 100kHz to 3 GHz frequencies. However, EMIRR can be measured for even higher frequencies when the high configuration (up to 10GHz) signal generator is available.

Figure 3.2: RF signal source

3 Bias tee

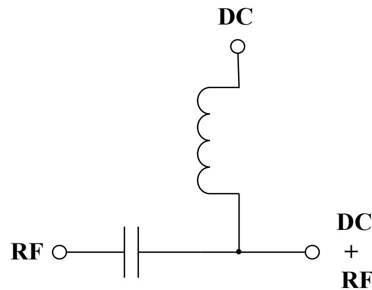

Figure 3.3: Bias Tee Circuit Model [4]

When working with RF systems, it is important to bias an amplifier to a with a dc common-mode voltage midway between the positive and negative power supply rails (0V in this case) before the signals from the RF source are sent to op-amp input. This method is a standard way of biasing an op-amp to operate linearly and avoid op-amp saturation [4]. The RF and DC signals require isolated

sources, to avoid signal interference and save the op-amp from the over-voltage state. Hence, a bias tee is used to separate RF and DC signals from causing the interference.

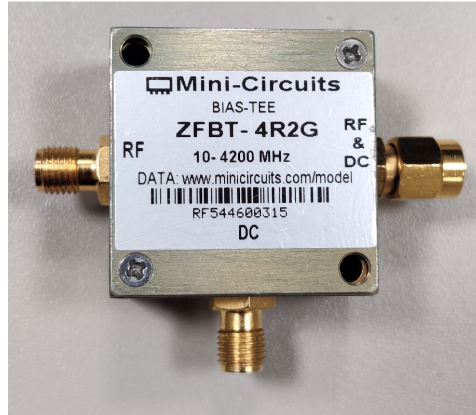

Figure 3.4: Bias Tee Circuit Model [4]

The bias tee is a three-terminal device with two input terminals for DC and RF signals and one output terminal to provide the superimposed DC and RF signal. The bias tee is designed with a large capacitor and an inductor as displayed in Figure 3.4. The capacitor only allows AC (RF) signals but does not allow the DC signals through port 1 and the inductor blocks the RF signal from getting through port 2 and allows all DC signals. Both RF and DC are then coupled up and passed through port 3 to op-amp input with minimal loss. The impedance of the bias tee is 50 Ω, which is suitable for impedance matching as well.

4 Dual-channel DC power supply

Figure 3.5: E3631A DC power supply

To power the amplifiers, a dudal channel DC power supply is used in the test setup. In the EMIRR setup, both the channels of the power supply are used. The first channel is used to supply DC bias voltage to the bias tee to bias the

amplifier and the second channel is used to supply positive and negative voltages to the amplifier. E3631A from Keysight is used in the test setup to serve this purpose.

5 Low pass filter

Figure 3.6: TTE 8th order low pass filter

Although the amplifier rejects the high-frequency RF interferences, some residual RF signals might pass through the feedback path or the path created by parasitics. Thus, a passive LPF placed at the output of the DUT helps in attenuating the residual RF signal to avoiding aliasing effect at the DMM by band limiting the input RF signals.

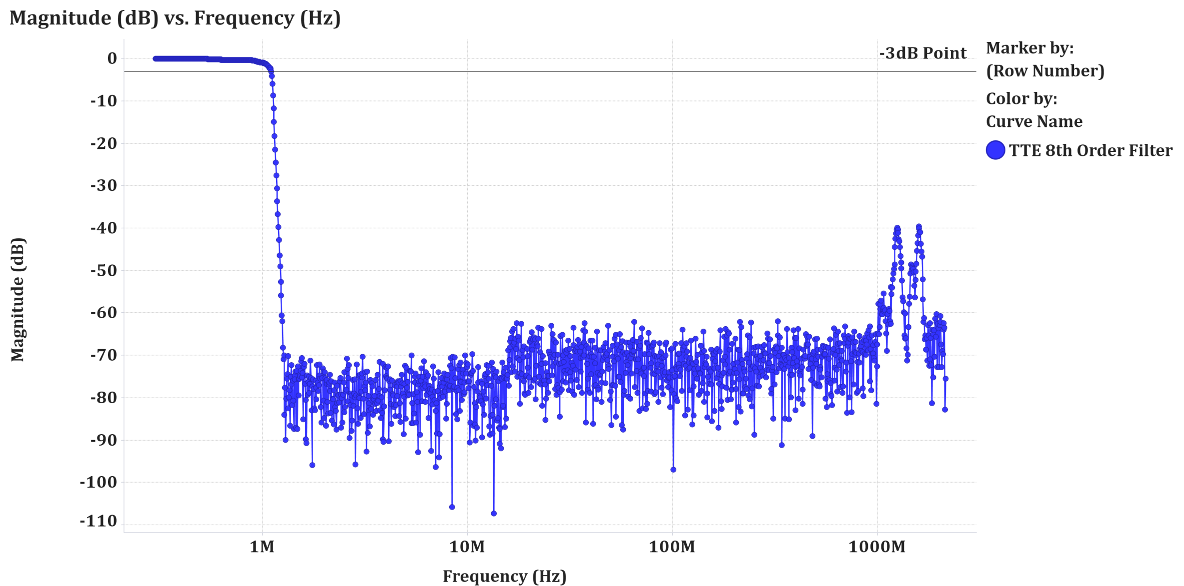

Figure 3.7: Frequency response of 8th order passive low pass filter

The cut-off frequency of the 8th order passive LPF used in the setup is 1MHz which is shown in the frequency response curve (Figure 3.7) of this filter. So, it attenuates the high-frequency RF residuals above 1MHz.

6 Digital multimeter

Figure 3.8: 34410A Digital Multimeter

A high-resolution DMM is connected to the output SMA of the test board (output of the amplifier) through LPF to provide the small DC offset voltage shift generated when the amplifier is subjected to RF interferences. In the current EMIRR setup, 34410A - 6½ digit DMM from Keysight is used.

7 Spectrum analyzer

To analyze the RF signal amplitude reaching the input of the amplifier, a spectrum analyzer can be used. When the DUT is not mounted, it can also be used to check for signal leakage at the output. R&S FSP spectrum analyzer with the frequency range 9kHz to 7GHz is used in the EMIRR setup.

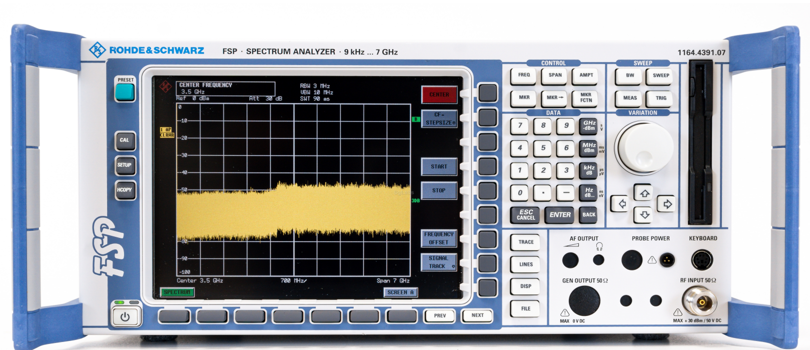

Figure 3.9: Spectrum Analyzer

3.2 Analyzing the Existing Op-amp Hardware Test Setup

All the instruments briefed above are commonly used in op-amp and INA test setups. Hence, the EMIRR measurement setup for op-amps and INAs is similar except for the hardware evaluation board part because of the difference in the device architectures. The existing hardware test board is analyzed for its design and signal reflections due to impedance mismatch. The evaluation board design can be made better by having the 50 Ω termination at the end of the RF input trace to minimise signal reflections. This helps the conducted RF input signal to reach the input of the amplifier whose immunity for RFI is evaluated. Therefore, along with this design change, some of the RF guidelines are followed while designing the INA test board for EMIRR setup. These RF guidelines are chosen from the International Standard IEC 61000-4-6 and are discussed in the next section. This is to ensure that the EMIRR test setup environment is not influencing the EMIRR results.

3.3 Hardware Test Board Design for INAs

3.3.1 Applying RF Input to INAs

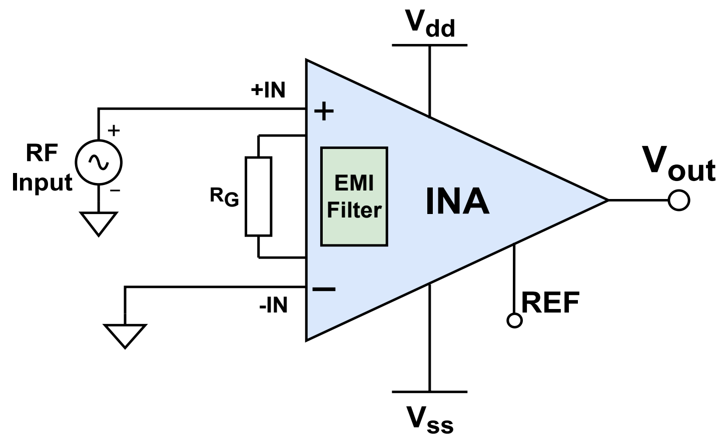

Figure 3.10: Differential mode RF input to INA

As amplifiers come in various packages such as SOIC-8 with Burr-Brown (BB) pinout and SOIC-8 with Analog Devices, Inc. (ADI) pinout, the design and layout of the PCB board become different from one another. INAs are tested for EMI by injecting the RF

signal in both differential and common-mode. So, now let us see the generic circuits to apply a differential or common-mode RF signal to the inputs of an INA, which are depicted in Figure 3.10 and Figure 3.11 respectively.

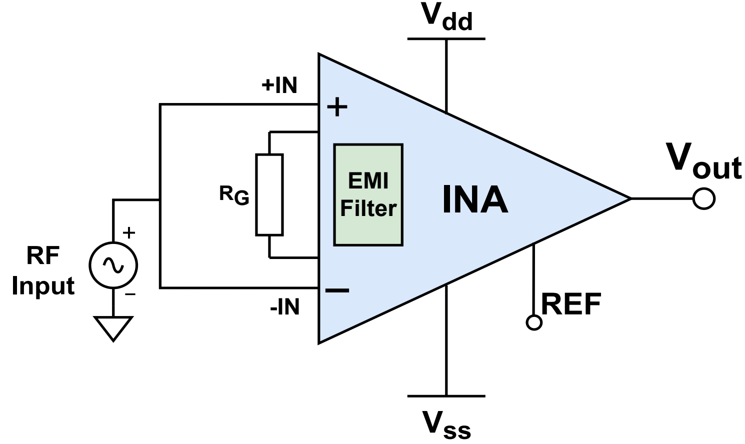

Figure 3.11: Common mode RF input to INA

In differential mode measurement, the RF signal is fed to the non-inverting input of INA while the inverting input is grounded and in common mode measurement, the RF signal is injected in both the inputs simultaneously. The common-mode capacitance (C_{CM}) at each input terminal along with the a differential capacitance (C_D) between both the input terminals constitutes the input capacitance of an INA which is shown in the Figure 3.12. The EMI filter bandwidth is determined by using (C_D) in differential mode measurement and (C_{CM}) in common mode measurement. Hence, the cut-off frequency of the EMI filter is expected to be influenced by the INA's input capacitance value in both the measurements.

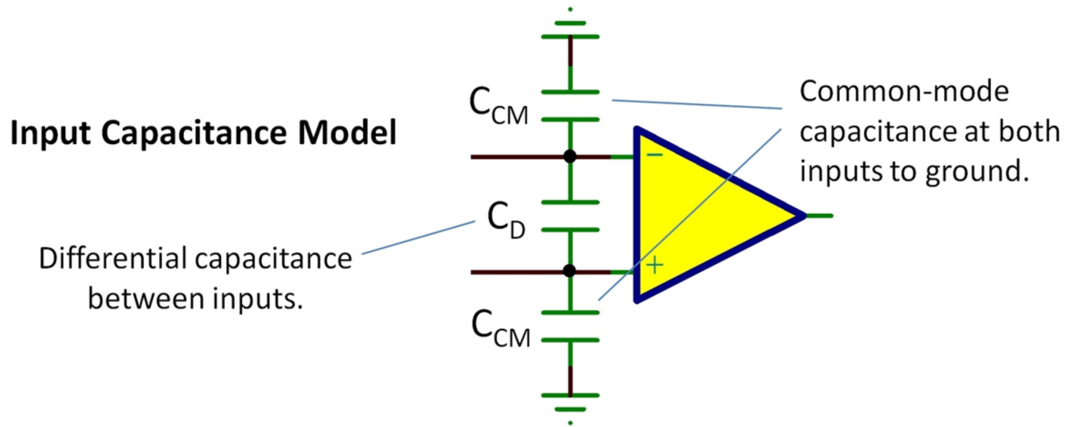

Figure 3.12: Input Capacitance Model [16]

3.3.2 Design of Evaluation Boards

Schematics of the test boards

The schematics of EMIRR test board for INA are shown for differential mode measurement and common mode measurement. In the differential mode circuit shown in Figure 3.13, U1 is an INA with BB pinout. R4 is the gain resistor to set the required gain to the circuit. R5, R6, and R7 are the 50Ω termination resistors placed near non-inverting, reference, and inverting inputs of the INA respectively. R1 with C17 forms a low pass filter on the output trace which is designed for debugging purposes. All the capacitors in the schematic are decoupling capacitors chosen with lower ESR values. The common-mode circuit shown in Figure 3.14 also has similar circuitry except for the input stage where the input RF signals are applied in common-mode.

Test boards to measure EMIRR

RF-compatible PCBs require careful design and routing to maintain signal integrity. The routing style should be chosen in such a way that it provides noise isolation. The test board and the layout were created in Altium Designer software. The test board designed for the INAs with SOIC-8 BB pinout is shown in Figure 3.15. To test the EMIRR of INAs which come with SOIC-8 ADI pinout, another test board is developed which is shown in Figure 3.16. The test board with BB pinout is designed for dual in-line packages and the test board with ADI pinout is designed for SMT packages to investigate whether the EMIRR measurement results differ due to the intervention of coupon boards used in the case of the test board with BB pinout.

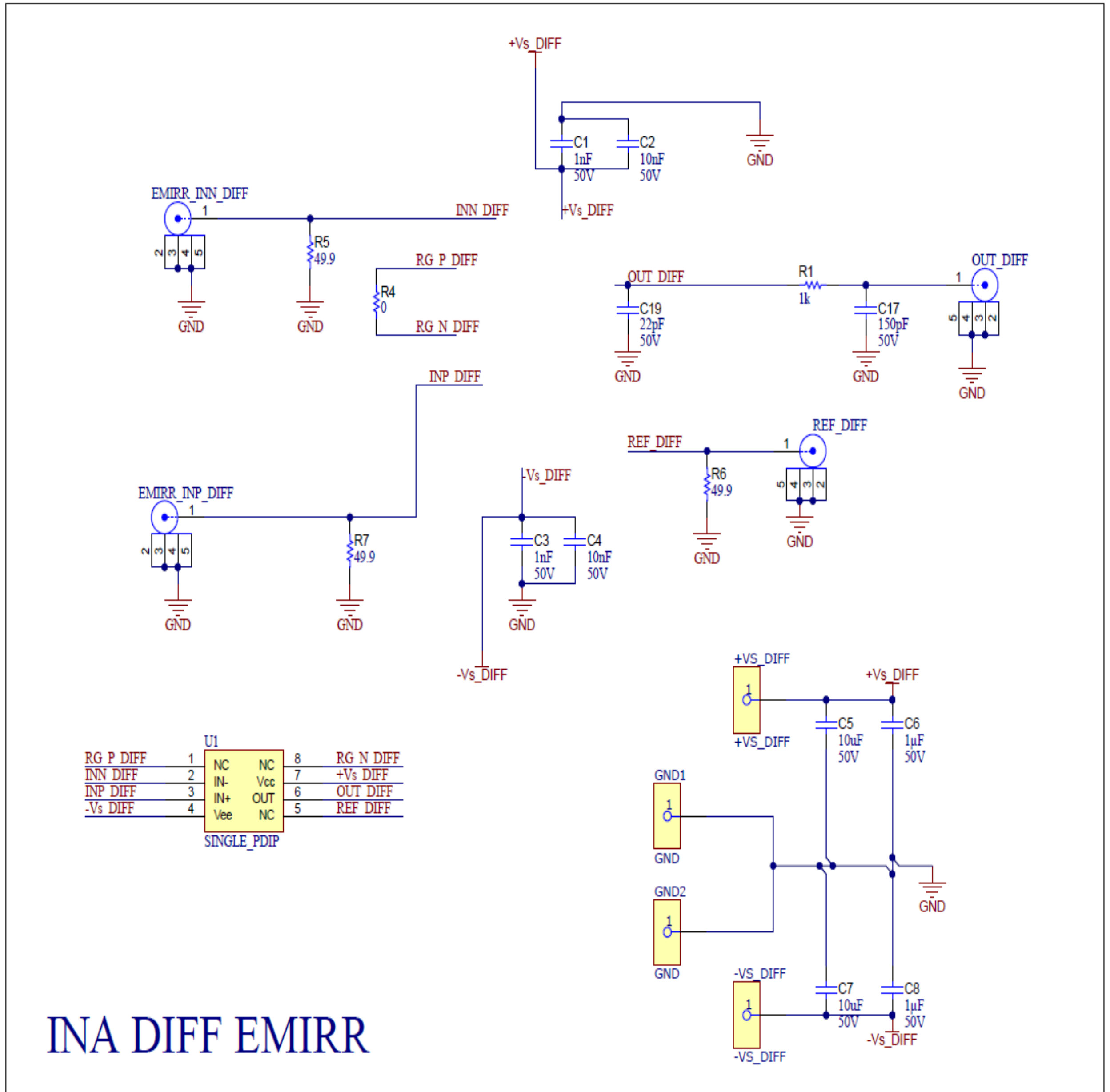

Figure 3.13: Schematic of INA for differential mode EMIRR measurement

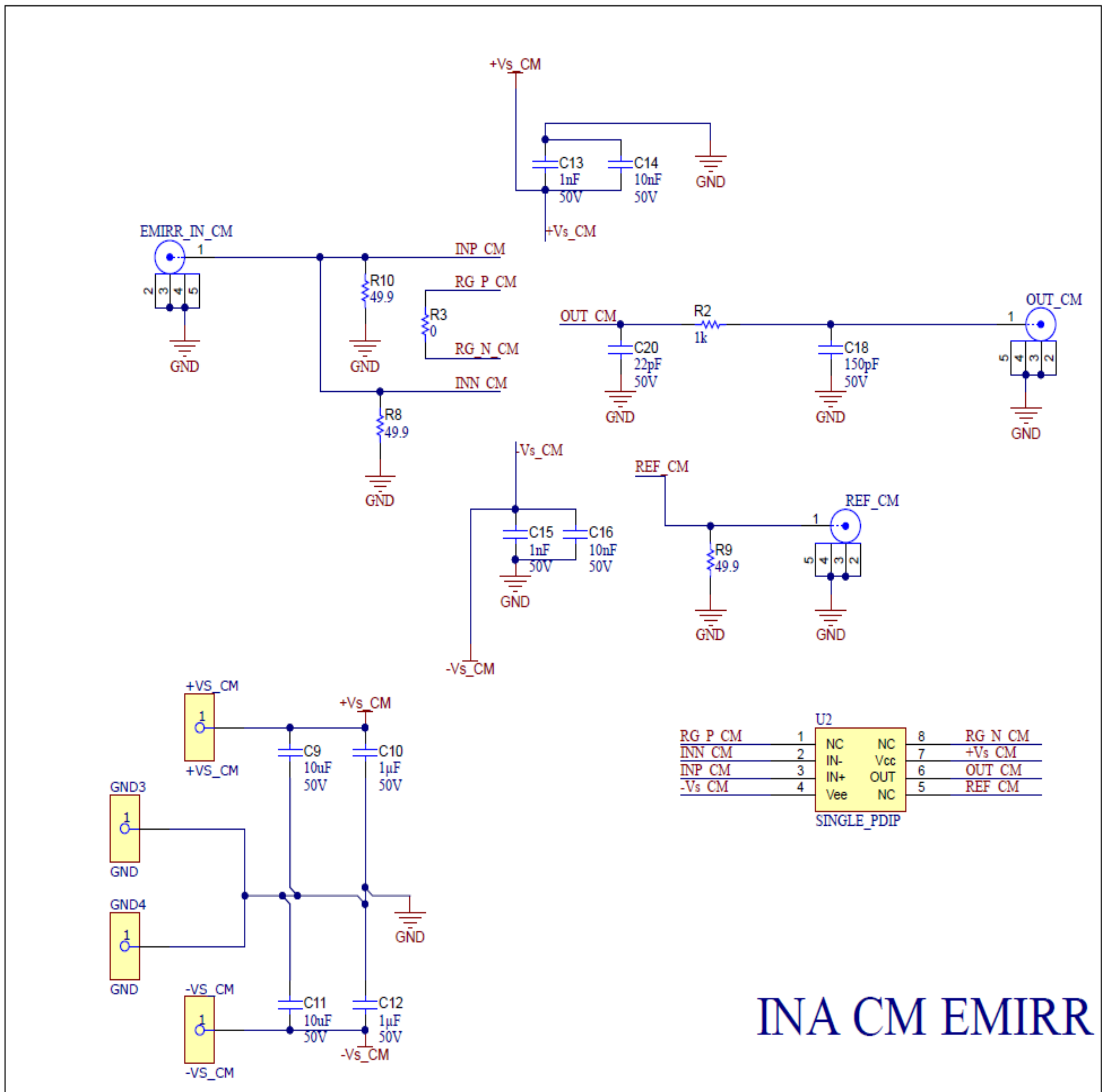

Figure 3.14: Schematic of INA for common mode EMIRR measurement

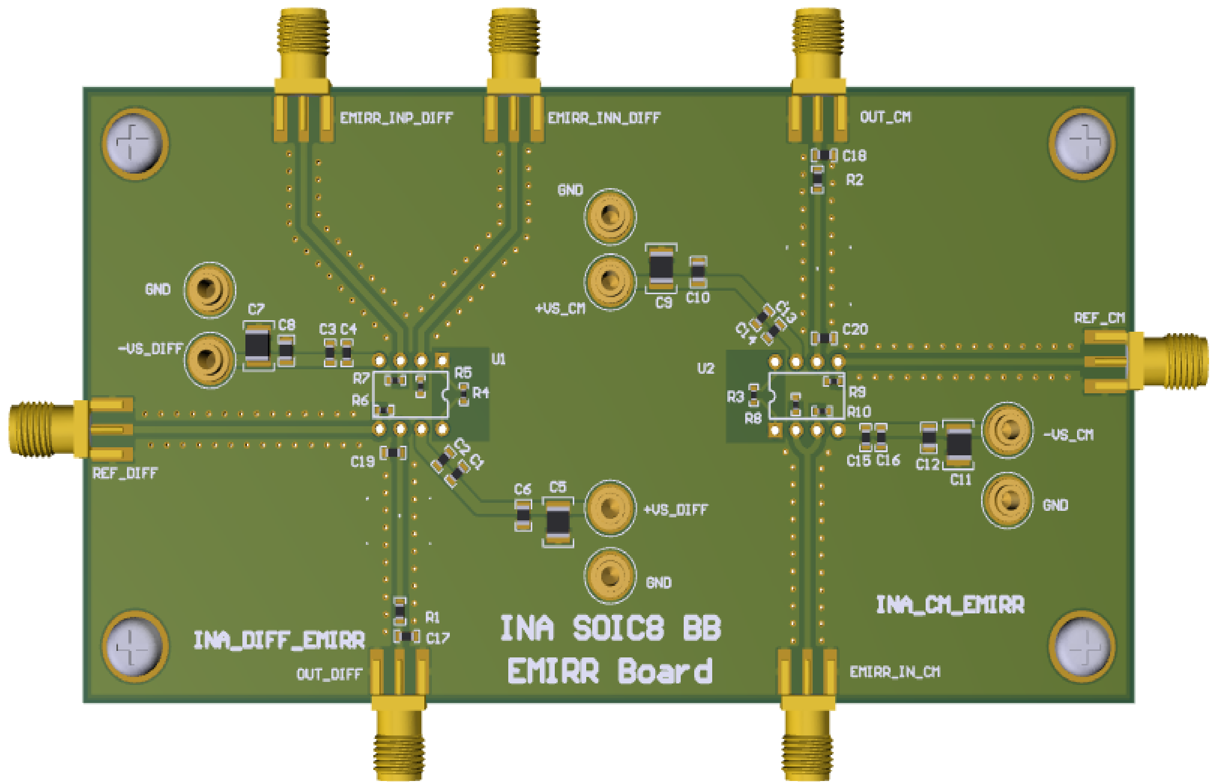

Figure 3.15: INA SOIC8 EMIRR Test Board with Burr-Brown Pinout

Both the test boards are designed symmetrical and accommodate differential-mode and common-mode circuits on them with no common connections. This enables the tester to carry out EMIRR measurements in both differential and common modes simultaneously. These test boards are four-layer boards with a signal layer on top and a ground layer on the first internal plane. The second internal plane and the bottom layer are positive and negative power supply planes respectively. The layer spacing, FR-4 permittivity, and overall thickness of the board are known and can be controlled. Furthermore, inverting terminal and reference pin of the INA can also be tested as they are connected with the SMA adapters through which RF can be injected. A passive RC filter and vertical SMA SMT connector are provided the output path of INA for debugging purposes.

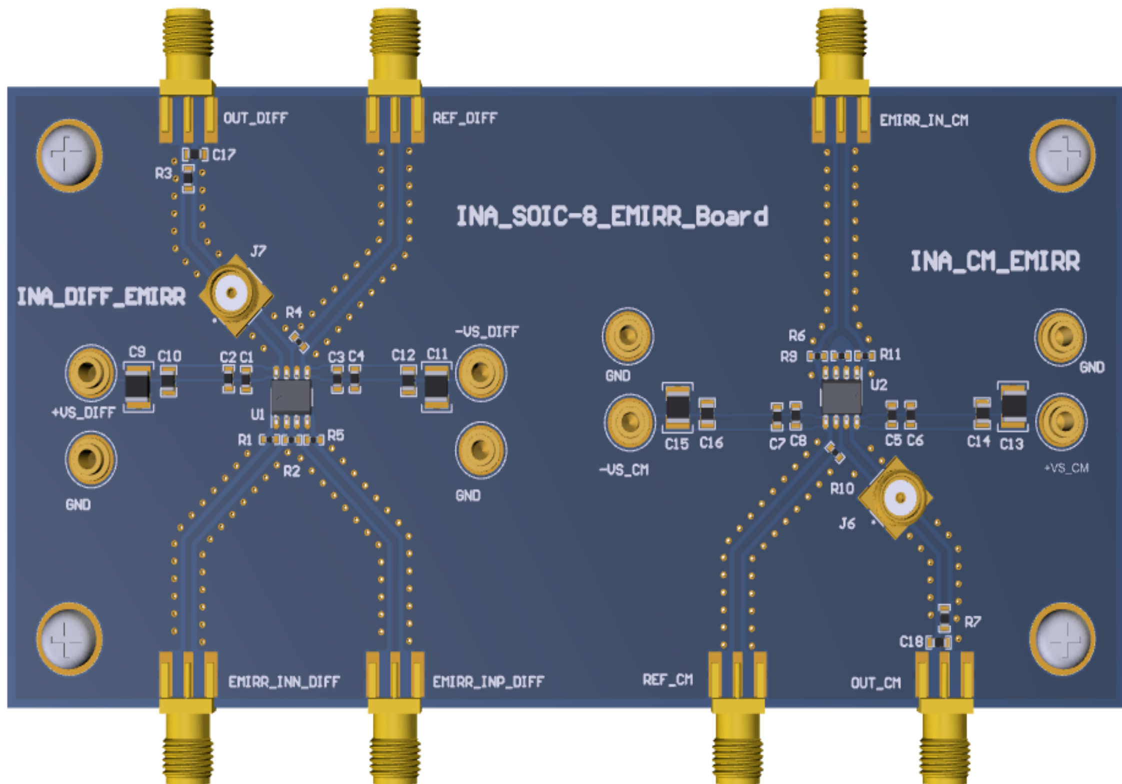

Figure 3.16: INA SOIC8 EMIRR Test Board with ADI Pinout

3.3.3 RF Design Guidelines that are Considered

Designing an RF test board to measure EMIRR is easy if the EM complaint rules are being considered before starting the PCB design. Some of the RF guidelines that are followed for the design are explained briefly.

1. Transmission line impedance

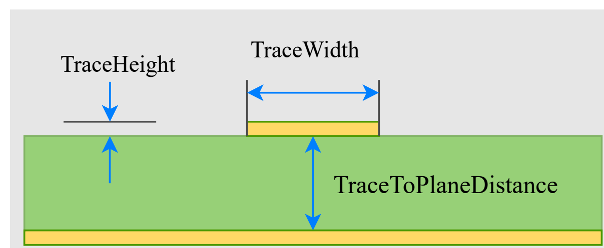

Figure 3.17: Impedance Calculation for Microstrip trace [19]

As PCB traces are significantly longer than the amplifier's size, they might behave as effective EMI antennas at higher frequencies (MHz to GHz range). Thus, PCB

traces should be designed carefully to avoid noise pickup. To, match the impedance of the trace with the impedance of the test setup, the traces are symmetrically designed with a 50 Ω impedance-controlled microstrip trace in Altium Designer. In Figure 3.17, TraceWidth, TraceHeight, and TraceToPlaneDistance are the parameters indicating length of the trace (yellow colored), thickness of the trace, and distance between the trace and polygon pour on the top layer respectively. The CharacteristicImpedance of the trace is calculated by the equation [19]:

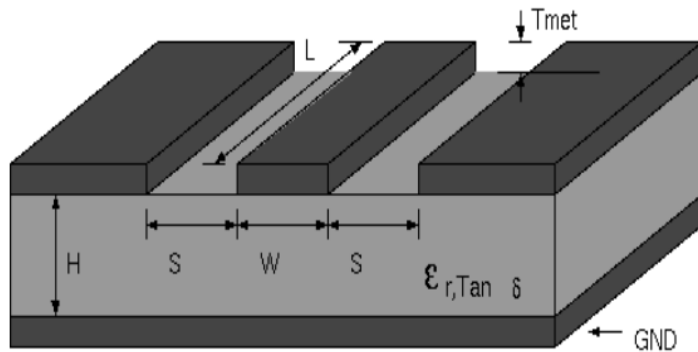

Metal width (W)	28.849	mil	calc
Metal spacing (S)	25	mil	calc
Trace length (L)	1260.17	mil	
Metal thickness (Tmet)	1.4	mil	
Metal resistivity (RHO)	3e-08	Ohm - m	
Metal surface roughness (RGH)	0.001	mil -rms	
Substrate thickness (H)	20	mil	calc
Substrate relative dielectric constant (Er)	4.8		calc
Substrate loss tangent (tand)	0.01		
Frequency	900	MHz	
Analyze Reset	☑	Include bottom side ground	
Characteristic Impedance	55.5271	[ohms]	
Electrical Length	63.9659	[degrees]	

Figure 3.18: Coplanar waveguide analysis [20]

$$CharacteristicImpedance = (60/SQRT(Er*(1-EXP(-1.55*(0.00002+TraceToPlaneDistance)/TraceToPlaneDistance))))*LN(5.98*TraceToPlaneDistance/(0.8*TraceWidth+TraceHeight))$$

As we need to calculate the trace width, the equation is solved for TraceWidth as shown below [19]:

$$TraceWidth = ((5.98 * TraceToPlaneDistance)/EXP(CharacteristicImpedance /(60/SQRT(Er * (1 - EXP(-1.55 * (0.00002 + TraceToPlaneDistance)/ TraceToPlaneDistance))))) - TraceHeight)/0.8$$

After calculating the TraceWidth from the Altium tool to match the 50 Ω impedance, it is also verified in coplanar waveguide calculator as shown in Figure 3.18. By filling in all the fields, the characteristic impedance can be calculated. However, highlighted fields must be filled as they are the main parameters to compute the impedance of the PCB trace. As expected, the the impedance of the trace is around 55 Ω for both the boards.

2. Ground shielding across the traces

The unintended noise signals are picked up by the dielectric material on PCB. The effect of return currents induced on the signal layer can be coupled to the ground through via fencing around the traces. Thus, ground shielding helps to prevent cross-coupling of RF signals with signal lines across the PCB. Via fencing is advised on both sides of the Microstrip line to reduce noise impact on the conducting trace. When it comes to rejecting high-frequency noise, the distance between the via holes is important. When the via holes are placed close together, they function similarly to a coplanar waveguide below the cutoff frequency. As a result, the shorter the distance between via holes, the greater the high-frequency noise rejection.

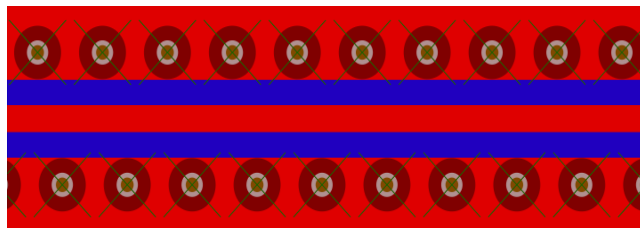

Figure 3.19: Via shielding around the PCB trace

3. 50 Ω termination at the end of RF transmission line

From the RF signal source to the evaluation board, coaxial cables with a 50 Ω impedance are used. As a result, the coaxial cable along with the microstrip trace on the test board serves as a transmission line between the RF source and the DUT. The 50 Ω termination at the end of the transmission line, acts as load resistance to match the characteristic impedance of the transmission line so that the calibration values can be improved which in turn reduces the error values in the measurement. Therefore, the EMIRR data is expected to be consistent when there is 50 Ω termination present on the evaluation board.

4. Solid ground plane in an internal layer

The test board is the four-layered board where the top layer has RF components and transmission lines. Ground planes should not be broken under the signal traces hence, it is recommended to use a continuous ground plane on one of the internal layers (preferably the second layer) because it acts as the common reference voltage. Ground plane also provides shielding, enables heat dissipation, and reduces stray inductance. As this board is a four-layered PCB board, the second layer is made as a solid ground plane.

5. Selection of decoupling or bypass capacitors

A decoupling circuit is required because of the high-frequency noise in power supply signals. It aids in the avoidance of unforeseen problems that might inflict damage on the system's performance. Broadband decoupling is essential when working with high-frequency RF signals, which can be accomplished by connecting capacitors of increasing size and capacitance, in parallel. The change in reactance of the capacitors over the frequency, however, necessitates the careful selection of such capacitors.

The impedance of passive components on the PCB changes as the frequency increases. For example, in reality, capacitors have a limited effective frequency range due to their Self-Resonant Frequency (SRF). The capacitor's impedance ($|Z|$) is lowest at SRF. The impedance at SRF is called Equivalent Series Resistance (ESR) of the capacitor. So, the impedance of the capacitor drops until the SRF is reached and then

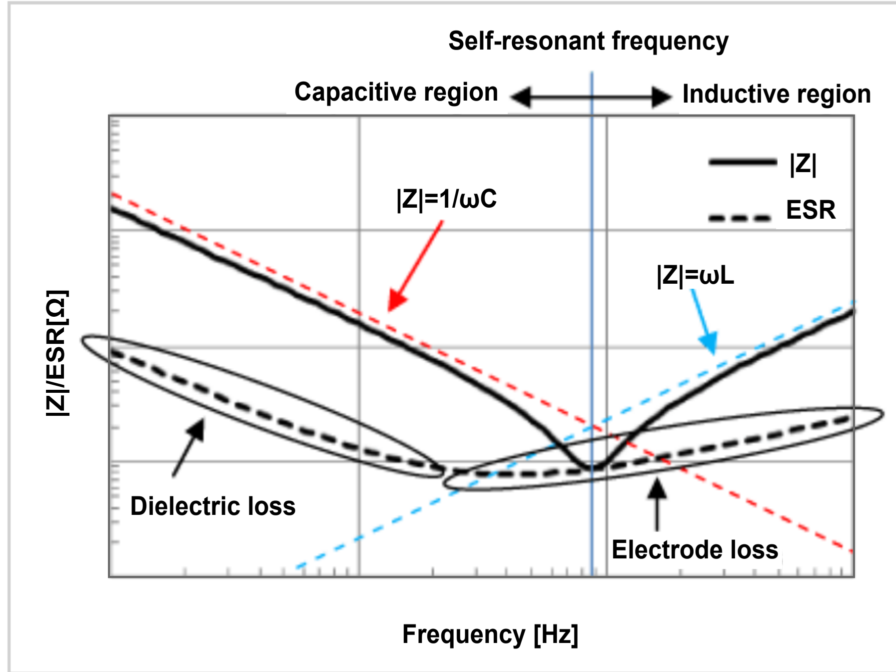

Figure 3.20: Impedance characteristic of decoupling capacitor [22]

the impedance of the capacitor begins to increase. The area below the SRF is called the capacitive region and the area above is called the inductive region. High ESR of the capacitor causes impedance mismatch which results in signal losses. Hence, low ESR capacitors are chosen for the RF decoupling circuit.

3.4 EMIRR Test Setup for INAs

Figure 3.21 depicts the EMIRR measurement setup, in which EMIRR for INAs is measured in a unity gain configuration. The VNA is calibrated at the start, including the cable connecting to the PCB input trace. The data for the reflection coefficients is then acquired from the VNA without placing the DUT on the test board. This data is collected in an excel file and then included in EMIRR calculations in the test software to compensate for signal losses. The RF interference generated by the RF signal generator is conducted through the coaxial cable to either the inverting or non-inverting input of the INA, while the other input is grounded. The remaining peripherals on the test board are all terminated with 50 Ω resistors. The impedance of all the instruments used in the setup is 50 Ω.

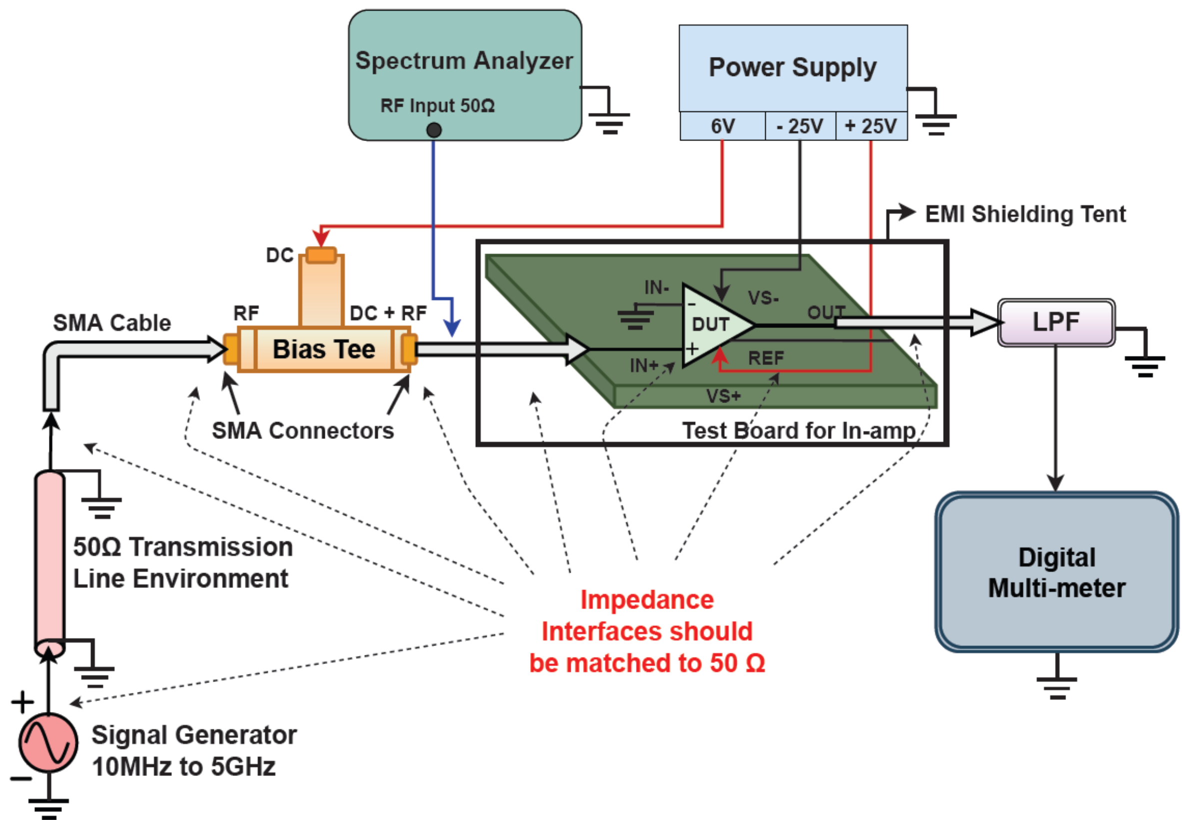

Figure 3.21: Block Diagram of EMIRR Test Setup for In-amps

A bias tee is connected between the signal generator and the test board, which not only prevents the RF signals from being coupled with the DC power supply signal but also helps to bias the INA with the common-mode DC voltage of 0V. So, a DC power source is required to provide DC bias voltage to the Bias tee. The magnitude of the input RF signal reaching the DUT is analyzed using a spectrum analyzer by connecting it to the inverting or non-inverting input of the INA as the impedance in the system is not always 50 Ω.Furthermore, when the spectrum analyzer is hooked to the INA's output, the DC offset at the output can be checked.

The complete EMIRR measurement set up along with the EMI shielding tent in the lab is shown in Figure 3.22. The DUT and the test board are placed inside the shielding tent. The DUT is powered with dual power supply voltage (e.g. $\pm$ 15V) as specified in its datasheet. The output of the INA is connected to an 8th order LPF with a -3dB frequency of around 1MHz. The residual RF signal is attenuated by the LPF to avoid aliasing at the multimeter. Finally, a DMM is connected after LPF to provide DC offset voltages when the INA is subjected to RF interferences during the

EMIRR measurement.

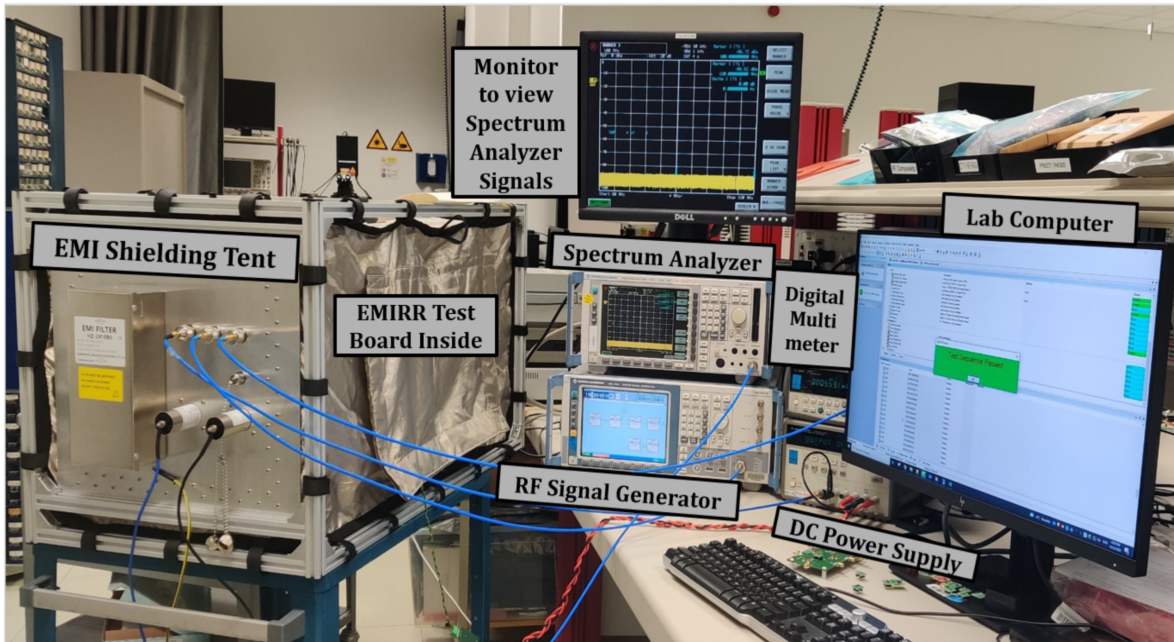

Figure 3.22: EMIRR Measurement Setup in Lab

3.5 New(INA) Test Setup Correlation with the Old(Op-amp) Test Setup

The EMIRR measurement setup for op-amps and INAs is nearly identical, except for the hardware test board. Both op-amp and INA EMIRR measurements can be performed with the same test software described in the subsequent chapter. The evaluation board follows the RF requirements before designing to minimize the error values that might add up to the EMIRR results. In the new test setup, the EMIRR measurement can be done by coupling the differential RF signals and common mode RF signals on the INA. Additionally, there are two different boards, for EMIRR measurement, one with PDIP connections (SOIC-8 BB pinout board) and the other with SMT connections (SOIC-8 ADI pinout board).

3.6 Chapter Summary

The correlation between op-amp and INA test setups is the subject of this chapter. The functionality of all of the hardware equipment employed in the measurement

setup is briefly discussed at first. This includes the VNA, RF signal generator, bias tee, power supply, LPF, digital multi-meter, and spectrum analyzer. The frequency response curve for LPF is also presented with a 1MHz cut-off frequency. Basic INA schematics for differential and common mode are given, as well as 3D images of two separate evaluation boards (SOIC-8 BB and SOIC-8 ADI) developed in Altium designer. The coplanar waveguide routing style with 50 Ω impedance microstrip, via shielding across the transmission line, termination resistor at the end of the RF transmission line, continuous internal ground plane on the second layer, mitigating parasitic capacitances on the test board, and selecting low ESR capacitors for the decoupling and bypass circuits are some of the RF standards followed while designing the boards. Finally, the comprehensive block diagram of the EMIRR hardware measurement setup for INAs is demonstrated.

4 Simulation and Test Software Implementation

4.1 Signal Integrity Simulations

The quality of the electronic signals that are prone to noise, signal loss, and distortion must be checked before the signals are injected into the device for measurement. Signal integrity testing is a technique for assessing the quality of such signals to ensure the measurement accuracy of analog circuits. The evaluation board or the prototype that is developed can be simulated before collecting a lot of data from measurements. Simulations are used not only to extract required electrical parameters and performance data but also to detect small design issues before sending the prototype to production. Let's first define S-parameters before moving on to the simulation procedure.

4.1.1 Scattering parameters

S-parameters are complex matrices that show the reflection or transmission characteristics of RF transmission lines in the frequency domain. Typically, VNA or Time Domain Reflectometer (TDR) test equipment is used to extract this data from RF PCBs. This type of simulation is usually a small-signal AC simulation which is most often used to evaluate a passive RF component and determine a device's small-signal properties at a certain bias.

A two-port VNA used in this project has four S-parameters (S11, S12, S21, and S22). The port where the signal enters is the first number following the "S" in S-parameters, and the port where the signal is transferred is the second number. S12 is therefore a measure of the signal exiting port 1 about the RF stimulus entering port 2. When the S-parameter numbers are all the same (e.g., S22), the transmitter and receiver ports are believed to be the same, indicating a reflection measurement at the ports. Smith

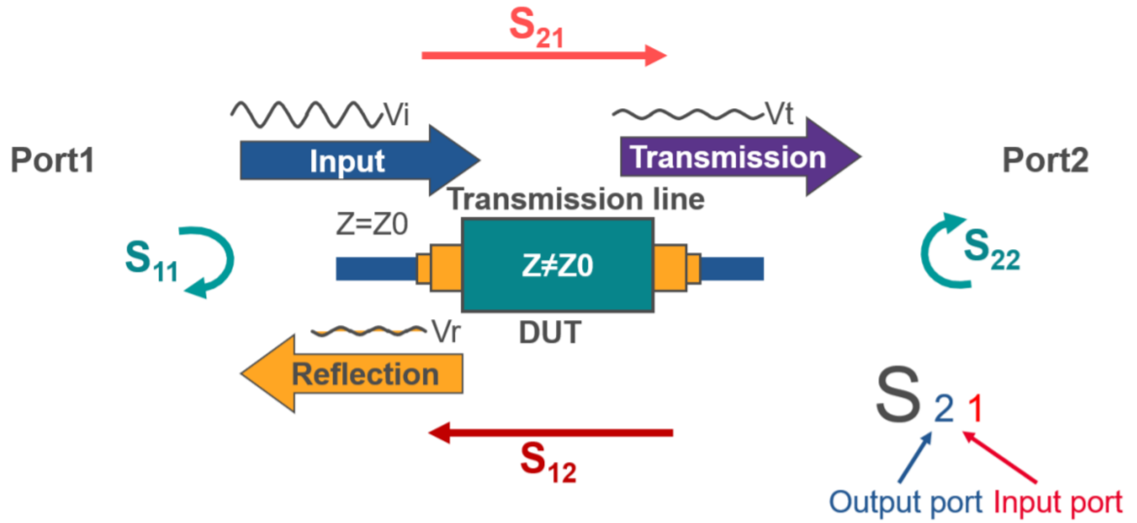

Figure 4.1: S-parameters overview considering 2 ports [21]

chart and Voltage Standing Wave Ratio (VSWR) are some of the display formats of such reflection or transmission coefficients. According to transmission theory, an impedance-matched transmission line must have a lower VSWR which means that the signal losses are less. The reflection and transmission coefficients are calculated by the following equations[21].

Reflection coefficient (return loss) → S11, S22 = (Reflection/Input)

Transmission coefficient (insertion loss) → S21, S12 = (Transmission/Input)

4.1.2 Signal Integrity Simulations in ADS

There are various tools to simulate a PCB such as Advanced Design Simulation (ADS) from Keysight, Hyperlynx from Mentor-graphics, Altium Designer and PSpice, etc. Furthermore, circuit simulation and layout simulation are two methods for simulating a PCB. The ADS software is used in this project for PCB layout simulations with EMPro setup to extract S-parameters. The steps to configure EM Setup for simulation are shown below.

1 Altium designer allows exporting design files in ODB++ format (Open DataBase). The generated file will have a .tgz extension.

2 Create an EMPro workspace in ADS and import the design files in ODB++ format. Also, create a library for the imported project and verify the material

thickness, conductivity, dielectric constant, and loss tangent, etc from the ODB stack import dialog box.

3 Next step is to configure the EM simulation setup which can be done by following the given steps.

a EM simulator selection

Momentum Microwave, FEM - Finite Element Method, and Momentum RF are the simulation algorithms available in ADS. Momentum RF simulator is chosen for our simulation because Momentum RF is quick, stable and it provides accurate electromagnetic simulation performance at RF frequencies.

b Define the PCB substrate

A substrate is an area where the complete layout resides. The substrate can be configured using the EM setup dialog box. It is recommended to add the cover on top and bottom layers of the substrate before starting the simulation because the cover layer acts as a perfect conductor on which the virtual ground ports can be placed to create reference potential.

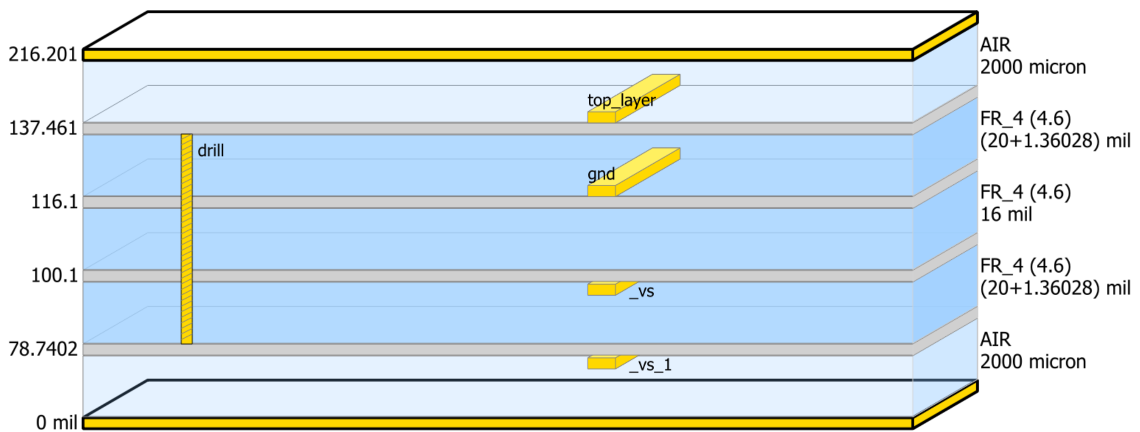

Figure 4.2: PCB layer stack-up for EM simulation

c Assigning the ports to transmission lines

There are various kinds of ports available in the ADS software. However, as this project requires the 50 Ω impedance, ports that have 50 Ω impedance

are used to inject the input signals into the circuit to analyze its behavior.There will be a potential drop in the flow of current if the ground reference points are placed too far from the transmission ports. So, it is important to place a virtual ground near each port on the cover layer. To eliminate potential drops during the simulation, virtual grounds must be used to provide zero reference potential near the port.

d Define the frequency and output plan

Using the EM setup dialogue box, the frequency sweep type, start and stop frequency with several data points, and range of frequencies can be set. Additionally, multiple frequency plans for a simulation can also be set. The output plan can be defined to decide whether the output data of s-parameters should be displayed once the simulation is over or it can be saved as a dataset, etc.

e Configuring simulation options

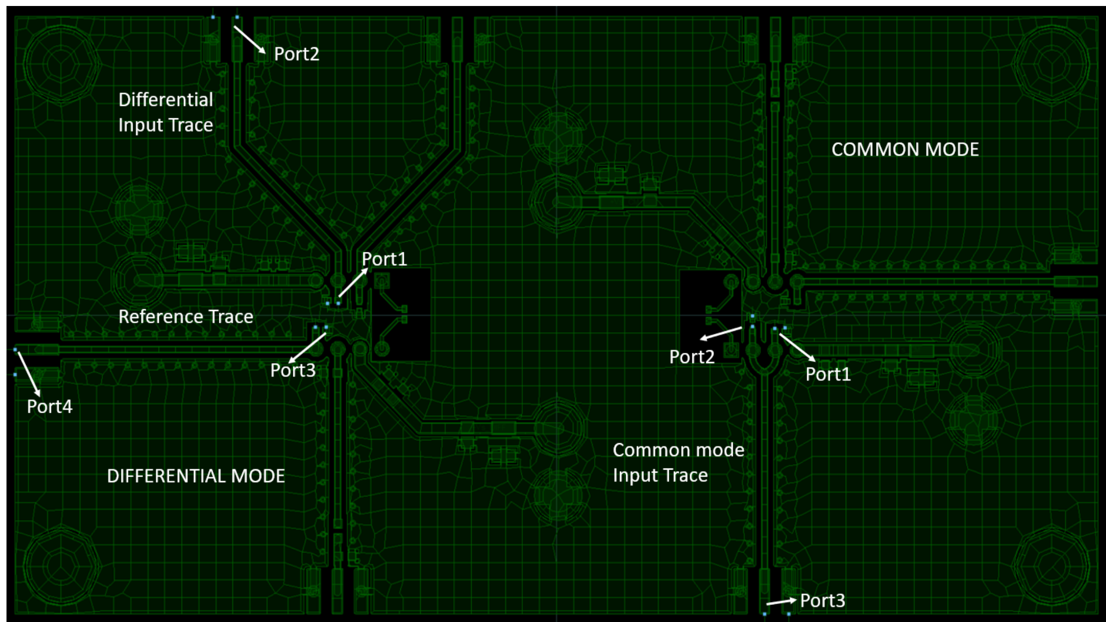

Figure 4.3: The meshed layout of SOIC-8 BB pinout board in EM simulation

Pre-processor parameters and mesh settings are defined in the simulation option. Mesh is a grid-like design comprised of circles and triangles, generally known as cells. During simulation, the mesh is applied to the layout to determine the current within each cell and detect any coupling effects in

the circuit. These mesh computations are used to determine S-parameters. A meshed layout structure is shown in Figure 4.3.

4 After finishing the EM setup settings, start the EM simulation by selecting the simulate option to generate S-parameters.

4.1.3 Simulation Results

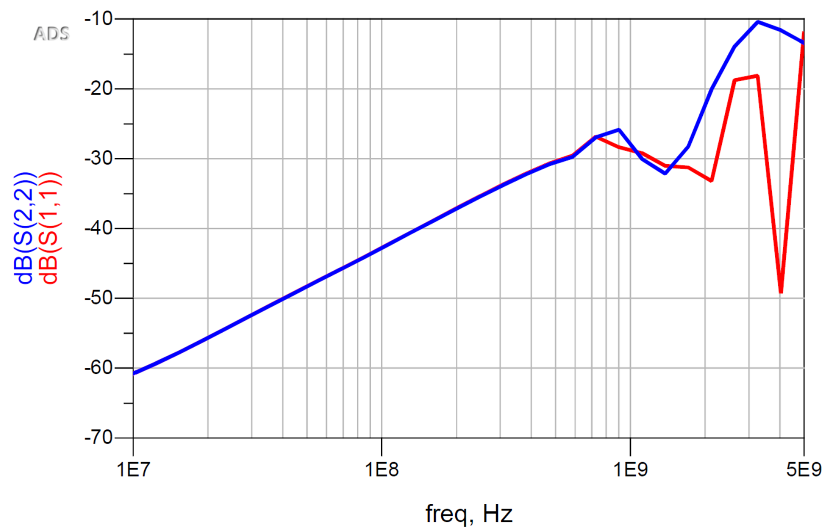

(a) Reflection coefficients

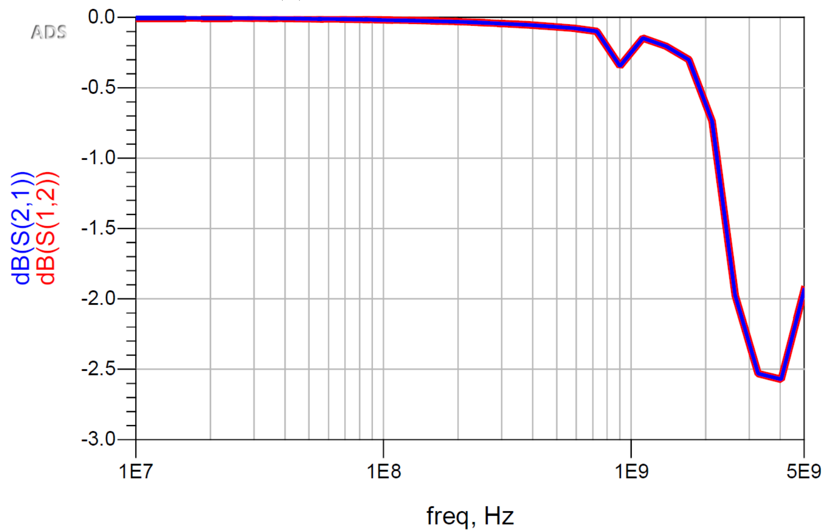

(b) Transmission coefficients

Figure 4.4: S-parameter data of differential mode input trace

The layout simulation for the SOIC-8 BB PCB test board shown in Figure 4.3 is performed. Three important traces from the board are chosen for simulation because of their different orientations, and the remaining traces are identical to one of these traces. The S-parameters for differential mode input trace, reference input trace, and common mode input trace (refer Figure 4.3) are displayed below in Figure 4.4, Figure 4.5, and Figure 4.6 respectively. Since both the boards have the same substrate and are simulated with the same settings, the simulation results of the SOIC-8 ADI test board are identical to those of the SOIC-8 BB PCB test board.

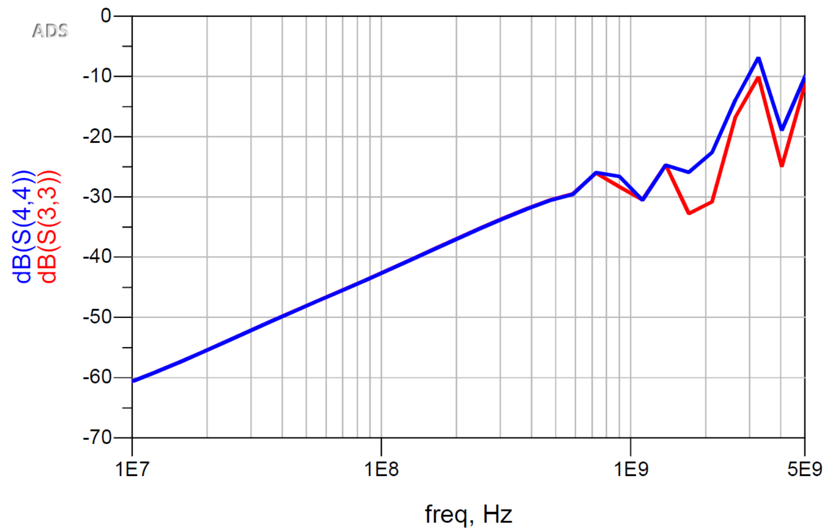

(a) Reflection coefficients

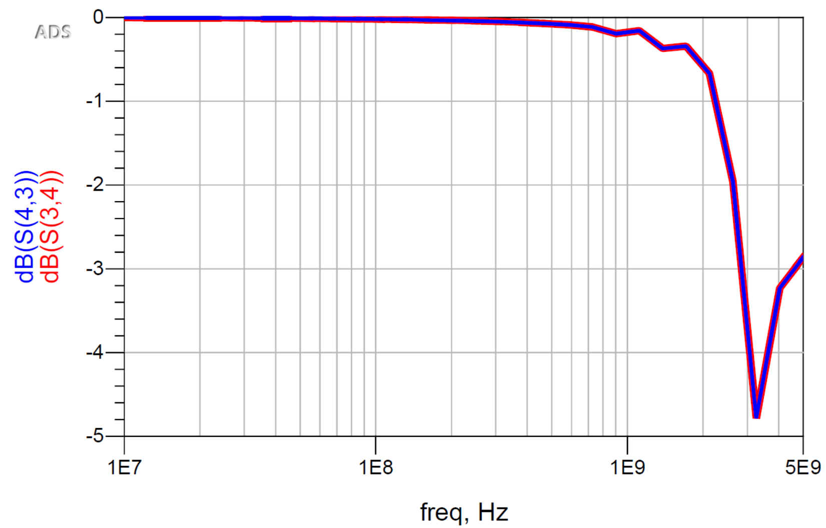

(b) Transmission coefficients

Figure 4.5: S-parameters data of reference trace

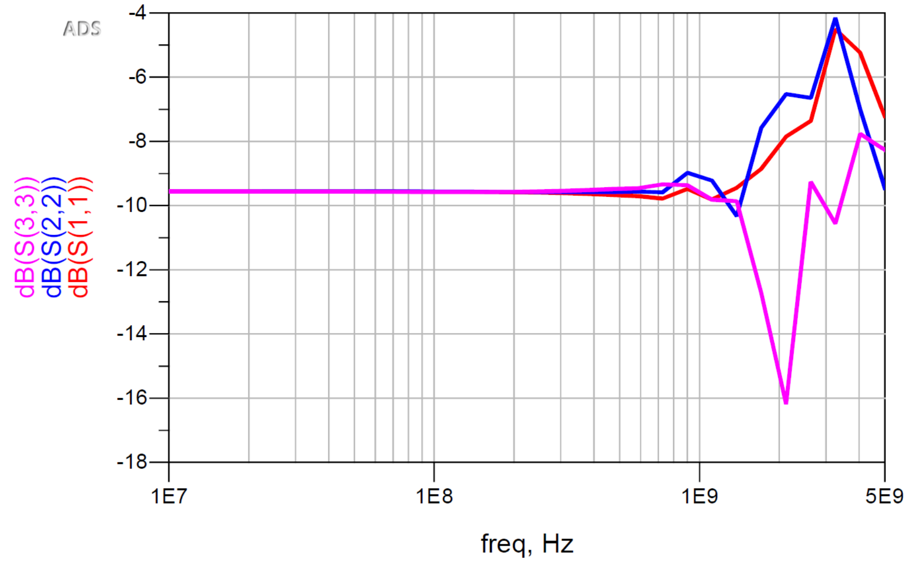

(a) Reflection coefficients

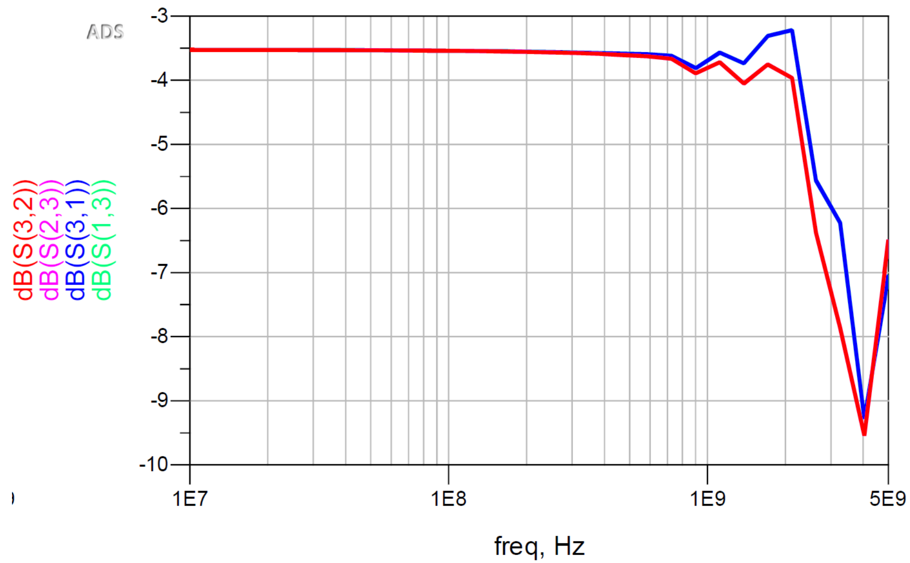

(b) Transmission coefficients

Figure 4.6: S-parameter data of common mode input trace

The signal reflections are lower (-60 dB) at 10 MHz and steadily rise with increasing frequency for differential input trace, as seen in Figure 4.4a. At lower frequencies most of the signal is entering the device. However, at higher frequencies the some of the signal is getting reflected. Figure 4.4b represents the loss-less transmission until 700MHz and then gradually the transmission loss occurs at higher frequencies. This signifies that the signal is well transmitted at lower frequencies but has considerable insertion loss at higher frequencies which can be expected as we are using FR-4 material for the PCB board.

Certainly, S-parameters of reference trace exhibit a similar pattern, with fewer signal reflections and higher transmission coefficients until roughly 1 GHz. The S-parameters for common mode input trace are displayed Figure 4.6a. The reflection coefficients (S11, S22, and S33) are around -9 dB, indicating that there is less return loss and some of the signals is reflected since the trace splits into two at the common-mode input stage. Since the input common mode trace is shorted with inputs and each input trace is terminated by 50 Ω, the power will split into half at each port. Therefore, it is expected to have a transmission loss of about -3 dB till 1 GHz and more loss at higher frequencies as shown in the Figure 4.6b. As a result, to obtain accuracy in EMIRR results, these reflection coefficients are compensated in the EMIRR test software.

4.2 Development of Test Software to Measure EMIRR

4.2.1 About NI TestStand and NI LabVIEW

LabVIEW is a graphical programming language from National Instruments that helps in the development of automated research, validation, and production test systems through data acquisition and instrument control [23]. LabVIEW programs are termed Virtual instruments (VIs). LabVIEW has two panels: the front panel, which displays the controls and indicators, and the back panel, which is a block diagram that contains the graphical source code. When applications need sequencing, LabVIEW can be used with the TestStand.

The test automation software for EMIRR measurement is developed using NI TestStand 2019 32-bit software with a data log library according to internal TI standards. NI TestStand is a test management system for creating automated software sequences for test and validation systems [23]. NI provides LabVIEW drivers for all of the hardware instruments used in this setup, that are used to handle the hardware instruments from the TestStand sequence. Furthermore, GPIB interfaces of all of these hardware instruments are connected to the same bus using star topology. The S-parameter measurement should be done before measuring EMIRR.

4.2.2 Setting-Up the VNA to Measure S-Parameters

Before starting the EMIRR measurements, the VNA must be calibrated along with the cable connecting to the input trace of the test board. The data for the reflection coefficients of input trace is then acquired from the VNA without placing the DUT on the test board. This data is collected in an excel file and saved in the local directory. This calibration data is then included in EMIRR calculations in the test software to compensate for the signal losses. First, we will go through the following steps to collect reflection coefficients data from VNA. To obtain reflection coefficients data from VNA, the below steps are followed.

1 Connect the input of the test board to the VNA's port. Ensure that all of the test board's peripherals are terminated with 50 Ω.

2 Connect VNA to the computer via the GPIB interface and verify that it is communicating with the computer.

3 Manually PRESET the VNA by pushing the green button on the VNA. Then, configure it by selecting the parameter to be measured (S11), specifying the frequency sweep type, setting the start and stop frequency, and defining the number of points to be swept.

4 Open the input/output console of the VNA Instrument and run the query FORM4;OUTPFORM to read the S11 parameters and save them to the temporary directory of the computer in an excel file(.xls, .xlsx, .csv). During runtime, data from this excel file is pulled from the TestStand sequence.

4.2.3 Building the TestStand Sequence

The TestStand sequence consists of the main sequence and four sub-sequences such as $HW_Configure$, Get_VNA_Data, VOS_RF_OFF, and $Meas_EMIRR$ are sub-functions called from the main sequence during runtime. The hierarchy of subsequences called during runtime is given in Figure 4.7.

All of the hardware instruments have NI drivers that can be used to control the hardware through the GPIB interface. Before executing the sequence, the user must input the DUT information in the variable section. The flowchart in Figure 4.8 and

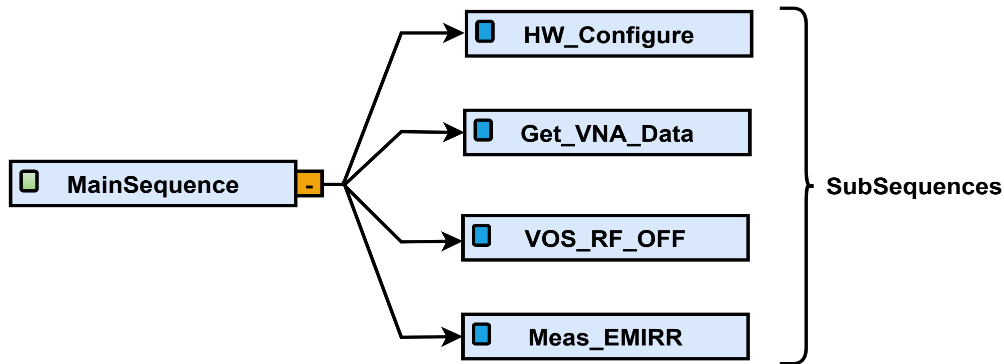

Figure 4.7: EMIRR test software hierarchy

Figure 4.9 represent the entire flow of the test program. The main sequence begins with datalog initialization and the creation of a local folder location where the measurement result files can be saved.

The main program calls the first sub-function ($HW_Configure$), which initializes and configures the hardware instruments employed in the setup, such as the signal generator, power supply, DMM, and so on. The next step is to load the reflection measurement data from the local folder, which may be accomplished with a submodule (Get_VNA_Data) developed in TestStand using an ActiveX/COM module. This module retrieves the excel file from the local folder path provided the user has entered the folder path name in the variables section before running the sequence.

A small voltage is present at the amplifier's output due to the inherent input offset voltage, but this voltage is not generated by the rectification process of RF signals. As a result, this should be excluded from the EMIRR calculation. To eliminate this offset from the multi-meter, a sub-function VOS_RF_OFF is called from the main function that captures DMM readings when the RF signal from the RF signal generator is turned off. The acquired DC output offset voltage is referred to as VOS1.

The DC output offset voltage measurements will be taken again when the RF signal generator is turned on. In the test program, this is performed by invoking the sub-module $Meas_EMIRR$, which sweeps the DC offset voltage readings from the DMM, when RF interference of -10 dBm power is applied to the amplifier at different frequencies ranging from 10 MHz to 3 GHz. This DC offset voltage is produced by

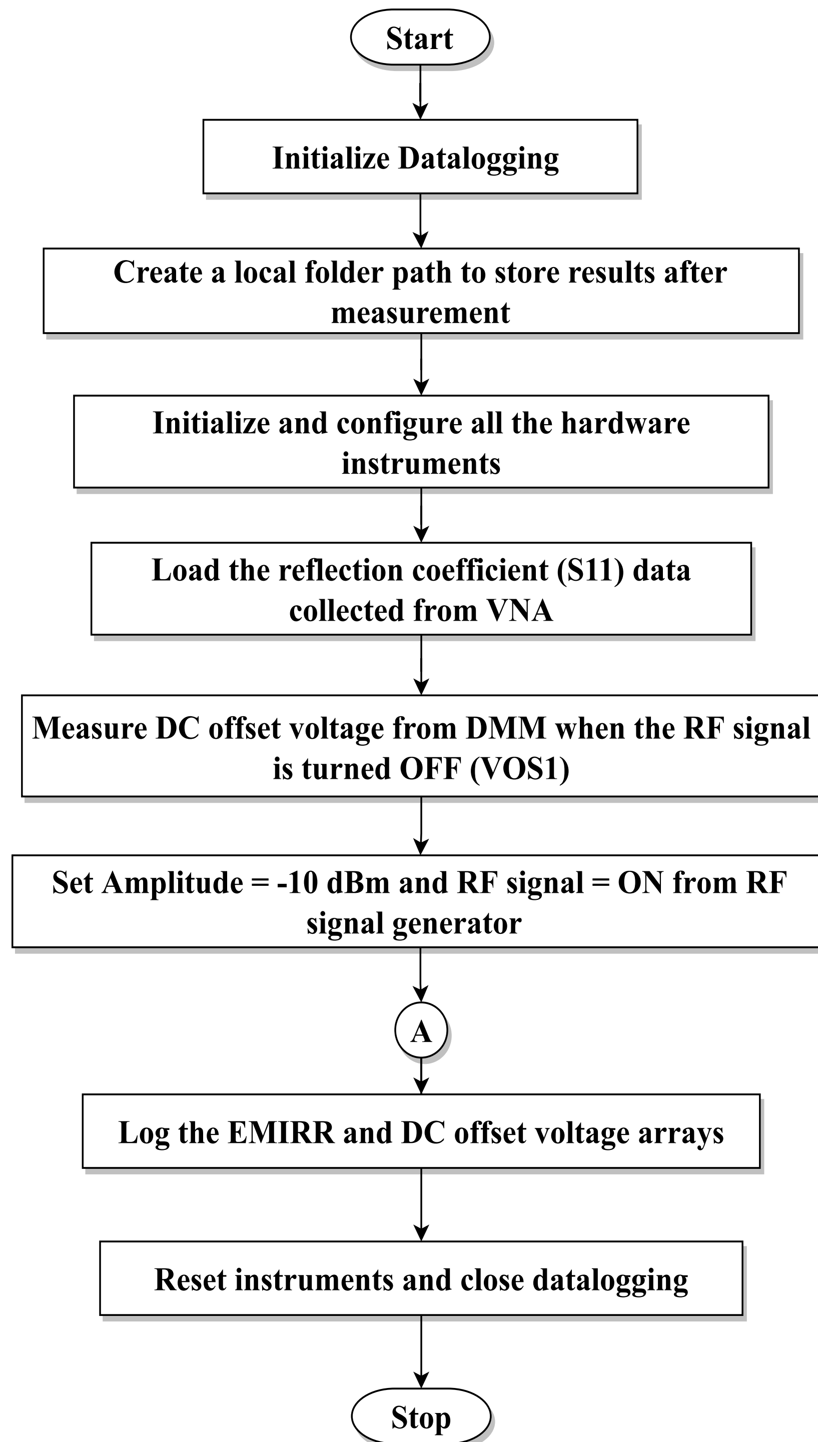

Figure 4.8: EMIRR test software flowchart for the main sequence

the DC rectification of the RF signal. The number of loop iterations is defined by the number of data points specified by the user. The DC offset voltage obtained for each loop iteration is referred to as VOS2. EMIRR is computed for each iteration using the equations as illustrated below.

4.2.4 EMIRR Calculation

Consider the amplitude of input RF signal to be -10dBm and system impedance to be matched to 50 Ω.

Step 1 V_{RMS} calculation: Convert the input power of RF signal from power in dBm to V_{RMS}. $R(\Omega) = 50\ \Omega$

$$V_{RMS_Applied} = (Power(W) * R(\Omega)) \tag{3}$$

$$V_{RMS_Applied} = 0.07071 V_{RMS}$$

Step 2 Conversion of RMS value to peak voltage (V_PEAK)

$$V_{PEAK} = \sqrt{2} * V_{RMS} = 0.1 V_{PEAK} \tag{4}$$

Step 3 Calculation of V_{RF_PEAK} by compensating the reflection coefficient (S11) data from VNA

$$V_{RF_PEAK} = (1 + |S11|) * V_{PEAK} \tag{5}$$

Step 4 Calculation of shift in DC offset voltage (ΔVos)

As the amplifier is in buffer configuration, gain (A) = 1. In case of other configurations, the DC offset voltage must be divided by the circuit gain. So,

$$|\Delta Vos| = |V_{OS2} - V_{OS1}| \tag{6}$$

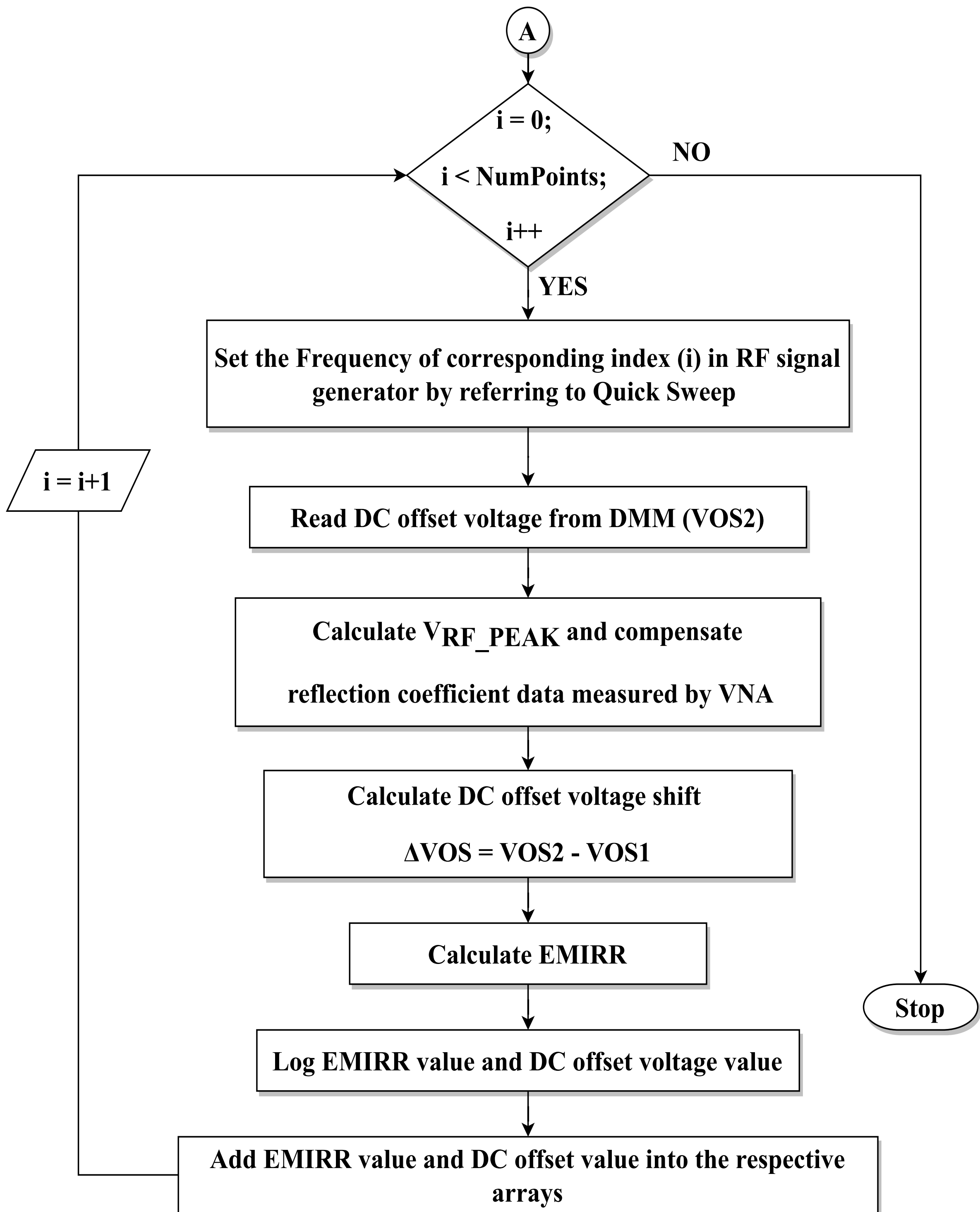

Figure 4.9: EMIRR test software flowchart for a submodule A

Step 5 Calculate EMIRR(dB) by substituting $|\Delta Vos|$ in equation (1)

$$EMIRR[dB] = 20 \cdot \log\left(\frac{V_{RF_PEAK}}{|\Delta Vos|}\right) + 20 \cdot \log\left(\frac{V_{RF_PEAK}}{100mV_p}\right)$$

Where,

V_{RF_PEAK} is the peak-amplitude of the applied RF voltage

ΔVos is the shift in DC offset voltage

$20 \cdot \log\left(\frac{V_{RF_PEAK}}{100mV_p}\right)$ term refers to the EMIRR to an input signal of $100mVp$

The computed EMIRR, DC offset voltage, and S-parameter values are stored in separate arrays after each iteration. These are logged in the output file, which helps in the characterization of the EMIRR data. The EMIRR setup is now ready for measurements. Let us check the working of the test setup in the upcoming section by performing some measurements. With this, the EMIRR setup is ready for measurements and let us see how it works in the next section.

4.3 Chapter Summary

The chapter deals with the signal integrity simulations at first, to check the magnitude of input RF signal reaching the device inputs, by performing layout simulations with EMPro setup in ADS software. Initially, for 2-port VNA, the basics of s-parameters are discussed. Furthermore, the ADS software is configured for simulating the transmission lines of the test board to extract the S-parameter data. For simulation, three representative PCB traces were chosen which are most important for measurement such as differential input trace, reference trace and common mode input trace.

The implementation of the test software for EMIRR measurements is covered in the second half of this chapter. The first step is to acquire the reflection coefficients from the VNA before starting the measurement. The extracted data will be added to the input signal during the EMIRR computations in the sequence to minimize the errors

due to calibration. A flowchart depicting the flow of the automation sequence is also presented. The relevant equations are used to describe the EMIRR computation.

5 Results and Discussions

5.1 EMIRR Measurements and Data Analysis

5.1.1 Test Setup Verification by Measuring EMIRR for Op-amp Sample

One of the goals of this thesis was to reproduce the generic EMIRR setup for op-amps and then optimize it for INAs. Therefore, the current test setup is tested with an op-amp sample using op-amp test board to verify that the test setup is not contributing any errors to the EMIRR results. So, OPA2227 is tested for EMIRR from 10MHz to 3GHz with a -10 dBm RF signal and a ±5 V supply to verify if the observed data matches the EMIRR curve from its datasheet. The OPA2227 is a high-precision amplifier with a wide bandwidth (8 MHz at unity gain) that is utilized in both DC and AC precision applications [25].

Figure 5.1 shows the EMIRR data curves of OPA2227 where the black curve represents reference data from a datasheet [25] and the red curve reflects the measured EMIRR data from the new INA setup. It is observed that the curves are nearly identical to the datasheet curve at lower frequencies and deviate a little at higher frequencies beyond 500MHz. This variation in the EMIRR curve at higher frequencies might be due to two factors: first, the calibration data collected from the VNA, varies from setup to setup, and second, the lack of input termination at the end of input trace on PCB may lead to setup dependencies that has to be included in the measurement results, if the setup is not fully replicated by the S11 data from the calibration step. Having a 50 Ω termination resistor at the end of the RF input trace on the test board improves the calibration data and so makes the EMIRR curve more consistent. The following chapter provides further detail regarding the 50 Ω termination. OPA2227 has a lower EMI rejection ratio at lower frequencies, which gradually increases as the frequency

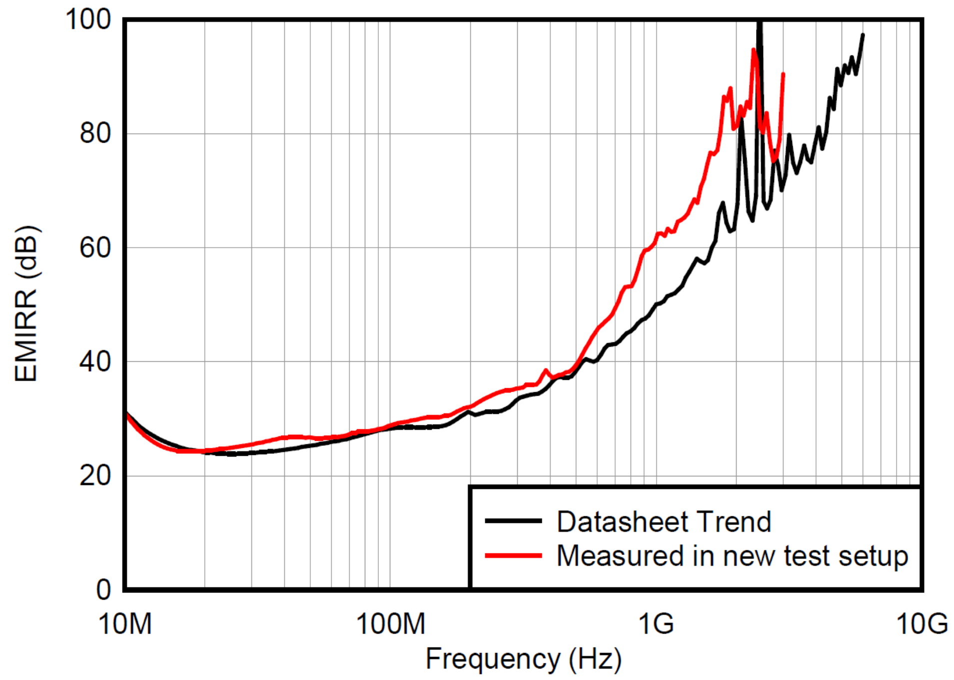

Figure 5.1: OPA2227 EMIRR Curve compared with that of the datasheet curve

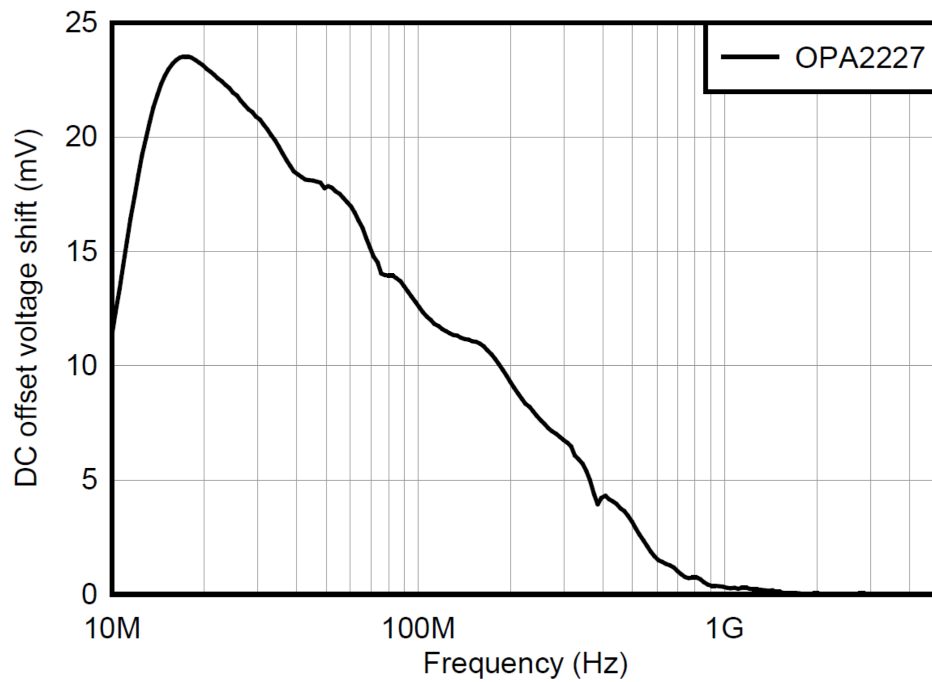

Figure 5.2: DC Offset Voltage vs Frequency curve for OPA2227

increases, which indicates the function of the EMI filter inside the op-amp. Higher frequency RF signals are attenuated by the EMI filter, resulting in good rejection at higher frequency RF.

We may deduce from equation (1) that the EMIRR value is determined by the DC offset voltage measured from DMM at the output of the op-amp. The DC offset voltage is fairly large at lower frequencies, as seen in Figure 5.2 , which explains the low EMIRR values in Figure 5.1. At increasing frequencies, the DC offset voltage drops. The shift in the DC offset voltage ranges from hundreds of microvolts to a few millivolts which can be measured with the chosen DMM (34470A - 6 $\frac{1}{2}$ digit) without additional measurement gain.

5.1.2 EMIRR Measurement for INAs

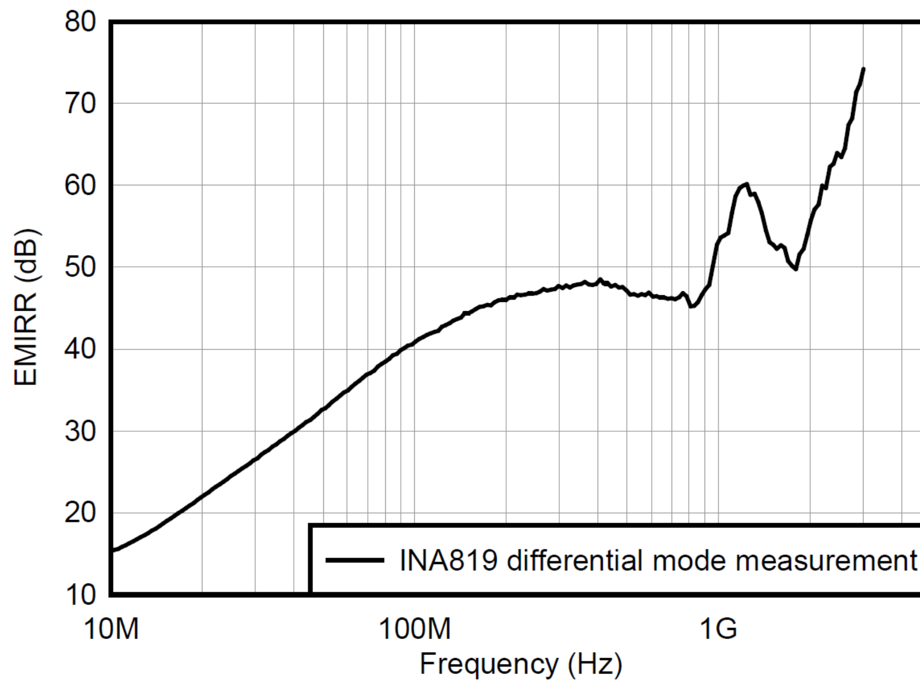

Figure 5.3: EMIRR vs frequency for INA819 in Differential mode

To perform EMIRR measurements for INA samples in the same setup, the test board has been replaced with a newly designed INA test board. For the EMIRR measurement, an INA819 precision instrumentation amplifier (very low input offset voltage and offset voltage drift precision INA) was used [26]. Before executing the test

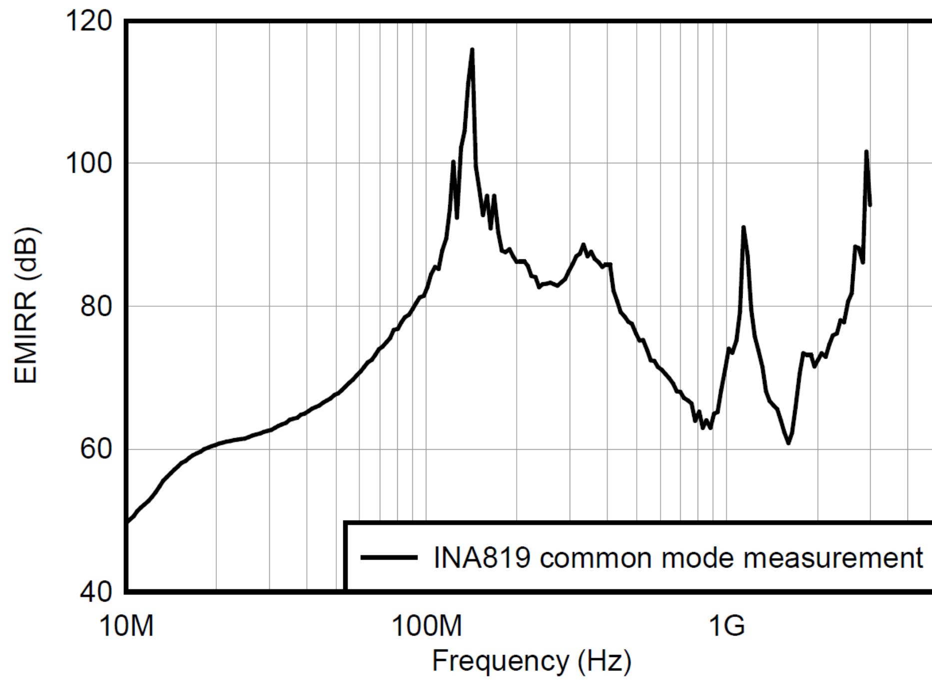

Figure 5.4: EMIRR vs frequency for INA819 in Common-mode

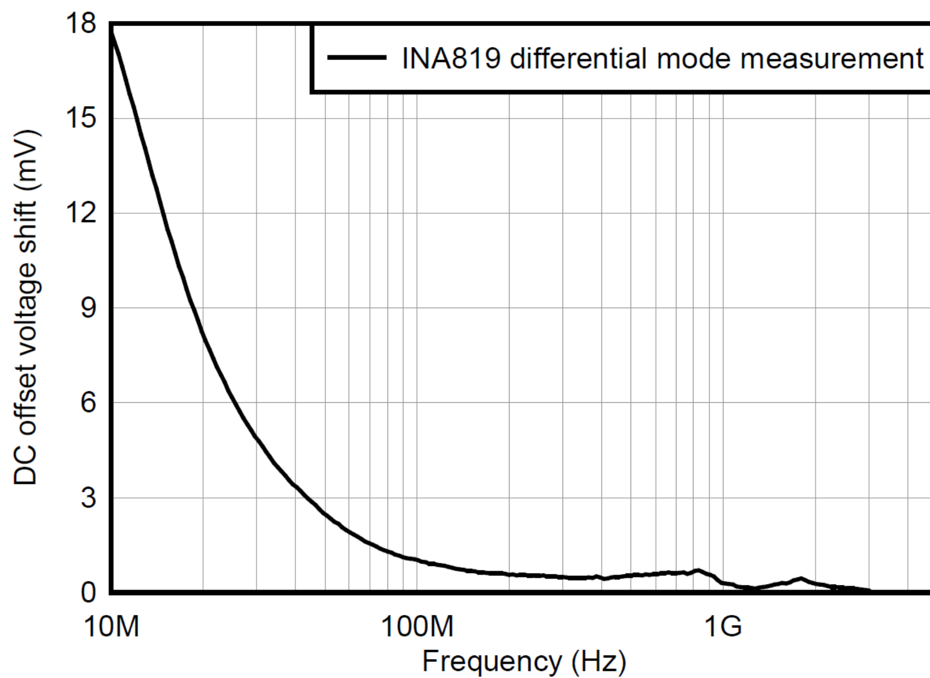

Figure 5.5: DC offset voltage shift vs frequency for INA819 in differential mode

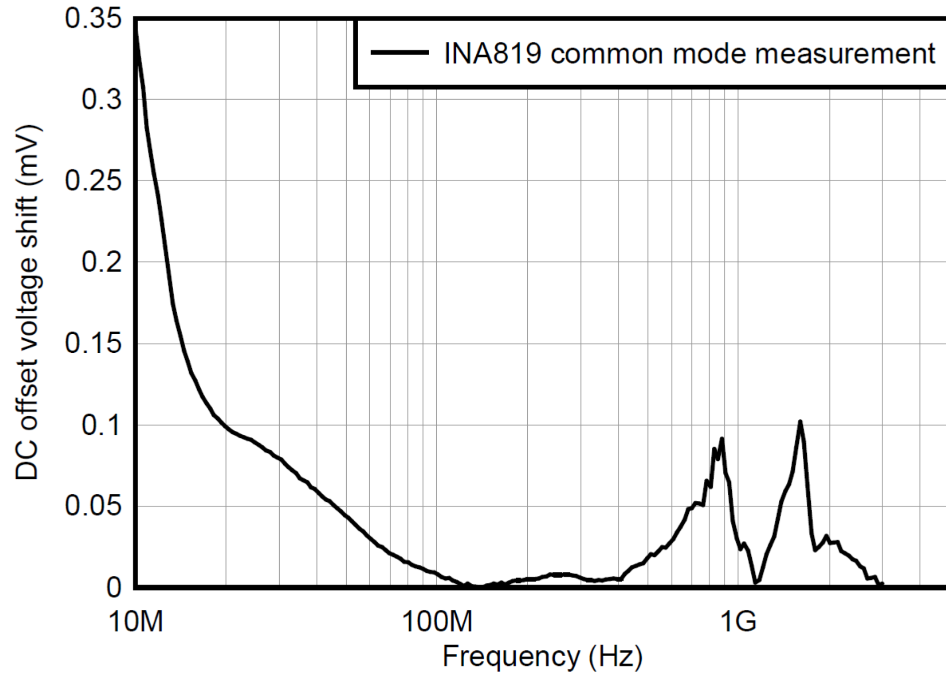

Figure 5.6: DC offset voltage shift vs frequency for INA819 in common mode

sequence, INA819 is mounted on a small adapter/extension PCB board known as a coupon board (as shown in the Figure 5.7) that is plugged into the test board. The EMIRR of the INA819 was measured from 10 MHz to 3 GHz with an RF signal of -10 dBm and power supply voltage of ± 15V. The EMIRR response of the INA819 for RF signals in the differential mode and common mode are shown in Figure 5.3, and Figure 5.4 respectively.

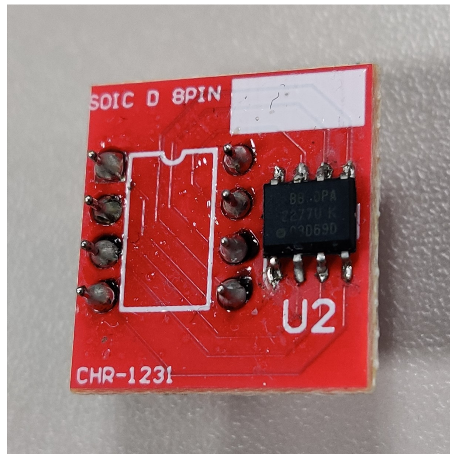

Figure 5.7: Coupon board

The INA819 is designed to provide a high CMRR (over 90dB at unity gain), which implies that change in the DC offset voltage is low, which might explain why it has better EMI rejection than differential mode. The EMI rejection rises to 113 dB at 134 MHz in common mode (as shown in Figure 5.4), possibly due to the notch filter created by the INA's internal circuitry attenuating the RF signal at this particular frequency. Figure 5.5, and Figure 5.6 also show that the variation in DC offset voltage at the output due to the applied RF signal throughout the frequency range of 10 MHz to 3 GHz. Since the DC offset voltage of INA819 in common-mode is fairly low, its EMIRR in common-mode is relatively high, because the EMIRR value is entirely reliant on the DC offset generated at the DUT's output.

5.2 Some Investigations on EMIRR and Data Analysis

The EMIRR test setup is carefully developed making sure that the test environment does not contribute any error values to the EMIRR measurements by coupling with the unwanted signals during measurement. So, the EMI robustness of each device is determined by the EMI filter and its internal circuitry, which makes the EMIRR response to differing significantly from one device to another. So, selected INAs with different characteristics are chosen for EMIRR measurements to examine if amplifier parameters such as bandwidth, input capacitance, gain, and device packages such as D, DGK, and DRG have any significant parasitic effect on the EMIRR curve. Furthermore, certain experiments on INAs are carried out to see if the EMIRR varies with and without a termination resistor (50 Ω), by reducing external EMI injection which can be added to the injected noise by using an EMI shielding tent. Finally, with varying power supply voltages and RF power levels, EMIRR behavior is evaluated. All these experiments are performed in both differential and common modes of INA. Let's take a look at each use case and analyze the EMIRR data one by one.

About TIBCO Spotfire

TIBCO Spotfire tool is used to analyze the obtained EMIRR data. Spotfire is a robust data analytics platform that allows data visualization, and predictive analytics [24]. It is a flexible and scalable tool that provides an effective dashboard and interactive analytical applications. It also enables users to integrate data in a single analysis and obtain a comprehensive view of data through interactive visualization.

5.2.1 Termination Resistor at the End of RF Input PCB Trace

The 50 Ω termination resistor at the end of the RF input trace improves the signal integrity on the input trace with the device having a high impedance. Thus, we have an open unterminated line. S11 measurement will be dominated by the unterminated line, to be able to use the dynamic range of that measurement. However, for the calculation purpose, we want to avoid introducing frequency-dependent reflections of an unterminated system. Hence, the measurements are performed on INA819 with and without a 50 Ω termination at the end of the input trace. The RF noise signal with the power of -10 dBm is injected into the non-inverting input of an INA and the supply voltage of $\pm$15V is provided.

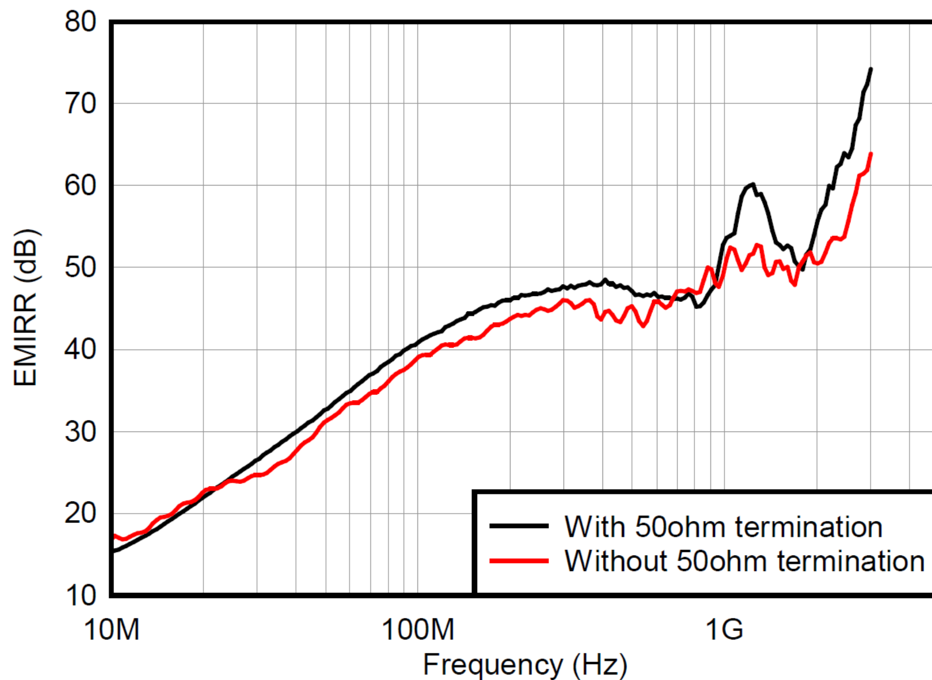

Figure 5.8: INA819 EMIRR curve in differential mode with and without 50 Ω termination

Figure 5.8 illustrates the measurement in a differential mode where the obtained EMIRR data (black curve) is stable without much resonance when there is 50 Ω termination compared to the EMIRR curve measured without termination that has small resonances throughout the frequency range. Figure 5.9 shows the measurement in a common mode where the EMIRR response is higher (red curve) when compared to the one measured without the 50 Ω termination (black curve). Hence, it is recommended to use a termination resistor if the application allows it and calibrate the test setup

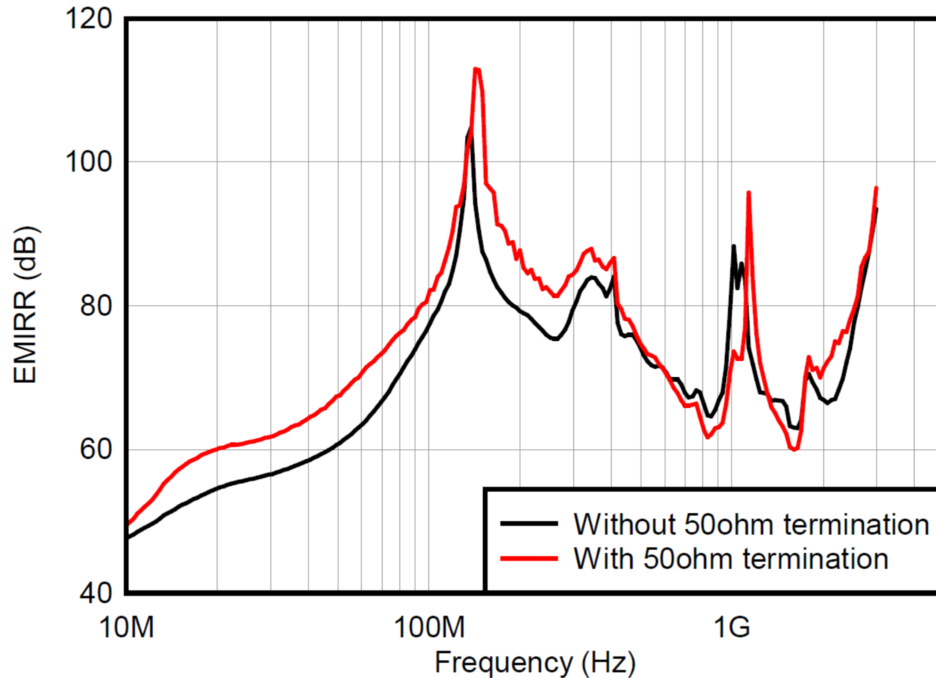

Figure 5.9: INA819 EMIRR curve in common mode with and without 50 Ω termination

before starting the measurement to minimize the errors added up to the measurements data. In this case, the selected INAs have sufficiently low bias currents so that the 50 Ω termination at the input is negligible.

5.2.2 Device Package Test

EMIRR measurements of INA819 with D, DGK, and DRG packages in differential and common-mode are shown in Figure 5.10 and Figure 5.11. The testing is done using the coupon boards (minimal impact) with -10 dBm input RF signal and $\pm$ 15V supply voltage. This test is conducted to check the influence of INA package parasitics on EMIRR as the bond-wire inductance or a capacitance to the lead-frame might have some impact on impedance which further affects the signal reaching the inputs of the amplifier where the RF rectification happens. The measurement results shows that for this figure of merit, the package(D, DGK, and DRG) parasitics variation is not a significant contributor or these INA variants are matched very well.

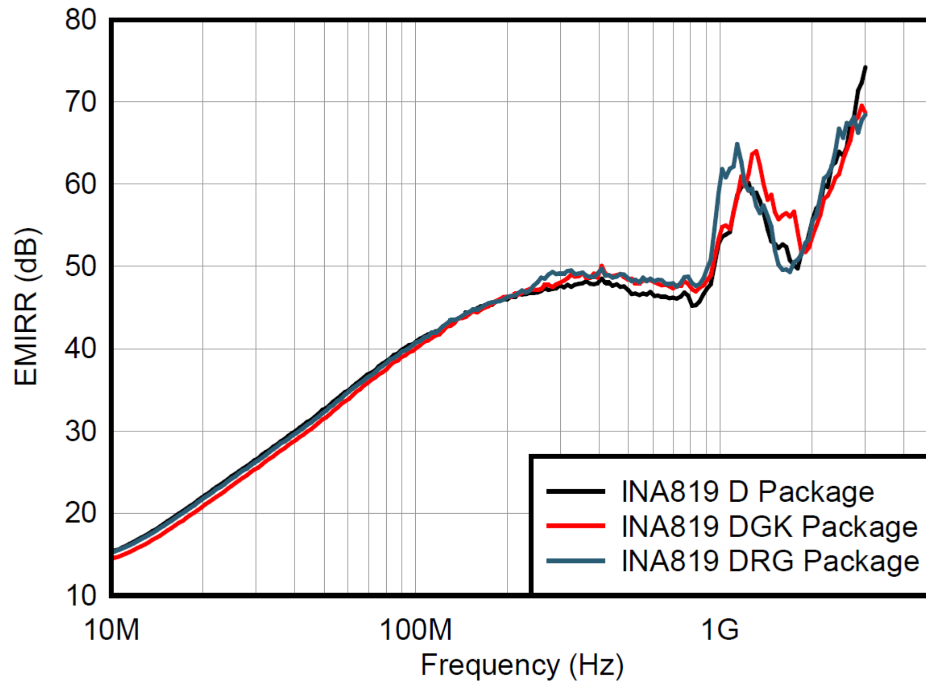

Figure 5.10: INA819 EMIRR curve in differential mode with D, DGK, and DRG packages

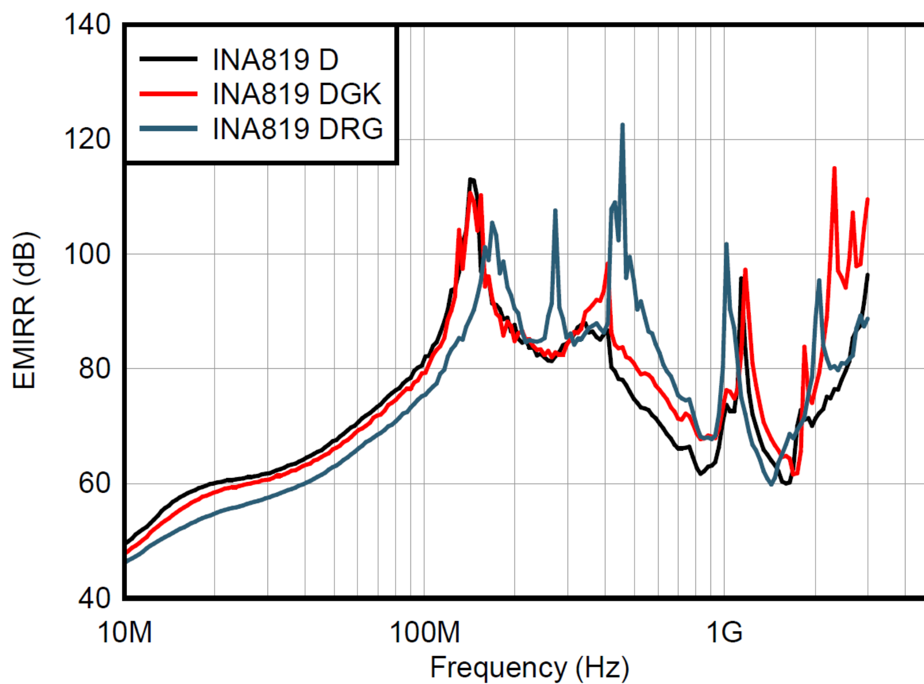

Figure 5.11: INA819 EMIRR curve in common-mode with D, DGK, and DRG packages

5.2.3 EMIRR Behavior for Different Amplitude Levels of RF

In general, the input RF signal injected into the amplifier's input pin is -10dBm. However, an experiment is done to check the EMIRR responds to various RF power levels at the amplifier's non-inverting input. The measurement is carried out with a DUT supply voltage of ± 15V. EMIRR is measured with -10dBm, -12dBm, -14dBm, -16dBm, -18dBm, and -20dBm amplitude levels of RF.

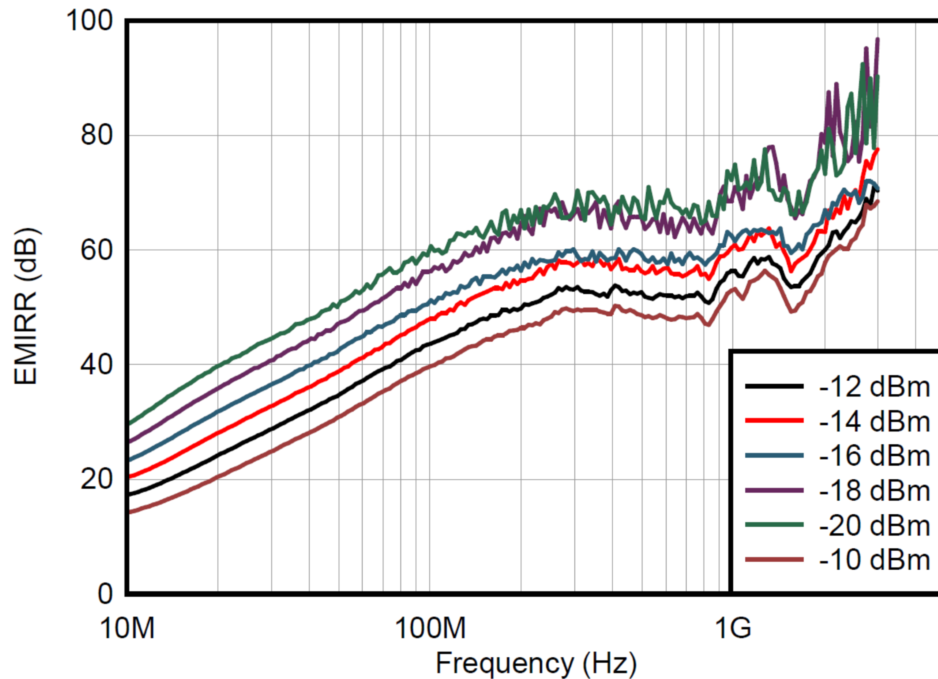

Figure 5.12: INA818 EMIRR curves in differential mode for different RF power levels

With this experiment, it was observed that for every 2 dBm drop in the RF power levels, the EMIRR increases by approximately 2 dB, implying that the lower the noise entering the system, the lower the change in DC offset voltage created at the amplifier's output, and therefore greater the EMIRR [7]. However, the DMM (34470A - 6 $\frac{1}{2}$ digit) can measure the DC offset from hundreds of microvolts to a couple of millivolts which should be considered during the measurement.

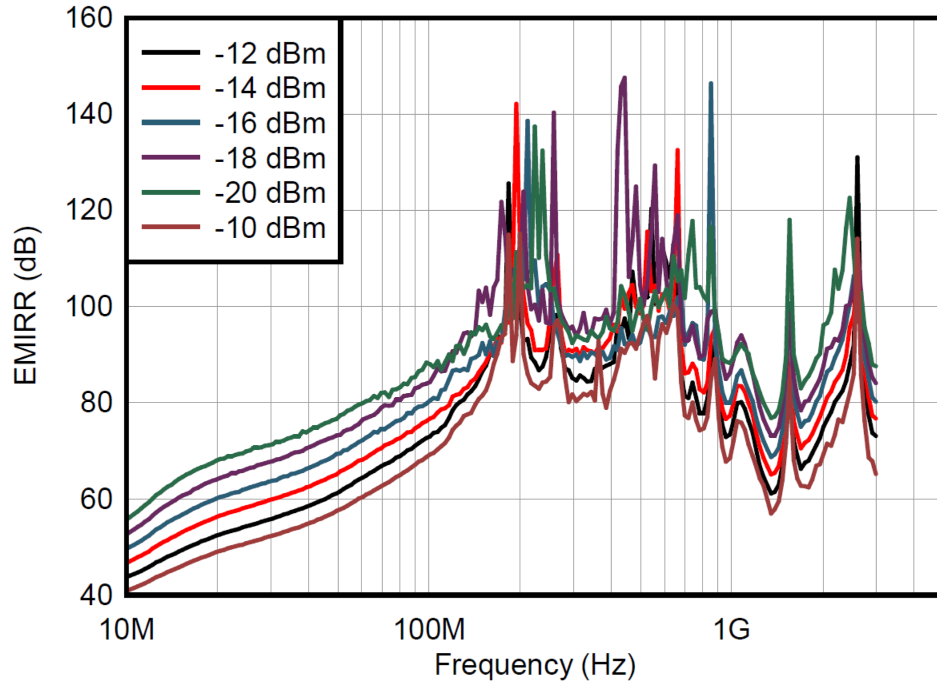

Figure 5.13: INA818 EMIRR curves in the common mode for different RF power levels

5.2.4 EMIRR Response for Different Power Supply Voltages

The INA819 is used as DUT in this experiment, which has a power supply range of ±2.25 V to ±18 V [26]. A fixed input RF signal of -10 dBm and DC power supply voltages of ±5 V, ±10 V, and ±15 V is applied to the test setup to assess EMIRR response. It is expected that the actual offset voltage of INA819 should not vary with power supply voltage because of its high PSRR (120 dB) for unity gain configuration. The ability of an amplifier to suppress any power supply changes on its output signal is described by its PSRR. It is observed that even the EMIRR does not vary with variation in the DUTs power supply. Therefore, change in offset voltage caused by rectification process is not influenced by the DUTs power supply.

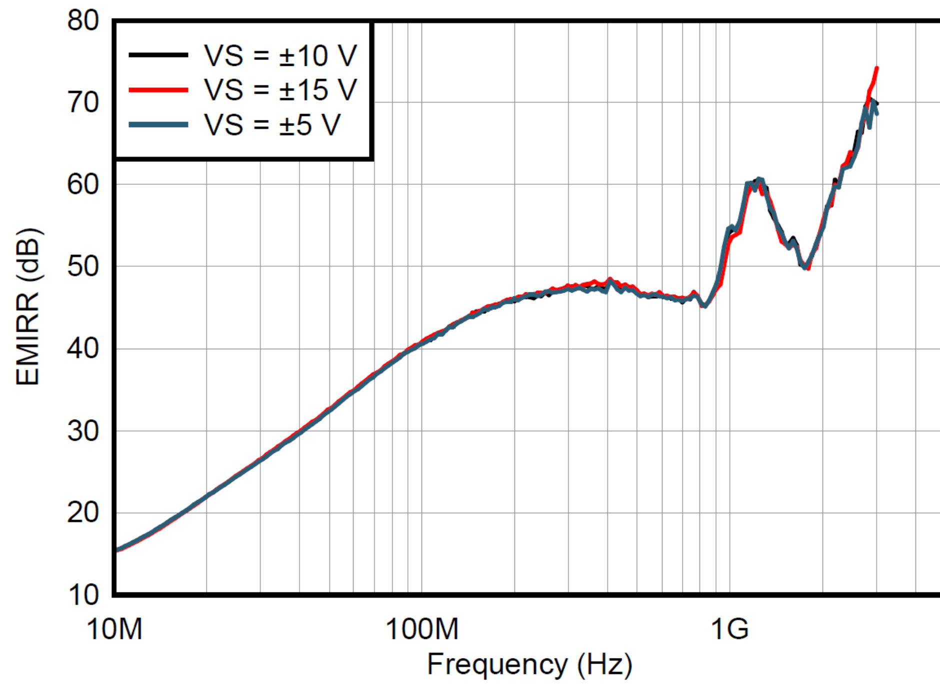

Figure 5.14: INA819 EMIRR curves in differential mode for different supply voltages

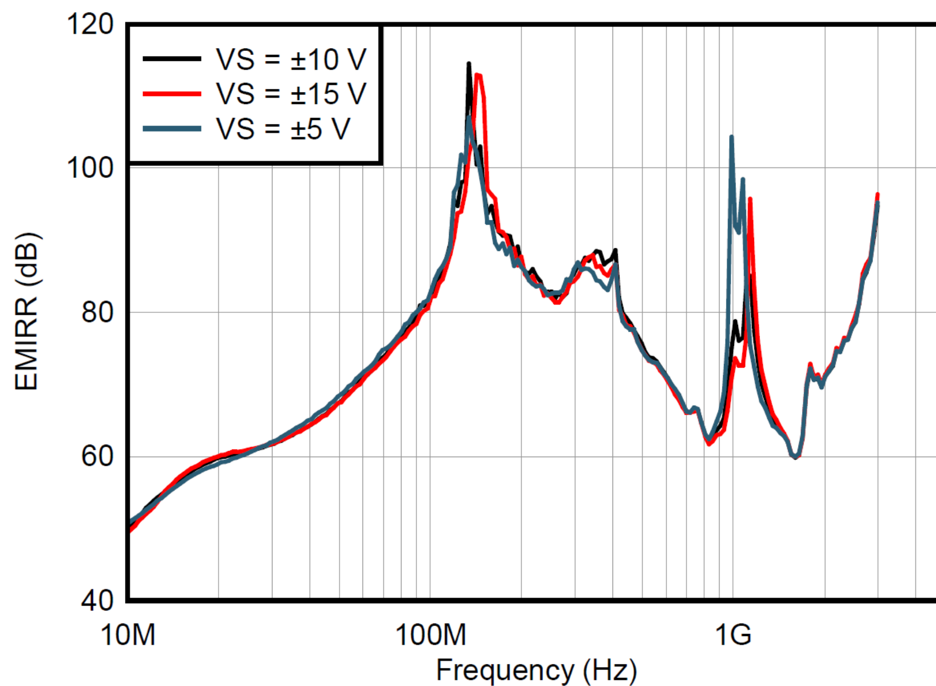

Figure 5.15: INA819 EMIRR curves in the common mode for different supply voltages

5.2.5 EMI Shielding Tent

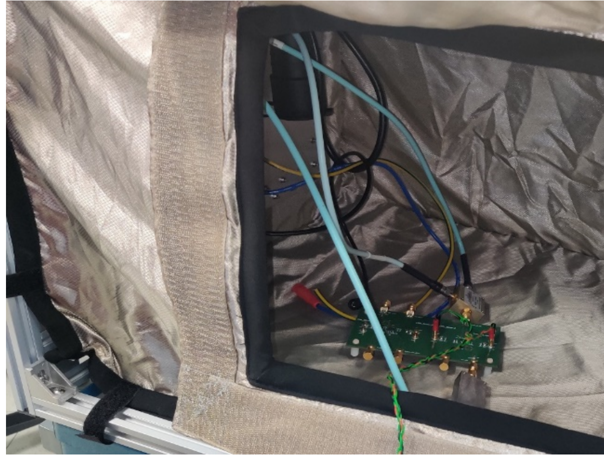

Figure 5.16: EMIRR test board placed inside the EMI shielding tent

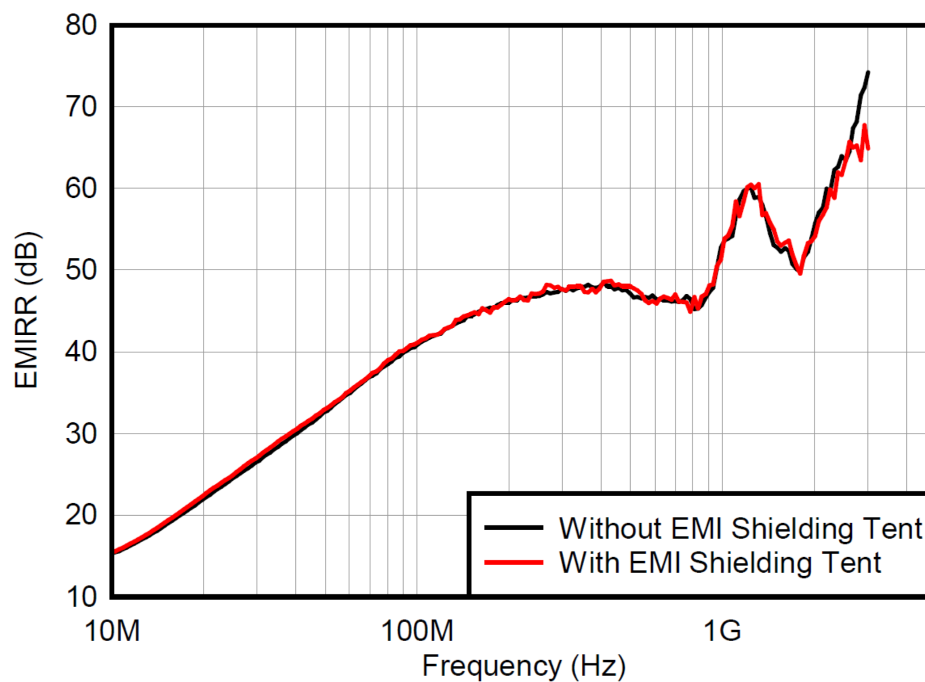

Figure 5.17: INA819 EMIRR data with and without EMI shielding tent in differential mode

If the electronic devices act as effective antennas to receive external RF signals, then RF radiations might affect their performance. Even though this is a conducted immunity test, an EMI shielding tent is used to determine if the device is impacted by any external radiations. The test board is placed within the shielding tent as shown in Figure 5.16, and the EMIRR for the applied RF signal is measured. However, in

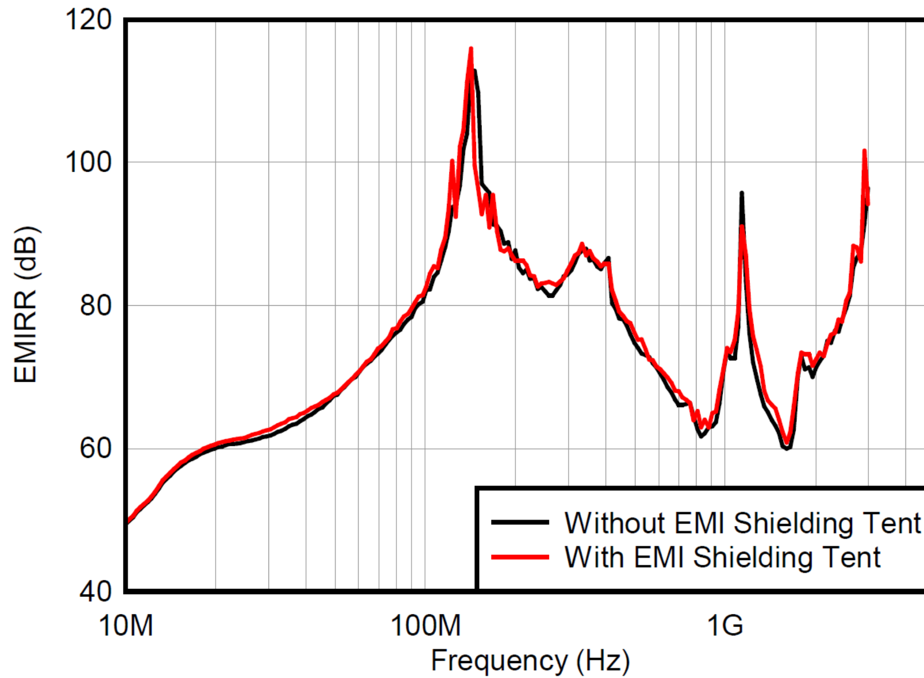

Figure 5.18: INA819 EMIRR data with and without EMI shielding tent in common mode

this scenario, the DUT does not receive any external RF signals which would be significant compared to the injected conducted signal, as evidenced by the EMIRR data in Figure 5.17 and Figure 5.18.

5.2.6 Coupling RF to Inverting and Non-Inverting Terminal of the Amplifier

RF can be coupled to any pins of the amplifier to check its ability to reject EMI. However, the input pins are so sensitive to signals that if the RF is coupled to the input terminals to check the EMIRR response when RF is injected in inverting and non-invering inputs of INA in the differential mode measurement. Due to the input trace symmetry in the test board design [17] [18], the amplifier's EMI rejection ability is same, when the RF is conducted in either the two input terminals, as illustrated in Figure 5.19.

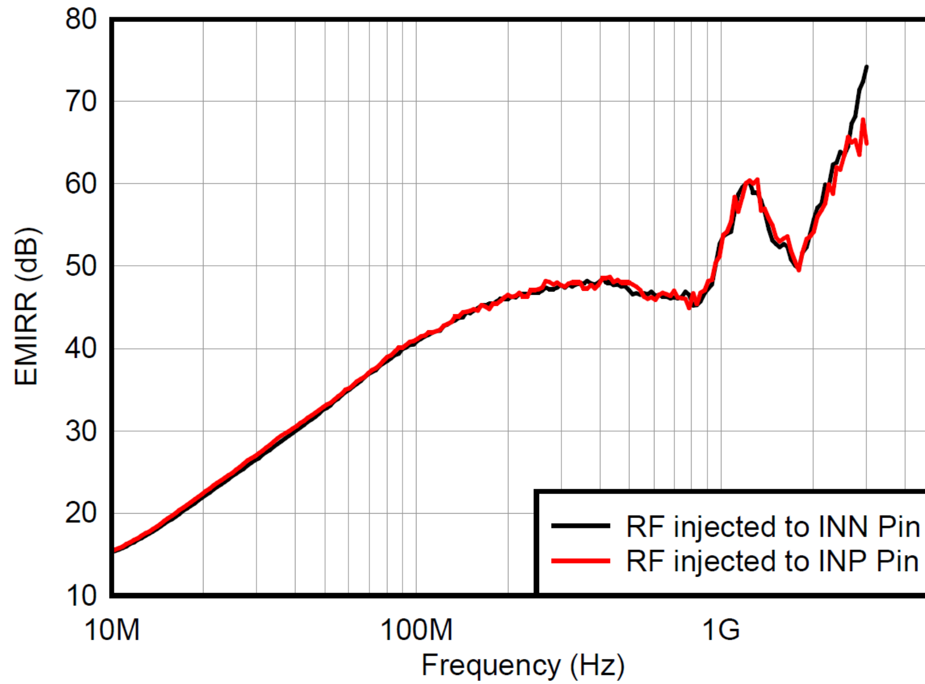

Figure 5.19: INA819 EMIRR measurement by coupling the RF to inverting and non-inverting input terminals

5.3 Comparison of the EMIRR Performance of INAs

Table 5.1: INAs with different specifications [26][27][28][29]

Names	INA819	INA821	INA828	INA118
Unity gain bandwidth	2 MHz	4.7 MHz	2 MHz	800 kHz
Differential mode input capacitance	1 pF	1 pF	1 pF	1 pF
Common mode input capacitance	4 pF	7 pF	10 pF	4 pF
EMI filter, –3-dB frequency	32 MHz	45 MHz	53 MHz	No EMI Filter

Some of the INAs listed in Table 5.1 with different bandwidths and input capacitances are picked for EMIRR measurement to compare their EMI immunity levels. Along with these characteristics, the cut-off frequency of the internal EMI filter is also mentioned by referring their datasheets. INA118 does not have an explicitly stated

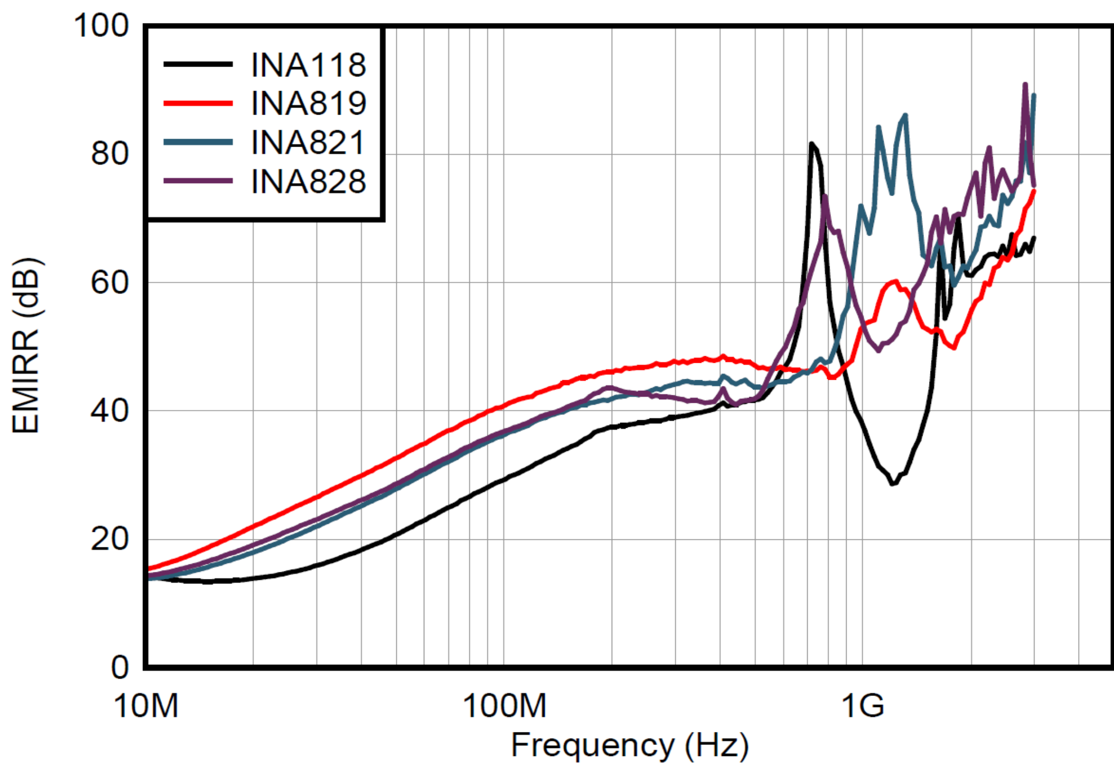

Figure 5.20: EMIRR responses of INA819, INA821, INA828, and INA828 in differential mode

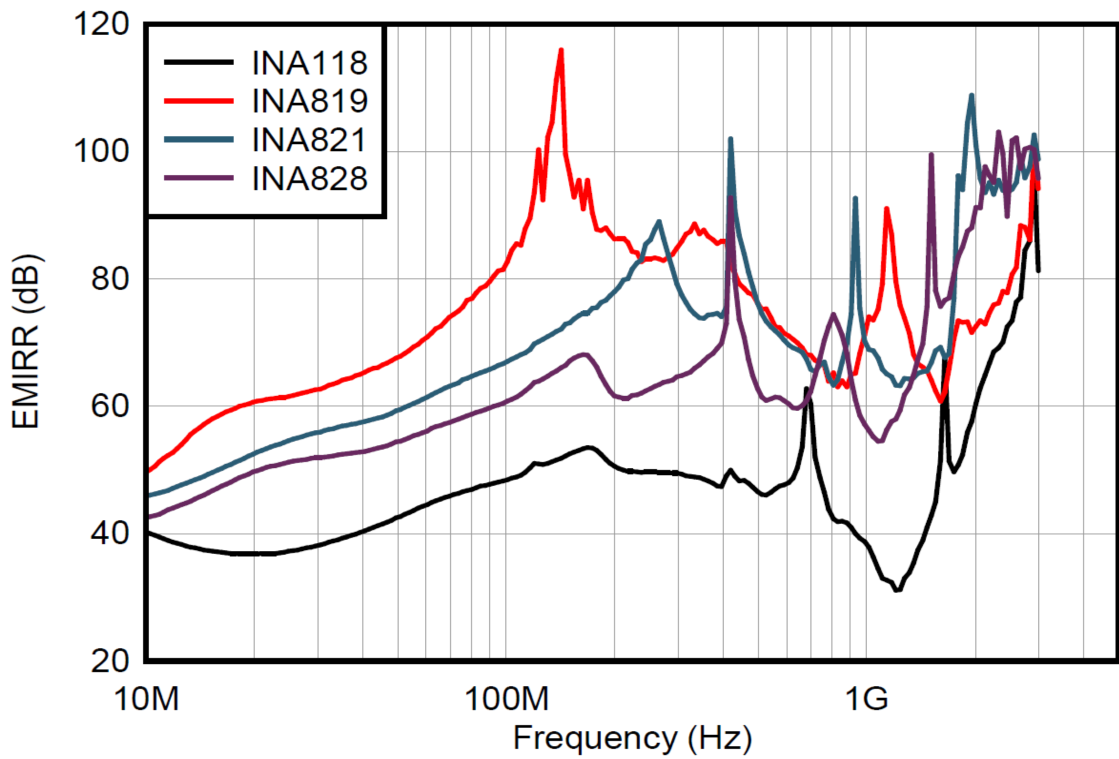

Figure 5.21: EMIRR responses of INA819, INA821, INA828, and INA828 in common mode

EMI filter according to the datasheet [29]. All these measurements are done with a fixed RF noise signal with an amplitude of -10 dBm and the supply voltage of ±15V for unity gain configuration.

The INAs show increasing EMIRR rejection in differential mode at lower frequencies (up to 500 MHz), but fluctuates at higher frequencies due to resonances, as illustrated in Figure 5.20. In case of common-mode EMIRR measurement, there is a significant difference between the highest (INA819) and lowest (INA118) EMIRR performance of INAs, as seen in Figure 5.21. The EMI immunity of INA is likely to be dependent on the EMI filter bandwidth, with the lower the filter bandwidth resulting in greater rejection of high-frequency RF signals. Therefore, when compared to the other INAs, the EMI immunity of INA819, which has the lowest cut off frequency of 32 MHz, has a larger EMIRR at lower frequencies. Following that are INA821 and INA828, with EMI filter bandwidths of 45 MHz and 53 MHz, respectively [27] [28].

Furthermore, the EMI immunity of the INA118 is lower than that of the other INAs, as it is an older INA that was designed before the designers developed the in-built EMI filters. Any rejection of it and other amplifiers that do not have EMI input filters may be due to inherent filtering or non-response to the RF. Inherent filtering is likely to be created by the combination of input pair junction capacitances with the inherent trace or junction resistances that might create the filter pole[12].

The EMI immunity of an INA is important at a certain frequency or range of frequencies required by the application. Table 5.2 lists some of the applications with their operating frequencies, for which the measured EMIRR values of all INAs are mentioned for both differential and common mode. This table assists the designer in selecting an INA with a higher EMI rejection capacity for EMI-sensitive applications. For example, if a mobile radio application that runs with 400 MHz requires an INA with high EMI immunity, INA821 is a good choice since it has 101 dB (highlighted in blue) rejection in common mode and 46 dB rejection in differential mode. Similarly, INA828 is a preferable option for 2.4 GHz frequency applications such as Bluetooth, ISM, and Wi-Fi. Finally, INA819 is suitable for RF applications below 400 MHz as it has better EMI rejection at lower frequencies.

Table 5.2: EMIRR values listed for the applications with the frequencies of interest [26][27]

Frequency	Applications	INA819		INA821		INA828		INA118	
		DM (dB)	CM (dB)	DM (dB)	CM (dB)	DM (dB)	CM (dB)	DM (dB)	CM (dB)
400 MHz	Mobile radio, mobile satellite, space operation, weather, radar, UHF applications	**49**	85	46	**101**	44	92	40	47
900 MHz	Radio communication, navigation, GPS (up to 1.6 GHz), aeronautical mobile applications	48	72	57	**92**	**63**	75	41	40
1.8 GHz	GSM applications, mobile personal communications, broadband, satellite applications	51	75	60	**96**	**70**	85	56	50
2.4 GHz	Bluetooth, mobile personal communications, industrial, scientific and medical radio band, amateur radio applications	67	80	74	95	**75**	**103**	65	72

5.4 Influence of Amplifier Bandwidth, Input Capacitance on EMIRR

The RF rectification process happens mainly at the input stage of the amplifier but the resulting low frequency signals can pass through the forward path or the feedback control path [7]. As expected, Figure 5.20 and Figure 5.21 depicts that INA821 with unity gain bandwidth of 4.7 MHz shows greater EMIRR compared to that of INA118 whose unity gain bandwidth is 800 kHz. However, the EMIRR response of the INA819 and INA828 varies although they have the same bandwidth of 2 MHz for unity gain configuration. Thus, some analog circuits with low bandwidth will respond to EMI signals in an undesirable way because the sub-circuits inside them might have greater bandwidths that sense and respond to high-frequency EMI. As a result, an amplifier's bandwidth has no direct influence on its EMIRR response.

Similarly, while the input capacitance of the INA819 and INA828 in differential mode is same, i.e., 1 pF with the unity-gain bandwidth of 2MHz, their EMIRR responses differ. As a result, like bandwidth, input capacitance also has no direct influence on EMIRR.

5.5 Chapter Summary

The goal of this chapter is to measure EMIRR for INAs and analyze the EMIRR data. So as a first setp, the OPA2227 DUT is tested for EMIRR first to ensure that the newly built test setup is not contributing any offset to the measurement results. And then for selected INAs, the EMIRR measurements are performed, and the EMIRR measurement results for one of the samples i.e., INA819, are displayed both in differential and common modes.

Furthermore, some experiments were carried on EMIRR and the results were analyzed to draw possible inferences. The findings are summarized below.

1 The termination resistor of 50 Ω at the end of the transmission line improves the calibration values to minimize the error values in the EMIRR measurement.

2 EMIRR measured with different packages such as D, DGK, and DRG of the INA819, gives similar results. Hence the device packages have no major influence on EMIRR.

3 Different RF signal amplitudes are injected to the amplifier to see the how EMIRR varies. It was observed that lower the RF noise entering the system, the lower the DC offset voltage created at the amplifier's output, and therefore greater the EMIRR.

4 Changing the power supply voltages within the supply range of the INA has no significant impact on its EMIRR response.

5 EMIRR is measured by keeping the test board within the EMI shielding tent. In this case as it is a conducted immunity measurement, the DUT is not affected by external RF signals.

6 Due to the input trace symmetry in the test board design, the amplifier's EMI rejection ability is similar, when the RF is conducted in either the INV or NINV inputs of the amplifier [17] [18]. This also assures that the EMI effect obtained is from the DUT but not from the setup.

7 EMI filter bandwidth influences the EMIRR, the lower the EMI filter cut-off frequency, the greater the EMI rejection.

8 The bandwidth and input capacitance of an amplifier have no direct effect on its EMIRR response.

Furthermore, EMIRR measurements on a couple of INAs with different bandwidths and input capacitances were performed to compare their EMI immunity levels. Finally, several RF applications and their operating frequencies were listed, and suitable INAs for designing such applications were suggested based on the EMIRR values of measured INAs at that frequency.

6 Conclusion

This thesis study starts with an elaborate discussion on the theoretical background of EMI briefing the essential elements required for EMI to be formed, sources of EMI, and two different EMI transmission types such as EMI by radiation and EMI by conduction. Amplifiers, used in the front-end of analog and mixed-signal integrated circuits must be evaluated for EMI. So, a most practical and accurate conducted immunity testing technique is implemented to measure EMI immunity of precision INAs using a figure of merit – EMIRR which quantifies the immunity of an amplifier when subjected to EMI.

As part of the test setup, two hardware evaluation boards were designed in Altium Designer implementing best practice RF design considerations. Signal integrity simulations were performed on both the hardware test boards in ADS software to extract signal path impedance and verify reflection behavior at the PCB traces. Furthermore, the test automation software using NI TestStand was developed to run EMIRR measurements in the lab setup.

Designing EMI-sensitive circuits necessitates careful consideration of the amplifiers used in the circuit, since their EMI robustness can vary significantly. This decision may be made based on the amplifier's EMIRR value. Hence, EMIRR measurements were performed for several INAs with different specifications to compare their performance for EMI and rank them on their EMI immunity. Some of the RF applications with their operating frequencies were listed, and the best performing INAs for developing such applications were proposed based on their EMIRR values.

Finally, the measured EMIRR data is analyzed to draw possible conclusions on the factors influencing EMIRR of INAs. Some of those inferences are,

1 Placing 50 Ω termination resistor at the end of the RF input trace on the PCB

improves the calibration values to minimize the error values in the EMIRR measurement.

2 Changing the power supply voltages within the supply range of the INA has no significant impact on its EMIRR response.

3 Rectification of EMI happens mainly at the input stage of the INA, where the EMI filter is designed. Thus, the EMI filter bandwidth influences the EMIRR, the lower the EMI filter cut-off frequency, the greater the EMI rejection.

4 The bandwidth, input capacitance and device packages of an INA have no direct effect on its EMIRR response.

Future Work

Future work concerns deeper investigations about IC level simulations to analyse the impact of internal INA parasitics on EMIRR which might also explain the resonances and spikes in the EMIRR curve at higher frequencies. It would also be interesting to implement the on/off keying of RF signal and finding a mechanism to look at the rectified RF signal. Hence, two DC values can be measured instead of single DC offset voltage at the output of the INA.

Bibliography

[1] N. M. D. A. HAQUE and A. P. PATEL, "An overview of an esoteric pollution emi-emc," 2019. [Online]. Available: http://www.irejournals.com/formatedpaper/1700935.pdf

[2] P. Crovetti and F. Musolino, "Digital suppression of emi-induced errors in a baseband acquisition front-end including off-the-shelf, emi-sensitive operational amplifiers. electronics 2021, 10, 2096," 2021.

[3] J. Yu, A. Amer, and E. Sanchez-Sinencio, "Electromagnetic interference resisting operational amplifier," *IEEE Transactions on Circuits and Systems I: Regular Papers*, vol. 61, no. 7, pp. 1917–1927, 2014.

[4] C. Hall, *EMI Rejection Ratio of Operational Amplifiers (With OPA333 and OPA333-Q1 as an Example)*, Texas Instruments, 2011, rev. A. [Online]. Available: https://www.ti.com/lit/an/sboa128a/sboa128a.pdf?ts=1633257946129&ref_url=https%253A%252F%252Fwww.google.com%252F

[5] "Operational amplifiers," CircuitBread, 2020. [Online]. Available: https://www.circuitbread.com/ee-faq/what-are-the-golden-rules-of-op-amps

[6] W. Yang, "Non-ideal op-amp circuit analysis," *International Journal of Electrical Engineering Education*, vol. 47, no. 1, pp. 73–85, 2010. [Online]. Available: https://journals.sagepub.com/doi/abs/10.7227/IJEEE.47.1.7

[7] C. Wu, G. Li, D. J. Pommerenke, V. Khilkevich, and G. Hess, "Characterization of the rfi rectification behavior of instrumentation amplifiers," in *2018 IEEE Symposium on Electromagnetic Compatibility, Signal Integrity and Power Integrity (EMC, SI & PI)*. IEEE, 2018, pp. 156–160.

[8] de Wagt; Gerrit; and A. van Staveren, *A Specification for EMI Hardened Operational Amplifiers*, Texas Instruments, 2010, rev. B. [Online]. Available: https://www.ti.com/lit/an/snoa497b/snoa497b.pdf?ts=1633258561240&ref_url=https%253A%252F%252Fwww.google.com%252F

[9] A. Boyer and E. Sicard, "A case study to apprehend rf susceptibility of operational amplifiers," in *2019 12th International Workshop on the Electromagnetic Compatibility of Integrated Circuits (EMC Compo)*, 2019, pp. 13–15.

[10] F. Fiori and P. S. Crovetti, "Nonlinear effects of radio-frequency interference in operational amplifiers," *IEEE Transactions on Circuits and Systems I: Fundamental Theory and Applications*, vol. 49, no. 3, pp. 367–372, 2002.

[11] P. Mathur and S. Raman, "Electromagnetic interference (emi): measurement and reduction techniques," *Journal of Electronic Materials*, pp. 1–24, 2020. [Online]. Available: https://link.springer.com/article/10.1007/s11664-020-07979-1

[12] T. Kuehl, "Analog basics workshop rfi/emi rejection," Texas Instruments, 2014. [Online]. Available: https://www.slideserve.com/svein/analog-basics-workshop-rfi-emi-rejection

[13] E. Bronaugh, "Helmholtz coils for emi immunity testing: stretching the uniform field area," in *Seventh International Conference on Electromagnetic Compatibility, 1990*, 1990, pp. 169–172.

[14] *Circular Helmholtz Coils*, Schwarzbeck Mess-Elektronik, 2021. [Online]. Available: http://www.schwarzbeck.de/Datenblatt/k5201-98.pdf

[15] F. Fiori, "Design of an operational amplifier input stage immune to emi," *IEEE Transactions on Electromagnetic Compatibility*, vol. 49, no. 4, pp. 834–839, 2007.

[16] B. Trump, "Input capacitance model," Texas Instruments, 2013. [Online]. Available: https://e2e.ti.com/blogs_/archives/b/thesignal/posts/input-capacitance-common-mode-differential-huh

[17] H. Zumbahlen, *Basic linear design*. Citeseer, 2007. [Online]. Available: https://citeseerx.ist.psu.edu/viewdoc/download?doi=10.1.1.480.3471&rep=rep1&type=pdf

[18] S. Mercer and C. Eng, "Minimizing rf pcb electromagnetic emissions," *RF DESIGN*, vol. 22, pp. 46–85, 1999. [Online]. Available: http://rfsilicon.com/home/measurement/19990103.pdf

[19] "Impedance formula editor," Altium, 2018. [Online]. Available: https://www.altium.com/documentation/altium-designer/pcb-dlg-impedanceformulaeditorimpedance-formula-editor-ad?version=18.1

[20] "Coplanar waveguide analysis/synthesis calculator," CGI, 2009. [Online]. Available: http://wcalc.sourceforge.net/cgi-bin/coplanar.cgi

[21] "S-parameter measurements," Keysight Technologies, 2019. [Online]. Available: https://literature.cdn.keysight.com/litweb/pdf/5991-3736ENDI.pdf

[22] "Capacitor guide," Murata Manufacturing, 2013. [Online]. Available: https://article.murata.com/en-eu/article/impedance-esr-frequency-characteristics-in-capacitors

[23] "Teststand," National Instruments, 2021. [Online]. Available: https://www.ni.com/en-us/shop/electronic-test-instrumentation/application-software-for-electronic-test-and-instrumentation-category/what-is-teststand.html#:~:text=TestStand%20is%20application%20software%20that,written%20in%20any%20programming%20language.

[24] "Analog basics workshop rfi/emi rejection," TIBCO Spotfire, 2021. [Online]. Available: https://docs.tibco.com/products/tibco-spotfire/

[25] *OPAx22x High Precision, Low Noise Operational Amplifiers*, Texas Instruments, 2022, rev B. [Online]. Available: https://www.ti.com/product/OPA2227

[26] *INA819 35-V Offset, 8-nV/Hz Noise, Low-Power, Precision Instrumentation Amplifier*, Texas Instruments, 2020, rev C. [Online]. Available: https://www.ti.com/product/INA819

[27] *INA821 35-µV Offset, 7-nV/Hz Noise, Low-Power, Precision Instrumentation Amplifier*, Texas Instruments, 2020, rev D. [Online]. Available: https://www.ti.com/product/INA821

[28] *INA828 50-µV Offset, 7-nV/Hz Noise, Low-Power, Precision Instrumentation Amplifier*, Texas Instruments, 2018, rev A. [Online]. Available: https://www.ti.com/product/INA828

[29] *INA118 Precision, Low-Power Instrumentation Amplifier*, Texas Instruments, 2019, rev B. [Online]. Available: https://www.ti.com/product/INA118

[30] J.-M. Redoute and M. Steyaert, "An instrumentation amplifier input circuit with a high immunity to emi," in *2008 International Symposium on Electromagnetic Compatibility - EMC Europe*, 2008, pp. 1–6.

TUC References

[TUC1] R. Banik, “Lvds transmitter design,” 2018.

[TUC2] H. Muhsen, S. Hiller, and J. Lutz, “Three-phase voltage source inverter using sic mosfets — design and optimization,” in *2015 17th European Conference on Power Electronics and Applications (EPE’15 ECCE-Europe)*, 2015, pp. 1–9.

TECHNISCHE UNIVERSITÄT CHEMNITZ

Zentrales Prüfungsamt

Selbstständigkeitserklärung

<table>
<tr><td>Name:

Vorname:

geb. am:

Matr.-Nr.:</td><td><u>Bitte beachten:</u>

1. Bitte binden Sie dieses Blatt am Ende Ihrer Arbeit ein.</td></tr>
</table>

Selbstständigkeitserklärung*

Ich erkläre gegenüber der Technischen Universität Chemnitz, dass ich die vorliegende
selbstständig und ohne Benutzung anderer als der angegebenen Quellen und Hilfsmittel angefertigt habe.

Die vorliegende Arbeit ist frei von Plagiaten. Alle Ausführungen, die wörtlich oder inhaltlich aus anderen Schriften entnommen sind, habe ich als solche kenntlich gemacht.

Diese Arbeit wurde in gleicher oder ähnlicher Form noch nicht als Prüfungsleistung eingereicht und ist auch noch nicht veröffentlicht.

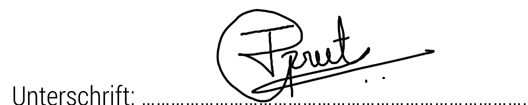

Datum: …………………………………. Unterschrift: ………………………………………………………………………

* Statement of Authorship

I hereby certify to the Technische Universität Chemnitz that this thesis is all my own work and uses no external material other than that acknowledged in the text.

This work contains no plagiarism and all sentences or passages directly quoted from other people's work or including content derived from such work have been specifically credited to the authors and sources.

This paper has neither been submitted in the same or a similar form to any other examiner nor for the award of any other degree, nor has it previously been published.